Abstract

Natarajan, Karthikeyan. Air Permeability of Elastomeric Fabrics as a Function of Uniaxial Tensile Strain (Under the directions of Dr. Abdelfattah M. Seyam and Dr. Tushar K. Ghosh)

It is known fact that the geometry of fabric changes when subjected to strain and fabric air permeability is affected by the fabric geometrical parameters. However, the literature disclosed that the influence of strain on the air permeability of the fabrics has never been studied. In this work an effort has been made to study the influence of strain on the air permeability of woven fabrics with elastomeric constituents. Forty two different fabrics were woven with range of in-loom pick density, filling yarn linear density and weave. A special device to impart uniaxial tensile strain on a fabric has been designed and built. The staining device was constructed so that the air permeability of a fabric could be measured while the fabric is in its stretched state.

Influence of uniaxial tensile strain and fabric structure parameters on fabric air permeability has been investigated. The results show that fabric air permeability is significantly affected by the fabric strain level. The air permeability increases with increasing in fabric strain. The increase in air permeability with strain is associated with the geometrical changes taking place in the fabric due to strain. The air permeability of an elastomeric fabric also depends on fabric construction parameters. For a fabric employed with particular weave, warp and filling yarns the air permeability decreases with increasing fabric tightness.

Air Permeability of Elastomeric Fabrics as a Function of Uniaxial Tensile Strain

By

Karthikeyan Natarajan

A thesis submitted to the Graduate Faculty of
North Carolina State University
in partial fulfillment of the
requirements for the Degree of
Master of Science

TEXTILE MANAGEMENT AND TECHNOLOGY

RALEIGH

2003

APPROVED BY:

Abdelfattah M. Seyam
Chair of Advisory Committee

Tushar K. Ghosh
Co-Chair of Advisory Committee

John F. Muth
Member of Advisory Committee

Biography

Karthikeyan Natarajan was born on January 1st 1979 in Erode, Tamilnadu State, India. He did his schooling in Mani Higher Secondary School, Coimbatore, India and completed his high school studies in 1994. He joined PSG College of technology, Coimbatore India in 1994 and graduated with a Diploma in Textile Technology in 1997. After completing his diploma he joined Bannari Amman Institute of Technology, Sathyamangalam, India and received an Undergraduate Degree in Textile Technology in 2000. In fall 2001, he joined North Carolina State University College of Textiles, Raleigh, USA to pursue a Master of Science Degree in Textile Technology and Management.

Acknowledgements

I would like to express my sincere thanks to my advisors Dr. Abdelfattah M. Seyam and Dr. Tushar K. Ghosh for their enthusiastic guidance and encouragement for this project and throughout the course of this study. They have been a tremendous influence on my academic and professional development over the last two years has assisted me a great deal in writing up this thesis. I am also grateful to Dr. John F. Muth for agreeing to serve on committee and for his valuable suggestions.

I would like to acknowledge Defense Advance Research Project Agency (DARPA) and MCNC the sponsors of this research. I would like to thank DuPont for providing Type 400 elastomeric yarns. My special thanks go to the staff of the College of Textiles for the help and suggestions during study period. I express sincere appreciation to all the lab managers for their technical assistance especially William Barefoot in the weaving lab.

Last, but not least, I am grateful to my parents, K. Natarajan and N. Padmavathi, my brother, N. Mohan Raj and my friends for their support, encouragement and love. I will always be indebted to these people without whom the higher education would have been a dream.

Air Permeability of Elastomeric Fabrics as a Function of Uniaxial Tensile Strain

Table of contents

List of tables

List of figures

1 INTRODUCTION

Air permeability is an important property of the fabric. It has a decisive influence on utilization of fabric for some technical applications (filters, parachutes, and sails) and clothing application as well. Air permeability is a measured by the ease with which the air passes through the material. ASTM D737-99 defines air permeability as “the rate of air flow through a material under a differential pressure between the two fabric surfaces” expressed in cubic feet per square foot per second. Air permeability of a fabric depends on parameters like the fabric cover and fabric porosity. Total cover of a fabric may be defined as the ratio of area covered by the warp and the filling yarns to the area covered by the fabric. Porosity of a fabric may be defined as the “ratio of the projected geometrical area of the opening across the material to the total area of the material” or the “ratio of air space to the total volume of the fabric expressed as percentage”.

Other fabric parameters that influence the air permeability of a fabric are type of weave, type of yarn (spun or filament), yarn size (linear density), twist factor in the yarn, thread density (ends and picks), and crimp%. Type of weave determines the manner in which the yarns are interlaced in fabric. By changing the order of interlacements the air permeability of the fabrics can be varied [7]. When the size of the yarn changes the area occupied by the yarn in the fabric and therefore the porosity of the fabric also changes. The twist factor in the yarn has a significant influence on the air permeability of the fabric since twist affects yarn size. The air permeability of the fabric increases with twist factor. The thread density has a negative relationship with the air permeability of the fabric, the air permeability decreases with increasing thread density.

If a woven fabric contains elastomeric threads either in the warp or in the filling or both directions, such a fabric can be extended to high degree of strain values. When the fabric with elastomeric components is strained, the degree of openness of the fabric changes as a result of changes in the fabric geometrical parameters. The extent to which the fabric can be stretched depends on the properties and the density of the elastomeric threads that is included in the fabric. The amount of stretch the fabric undergoes depends on the strain level applied to the fabric.

Studies have been conducted separately on the two topics “the behavior of fabric air permeability as a function of fabric parameters” and “the influence of strain on the fabric geometry.” This fact prompted undertaking research effort to understand behavior of air permeability of fabrics with elastomeric components in terms of fabric strain.

The objective of this research is to provide basic understanding of the air permeability behavior of fabrics with elastomeric constituents when subjected to different levels of strain. This study will help to understand the relationship between air permeability of the elastomeric fabrics and uniaxial fabric tensile strain. It also helps in understanding the effect of yarn and fabric parameters on the same. The study is believed to aid engineers designing fabrics with controllable porosity (air permeability) that could be used to construct active fabrics for technical applications such as parachutes, Parafoils, sailing, and windscreens.

2 BACKGROUND

ASTM D737-99 defines air permeability as "the rate of air flow through a material under a differential pressure between the two fabric surfaces" expressed in cubic feet per square foot per second.

The rate of airflow through a material under a differential pressure between the two fabric surfaces is a very important parameter. Many fabric functionalities like the performance of parachute and sailcloth, efficiency of filtration in industrial cloths, apparel comfort, flammability, thermal insulation efficiency, barrier fabric performance, and precision of the filter media depends on the resistance offered by the fabric to the passage of air and other fluids. The resistance offered by the fabric depends on the proportion of the void volume and the accessibility of the void.

2.1 Relationship between air permeability and fabric structure

Fabric geometrical parameters like fabric thickness, interstice size, the number of interstices in a given area, pick density, warp density, type of yarn and yarn twist influence fabric air permeability. The influence of fabric geometry on the air permeability has been studied by numerous investigators on both an empirical and theoretical basis.

Clayton [1] has conducted series of experiments to determine the relationship between air permeability and cloth structure. In his first series of experiments he chooses pick density as the main variable. He describes a new term called sectional air permeability. The sectional permeability is a value indicating the airflow and is used to express the openness of a fabric of unit thickness. It is a product of P and d, where d is the fabric thickness in millimeters and P is the permeability. His experimental results of the first series show that when the pick density increases from 35 to 65 picks/in, the sectional permeability (P_s) decreases at a constant rate, the curve flattens out beyond pick density of 65 picks/in. This can be seen in Figure 2.1. He explains that the decrease in P_s is due to of the closing of holes or the open area in the cloth.

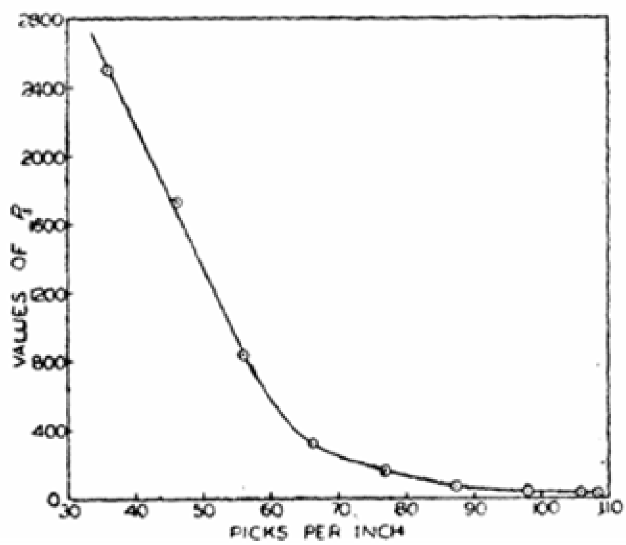

Figure 2. 1: Sectional Permeability (P_s) as a function Pick Density [1]

Similar studies conducted by Brown and Rusca [2] and also by Mohamed and Lord [3] indicate that air permeability decreases with increasing pick density.

In the second series of experiments Clayton [1] took filling count as the primary variable and the subsidiary variable being warp crimp % and cloth weight. His experimental results show that the sectional air permeability varies linearly with filling count. I.e. the air permeability increases linearly with increase in filling count (Ne), as it can be seen in Figure 2.2.

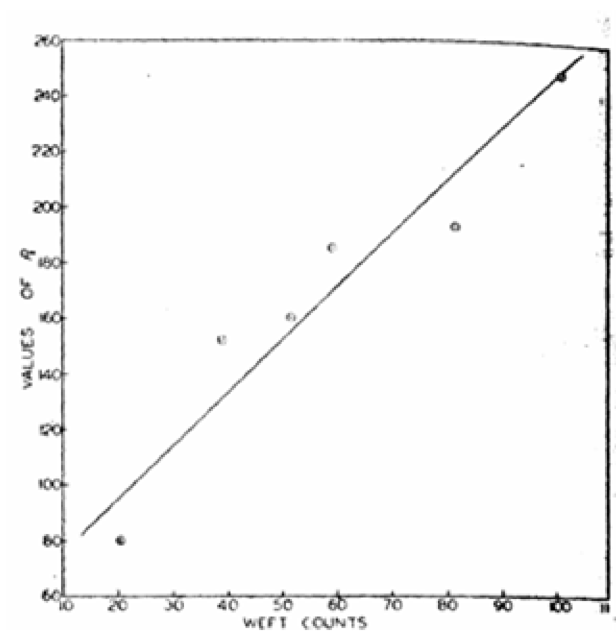

Figure 2. 2: Sectional Permeability (P_s) as a function of Filling Count (Cotton count)[1]

In the third series Clayton [1] kept filling count and the picks per inch as two primary variables so that the number of picks per inch / Square root of filling count = Constant. The intention of this relation was to keep the cover constant. Filling crimp and thickness of the fabric were kept as subsidiary variables. The results show that the logarithm value of sectional permeability varies linearly with logarithm of pick density and the logarithm of the filling count. This can be seen in Figure 2.3.

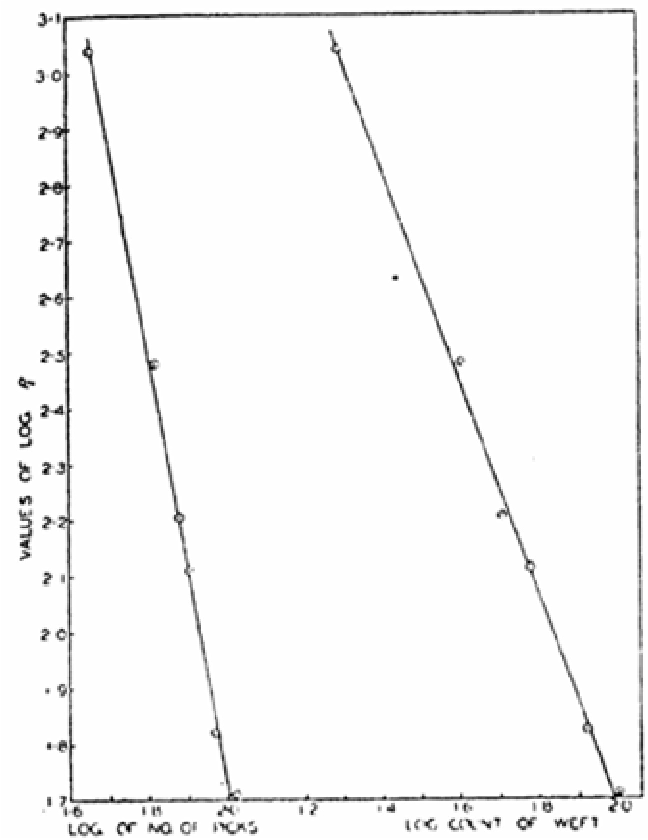

Figure 2.3: Sectional Permeability (P_s) as a function of Filling Count & pick density[1]

In the fourth series Clayton [1] kept the twist factor of the filling yarn as the main variable. The results show that the sectional permeability varies linearly with the twist factor. This can be seen in Figure 2. 4.

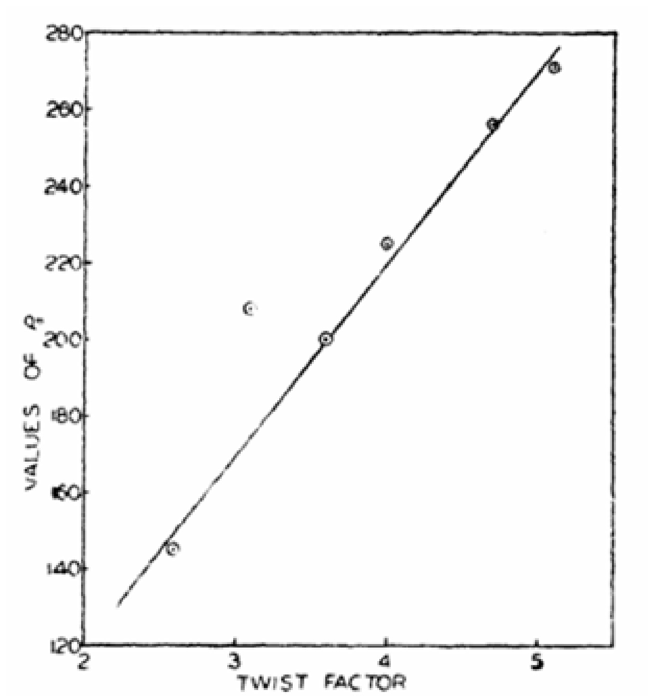

Figure 2. 4: Sectional Permeability (P_s) Vs Twist Factor [1]

Although the relations between cloth structure and air permeability are given for one type of poplin, Clayton [1] believes that the general nature of the variation will be the same for most of the cloths. Studies conducted by Lord and Mohamed [4] and also by Peak [5] prove that the air permeability increases with increasing twist factor.

The air permeability of the fabric reduces with the finishing process like bleaching, dyeing, and calendering. During the bleaching process the size material in the warp yarns is removed and thus increases the yarn hairiness. The increase in hairiness tends to close the holes of the cloth there by decreasing the air permeability. The reduction is air permeability is also because of the shrinkage in the cloth during the finishing process. During the calendering process the yarns get flattened and there by decreases the fabric air permeability [1].

Lord [6] made an effort to study the influence of certain variables such as the pressure drop across the specimen, area of test specimen and number of fabric layers on the air permeability of fabrics. He found that the airflow through the fabric is proportional to the pressure drop across the fabric for tightly woven fabrics and is linearly related to the square root of pressure for open constructions and also airflow through the fabric is proportional to the area of the test specimen. His research finding also includes that the resistances offered to the airflow of air through multiple layers of same fabric or superimposed layers of fabric used in a clothing assembly is additive. He mentioned that for a closely woven fabric the measured resistance of several superimposed layers may be somewhat greater than the sum of the resistances.

Schiefer et al [7] have also conducted experiments to find out the influence of fabric parameters on the air permeability behavior of the fabrics. He produced a set of 42 fabrics of similar yarns (warp 57's, 4.0 Twist multiplier and filling yarn of 60's, 2.6 T.M.) with a thread count in the loom of 90x90. He considered weave as the primary variable. The different kinds of weaves include plain, twill, rib, mock leno, basket, sateen, and combinations of these. He analyzed the physical properties of these fabrics and concluded that the fabrics which are closely woven and have a large number of thread interlacing per unit area and short floats will have lower air permeability than the cloths of the same weight which are loosely woven, sleazy and have a smaller number of thread interlacing per unit area and long floats [7].

Rainard [8] have also worked on the air permeability of fabrics. The objective of his research was to device a method for obtaining significant data on the air permeability of fabrics and to consider the general description of the fabric in terms of air permeability over a wide range of velocities of air. For his experimentation purpose he used the Frazier air permeability tester designed by Schiefer and Boyland [7] and an apparatus designed especially for determining permeability at low pressure. He measures air permeability in at least 3 spots and for each spot the amount of air passed through the fabric was determined as a function of differential pressure.

Seyam and El-Shiek [9] studied the relationship between air permeability and fabric cover factor (K_1+K_2), where K_1 is the warp cover factor (=ends per inch/square root of warp yarn cotton count) and K_2 is the filling yarn cover factor (=picks per inch/square root of filling yarn cotton count). Their experimental result shows that the air permeability of the fabric decreases with increasing cover factor. They explain that the decrease is because of the reduction in the uncovered fabric area, which contributes mainly to the air permeability with increasing cover.

Rainard [8] plots the air permeability value as a function of pressure differential Δp. He defined a new parameter termed "intrinsic air permeability" obtained by extrapolating the curves of ($F_a/\Delta p$) versus Δp at $\Delta p=0$. He derived an equation to calculate air permeability as a function of pressure differential in terms of any known airflow, in corresponding pressure differential and intrinsic permeability,

$$F_a = \left(\frac{\frac{F_{a0}}{\Delta p_o} - P_i}{\Delta p_o} \right) \Delta p^2 + P_i \Delta p$$

where,

F_a= Air permeability in cubit feet per min per square foot,

Δp= Pressure differential in inches of water,

Δp_o= any chosen arbitrary pressure whose corresponding air flow (F_{ao}) is known,

P_i = Intrinsic air permeability P_i.

Backer [10] studied the relationship between the structural geometry of a textile fabric and air permeability of the fabric. He showed that the air permeability of a fabric is related to the number and size of the interstice in a fabric and it is impossible to define the nature of the fabric interstice in a highly dense fabric. He assumes that the airflow through the pores (interstice) in the fabric is similar to fluid flow through an orifice through a channel of varying cross-section and that the flow through fabric structure is influenced by the minimum cross sectional area of the pore. The minimum cross sectional area can be computed by geometric relationships or mechanical integration or through use of models or by approximation of pore shapes. The degree of accuracy of the minimum pore area depends on how far the assumption is met in the material under consideration. It’s assumed here that the yarn structures are solid, flexible cylinders, which maintain their circular cross section in bending.

Backer [10] uses the minimum cross sectional area to determine the relationship between cloth design and air permeability. Similar to the classification of pore structures by the geophysicists into 6 types, Backer classified the pore structure occurring in textile fabric into four basic categories as shown in Figure 2. 5, assuming that the planes perpendicular to the fabric surfaces and bisecting any two adjacent warp and filling yarns are used to form a unit cell.

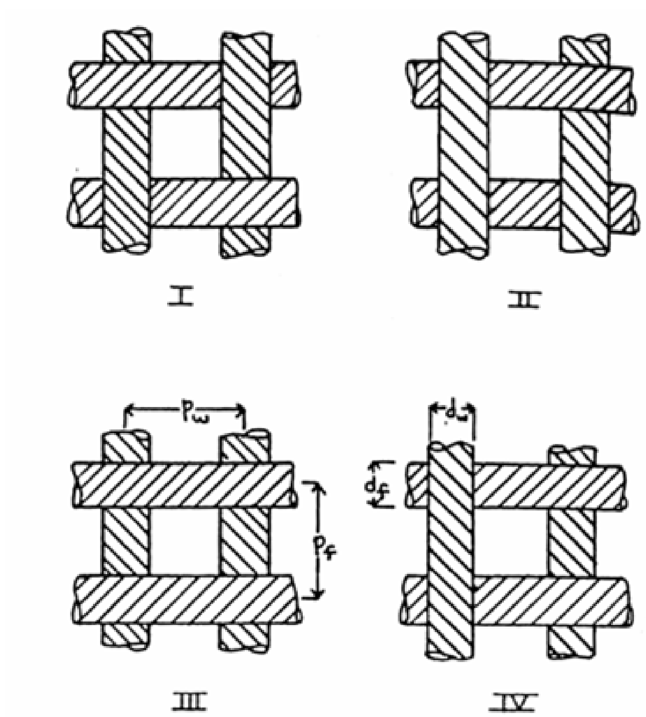

Figure 2. 5: Four basic types of pore structure occurring in fabric [10]

Type 1: In this type the four yarns of a unit cell alternate from top to bottom surface of the cloth and vice versa

Type 2: Here one warp and one filling alternate

Type 3: No alteration of yarns

Type 4: Here either two warp yarns or two filling yarns alternate from top to bottom surface and vice versa

At least two or three types of pores will be there in most of the commercial fabric constructions. The fabric having the plain weave construction consists entirely of type 1 pore structure.

Pore volume and shape of two fabrics woven with identical yarn diameter and yarn spacing will vary depending on the manner of interlacing of the threads. The number of each type on interstice present in the fabric and hence the cross sectional area of the pores depends on the weave [10].

Backer [10] studies the shape of the interstice types by drawing the progressive horizontal sections of the four pore types in the same manner as Bailey [11] did with the longitudinal sections of the actual fabrics. Figures 2.6-2.9 show the variation of the shape of each of the interstice. It can be seen from the figures that the interstice with the greatest number of yarn interlacing (i.e. Type 1) has the smallest minimum cross sectional area while the pore with no interlacing (i.e. Type 3), has the largest minimum cross sectional area.

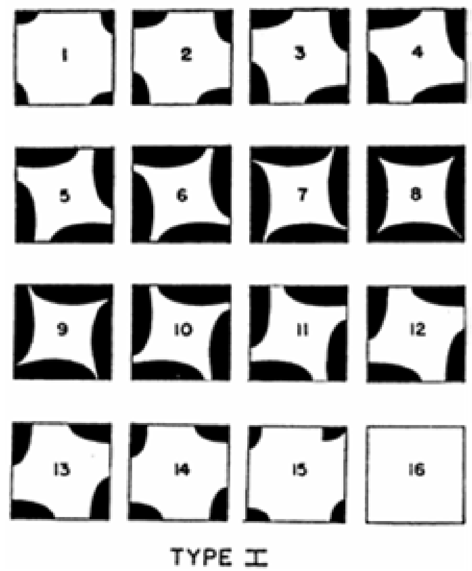

Figure 2. 6: Progressive horizontal sections of Type1 interstice [10]

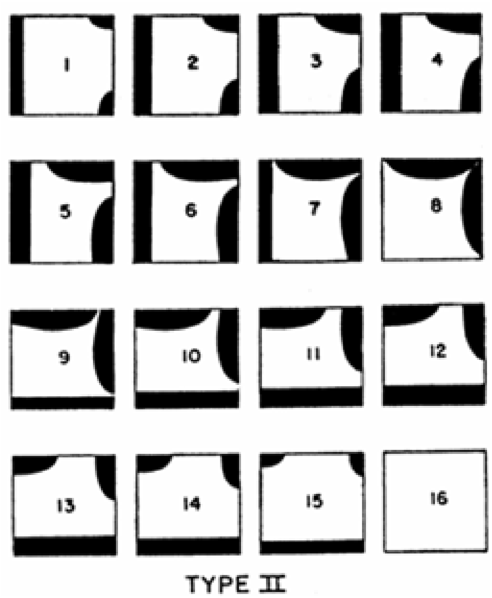

Figure 2. 7: Progressive horizontal sections of Type2 interstice [10]

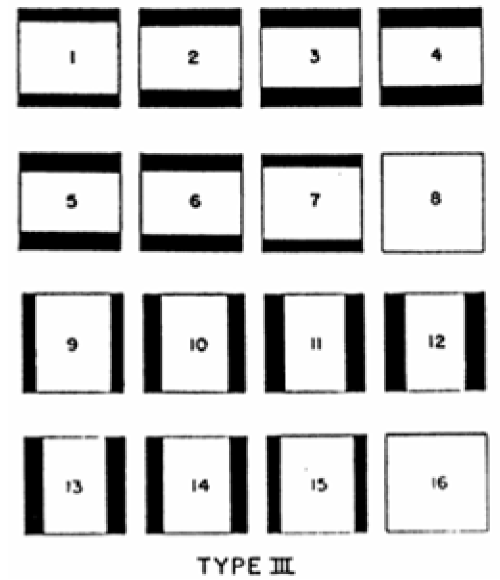

Figure 2. 8: Progressive horizontal sections of Type3 interstice [10]

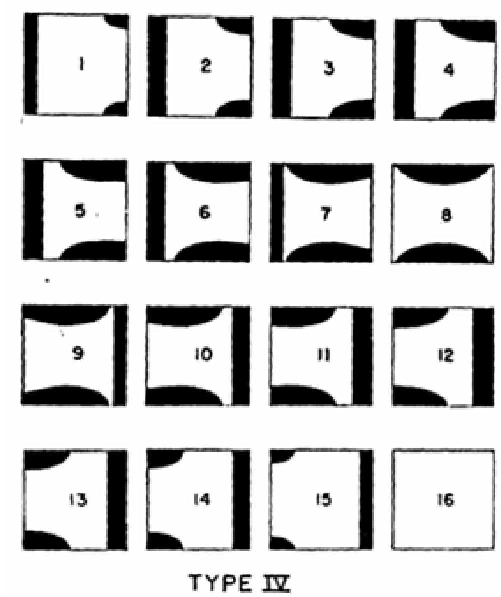

Figure 2. 9: Progressive horizontal sections of Type4 interstice [10]

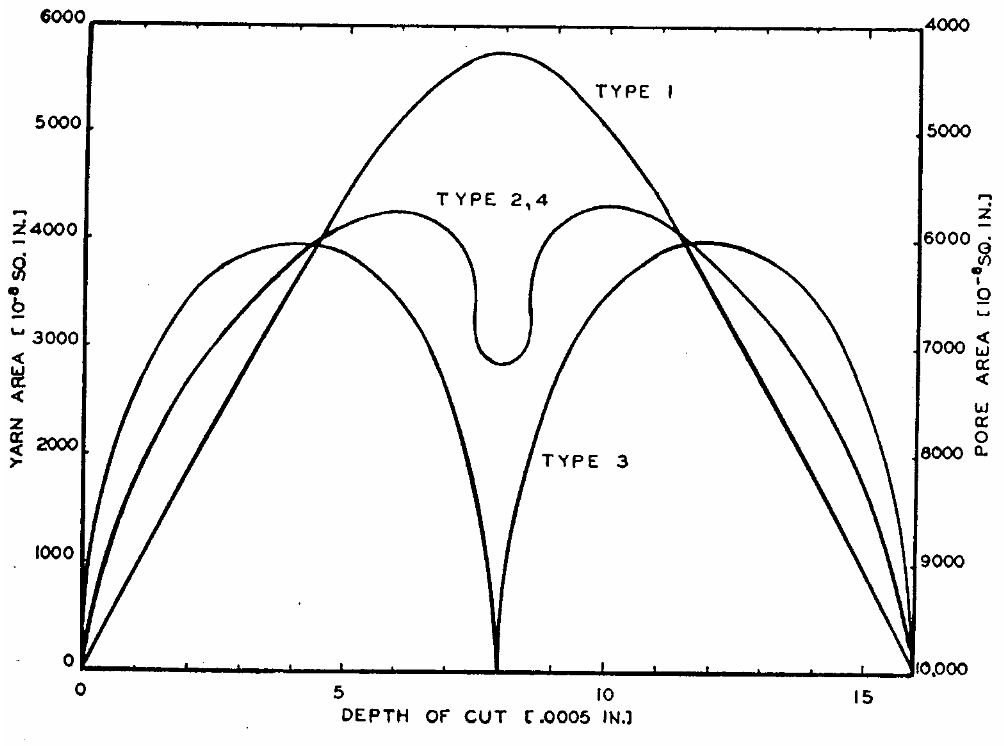

Figure 2. 10: Cross sectional area of unit cells [10]

He calculated the average minimum pore cross sectional area for each weave and then plotted this value against the air permeability as shown in Figure 2.11.

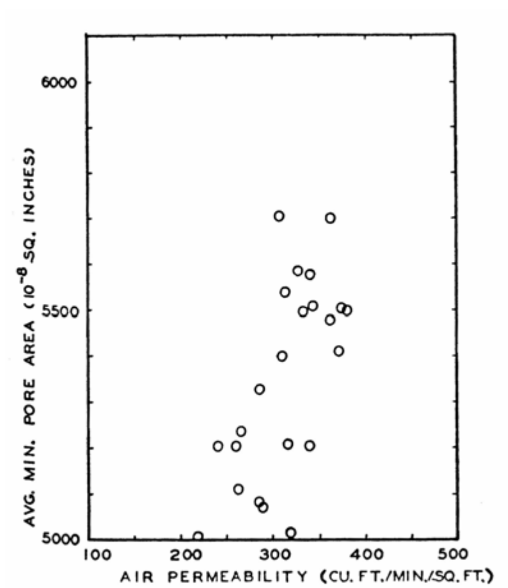

Figure 2. 11: Air permeability and average minimum pore areas [10]

The type of fabrics he considered here were relatively open fabrics. He found that fabrics which were closely woven and firm and had a larger number of thread interlacing per unit area and short floats had lower air permeability than cloths of the same weight which were loosely woven and sleazy and had a small number of thread interlacing per unit area and long floats.

He also found out that for a balanced fabric with equal textures and yarn diameters there exists a relationship between the air permeability and total crimp (defined as the crimp of warp or filling yarn since the fabric is square) which could serve indirectly as a basis for predicting air permeability. Figure 2.12 show the relationship between air permeability and total crimp.

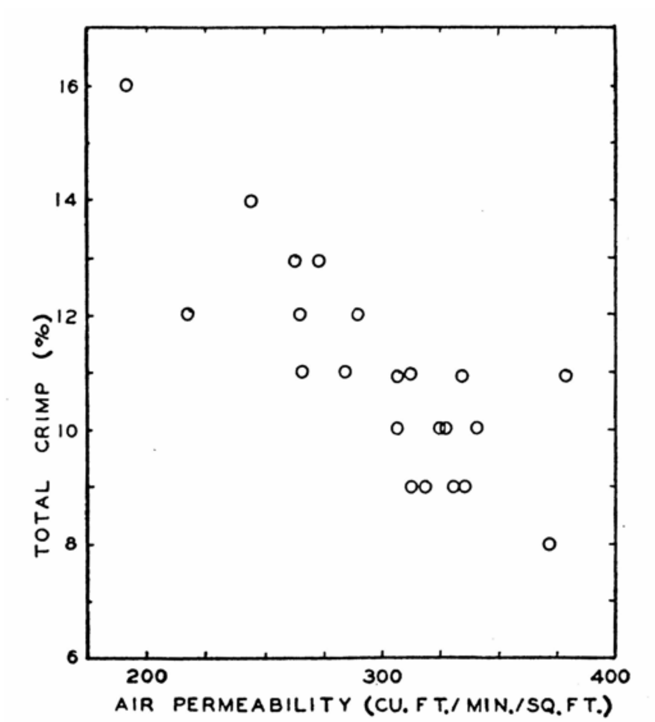

Figure 2. 12: Air permeability as a function of total crimp %[10]

Backer [10] also studied the air permeability behavior of very tightly woven fabrics. He mentions that in a closely packed fabric when the limiting condition (warp or filling yarns are so closely packed that adjacent yarns of the same parallel set touch) occur the minimum cross-sections of the interstice changes. Figure 2.13 show the minimum cross sections of the four interstices in closely packed warp fabric. It can see that the relative difference between the minimum pore areas of the four-interstice type is greater for a tightly woven fabric than for more open cloths.

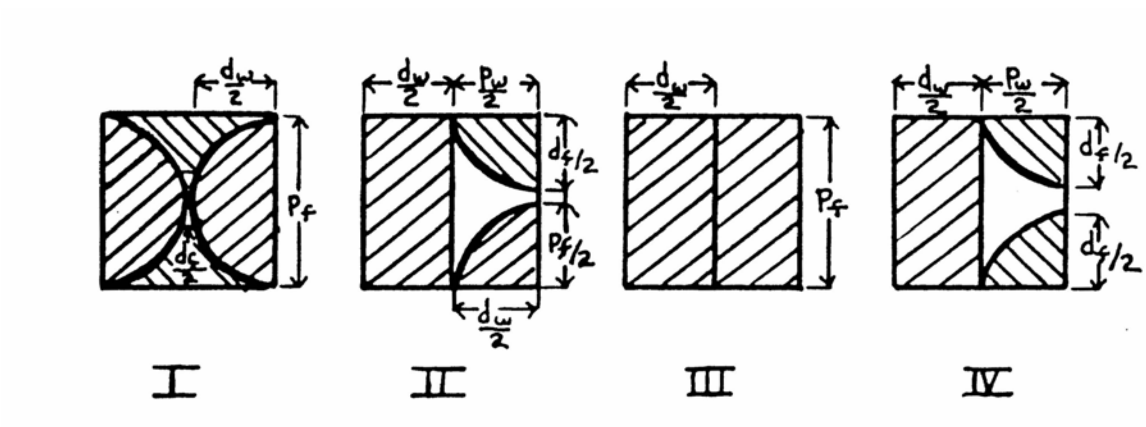

Figure 2. 13: Minimum cross sections of the four interstices in close packed-warp fabric [10]

Backer [10] calculated the air permeability values of the tightly woven fabric samples using the Schiefer apparatus under a pressure differential of 0.5 inch of water and plotted it against the projected area left open per square inch of the fabric as shown in Figure 2.14 which he calculated using the expression derived by Peirce[12].

$$\frac{(p_w - d_w)(p_f - d_f)}{p_w p_f}$$

where $1/d = 28\sqrt{N}$ (N is the cotton count)

d_w and d_f are warp and filling yarn diameters in inches

p_w and p_f are the yarn warp and pick spacing in inches

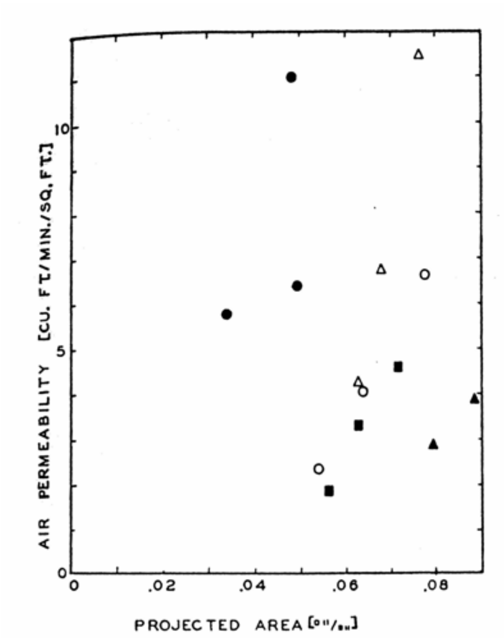

Figure 2. 14: Air permeability as a function of projected area [10]

Figure 2.14 shows that the relationship between the projected pore area and air permeability's of the fabrics is very poor. He also computed the minimum pore area using the geometric forms and plotted it against the air permeability values of the tightly woven fabric samples using the Schiefer apparatus under a pressure differential of 0.5 inch of water as shown in Figure 2. 15.

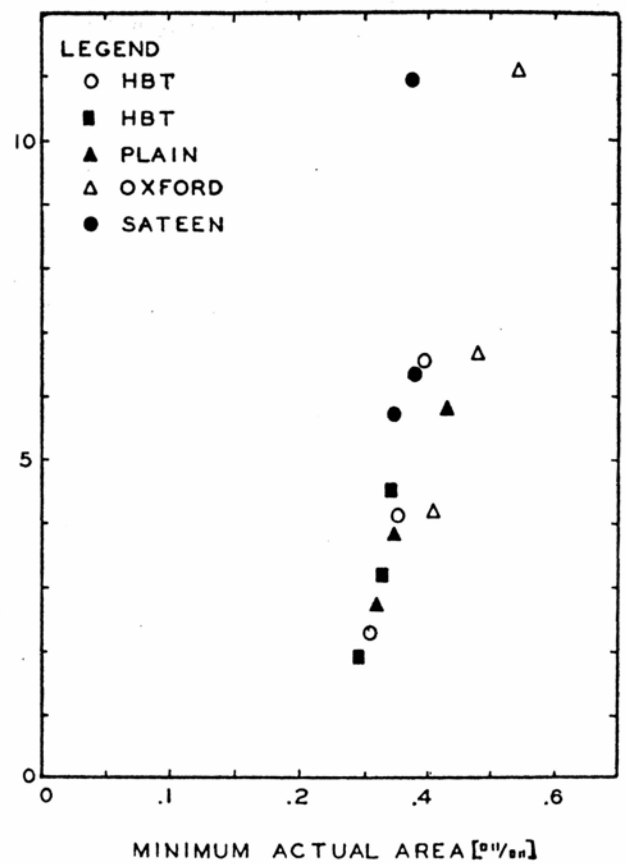

Figure 2.15: Air permeability as a function of minimum pore area [10]

We can see from Figure 2. 15, that there is an improved relationship between the minimum pore area and air permeability when compared to the relationship between projected area and air permeability.

Backer [10] found out from his research that the inter fiber spacing with yarn also contributes to the airflow through the fabric woven with maximum tightness. The inter yarn pores or spacings dominates the flow through the fabric in which a moderate tightness and a reasonably circular cross section of the yarn is maintained.

Penner and Robertson [13] have made an effort to study the flow of fluid through the fabric. They studied the relationship between the weave structure and fluid flow in the range of Reynolds numbers from 10 to 400. In their study they considered the fabric pores as orifices.

They used the four basic models of yarn combinations in a woven fabric interstice created by Backer [10]. The four models that were constructed have nearly constant d/p (where d is the yarn diameter and p is the yarn spacing) ratio. Liquid is forced past the models and air bubbles are used to visualize the fluid motion. The movement of the air bubbles is detected by means of suitable light source. This helps to get an undistorted visualization of the fluid flow through the fabric like structures, since the refractive indices of the fluid and the construction material for the model and viewing chamber are same and are translucent [13].

The effect of fabric constructions and the variations of the Reynolds number on the area available for the passage of the fluids through each pore type or the effective pore area can be analyzed with help of the photographs taken parallel to the direction of flow. The construction of the four basic models is shown in Figure 2.16. The photographs revealed that the four pore types do not behave like geometrically similar orifices. The minimum cross sectional area of the jet or the stream tube through the pore determines the effective pore area [13]. The shape of the jet is influenced by factors like Reynolds number, size and the surface of the pore and the manner of yarn interlacement in the fabric. At low Reynolds numbers (approximately 10) the flow around the cylinders is more nearly ideal, and there is very little separation or eddying taking place and the minimum jet area approaches the minimum pore area as proposed by Backer. As the

Reynolds number increases the effective pore area decreases. The photographic investigation revealed information about the development of wake with increasing Reynolds number. The size and the characteristics of the wake are influenced not only by the Reynolds number but also by the construction of the pore.

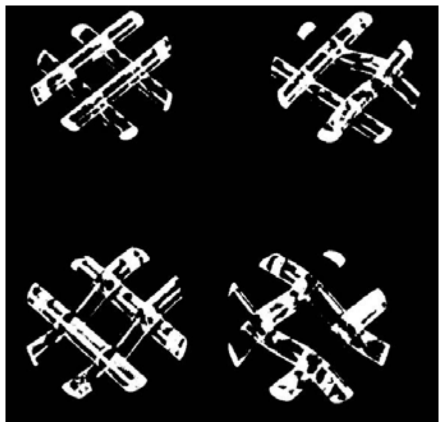

Figure 2. 16: The basic four models. Top left –No1, Bottom left –No2, Top right-No3, Bottom right- No 4 [13]

Penner and Robertson [13] studied the jet pattern emerging out from each of the pore types by study of photographs of each of the four pore types at flow corresponding to Reynolds number 400. The photographs help in estimating the jet widths, which were then plotted on the projection drawing.

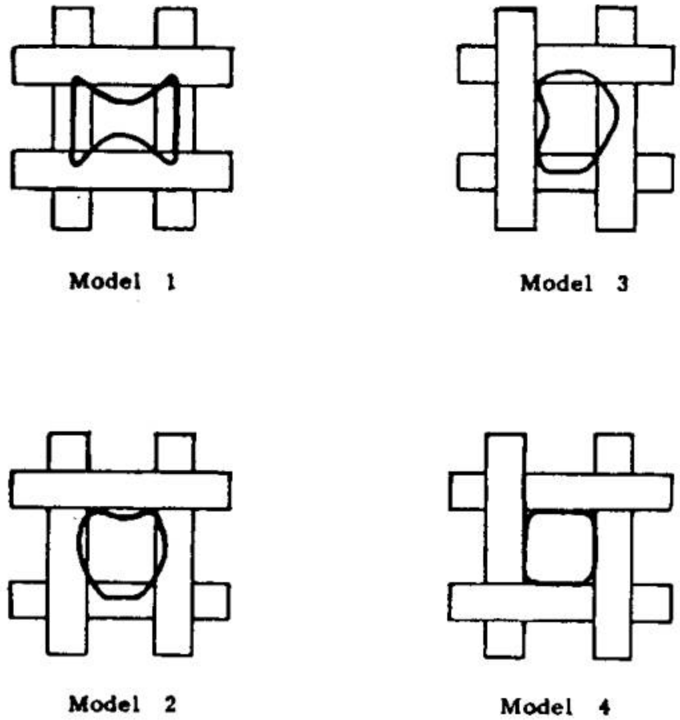

Figure 2. 17: minimum jet cross sectional areas of the four models at Re=400. Flow is normal to and out from the plane of the paper. [13]

Figure 2.17 shows the resulting minimum jet cross sectional areas obtained for each unit cell with the help of this method. From Figure 2.17 we can see that construction of the pore has a significant effect on the performance of each pore type and projected area or diameter/ pitch ratio have low or no effect on it [13].

Penner and Robertson [13] found out from their research that the jet areas of models No.1 and No.3 (most common type in sateen/satin weave fabrics) is approximately 30% higher than model No. 4 (plain weave pore type). Since the % open area of models No. 1, 2 and 3 is greater than model No. 4 they offer considerably less resistance or correspondingly greater porosity. For all other weave except plain weave, the projected area of the jet is smaller than the effective pore area and also the area available for the passage of fluids becomes lower than the minimum pore area proposed by Backer [10] due to the contraction of the jets at high Reynolds number [13].

Lu and Tung [14] have also studied the flow of fluids through the fabrics. They studied the flow pattern in 4 basic models, which were proposed by Backer [10] for his studies. They used fluid flow software called FLUENT for their flow analysis. Their study is similar to one done by Penner and Robertson [13] by using the tracer technique, the difference is the use of computer software. The software helps in getting the results of the flow pattern and resistance to flow in the interstices in the form of numerical solution [14]. The results of their studies vindicate the results obtained by Penner and Robertson [13] that plain weave gives the highest fluid flow resistance and satin weave has the lowest with the same thread count.

2.2 Porosity

Porosity is defined as the "Ratio of the two projected geometrical area of the opening across the material to the total area of the material"[15]. It is also defined as the "ratio of the void to the total volume"[16]. It is a complement of solidity.

Hsieh [17] defines porosity (P) as

$P=1-\rho_a/\rho_b$,

Where ρ_a= fabric density g/cm^3,

ρ_b= Fiber density g/cm^3.

Fabric density ρ_a is calculated by dividing the fabric weight per unit area (g/cm^2) by fabric thickness (cm).

Shinkle [18] defines porosity as the "ratio of air space to the total volume of the fabric expressed as %". He used the volume of the fabric estimated from length, width and thickness of the fabric and specific gravity of the component fibers for the porosity calculation.

$$P = \frac{100(AT - W/D)}{AT}$$

P= porosity of the fabric

A= Area of the specimen (cm^2)

T= Thickness of the specimen (cm)

W= Weight of the specimen in standard conditions (g)

D= Specific gravity or density of the fiber (g/cm^3)

Porosity can also be calculated from the projected geometrical area of the opening across the material.

Porosity = open pore area / Total area

$$= \frac{P_1 P_2}{(P_1 + d_1)(p_2 + d_2)}$$

P_1= Distance between warp threads

P_2= Distance between weft threads

d_1= Diameter of the warp yarn

d_2= Diameter of the filling yarn

Total and effective porosity:

Sieminski et al [20] defines total porosity as the entire void space of the material with no reference to its openness to the flow of fluids. With regarding to fabrics, inter yarn, inter fiber and intra fiber spaces all contribute to the total porosity

He also defines effective porosity as the void space available to the fluid flow. This is mainly due to the inter yarn space, but with fabrics made of different fibers inter fiber space also plays a major role.

Hsieh [17] studied the importance of intra fiber porosity in the overall porosity of the fabric. He found out from his studies that the porosity and liquid transport efficiency differ significantly between fabric samples that have nearly identical weight, thickness, weave type and fabric count but with different fiber density.

Burleigh et al [21] classifies the total porosity of the fabric in to three components

1. Inter yarn porosity
2. Inter fiber porosity
3. Intra fiber porosity

Intra fiber porosity: It represents the void space contained within the fiber walls

Inter fiber porosity: It represents the void space contained between the fibers in the yarn.

Inter yarn porosity: It represents the void volume contributed by interstices between the yarns

Burleigh et al [21] stated that the inter yarn and the inter fiber porosity mainly contributes to the effective porosity. They also mentioned that the inter fiber and inter yarn porosity depends upon fiber fineness, fiber shape, type of weave number of thread density and yarn twist.

Kullman et al [22] studied the relationship between air permeability and inter fiber porosity or the void volume within the yarn. For this purpose they made fabrics with five different yarn constructions, which are ring spun, no-twist, open end, cover spun and a twisted core wrapped yarn. Of these fabrics they found out that the fabric made of twisted core wrapped yarn produces the greatest air permeability while fabrics from twistless yarn had the lowest air permeability. They mentioned that the low air permeability of the twistless yarn fabric was because of the inherent yarn flatness and since there is no twist the fibers in the yarn spreads out in the fabric after processing resulting in smaller inter fiber pores.

2.3 Geometry of fabric as a function of uniaxial fabric strain

The geometry of fabric changes when strain is applied to the fabric. The change in the geometry of the fabric is due to various mechanisms of fabric deformation under the influence of uniaxial and biaxial stress. The mechanism includes yarn consolidation (diameter decrease), yarn flattening, yarn bending, fiber rotation, fiber extension and fabric shearing [15, 16].

Realff [24] explained regarding the various changes in the yarn geometry occurring during fabric deformation in uniaxial tensile loading. For the experimental purpose she constructed various plain weave fabrics with yarn count and yarn structure (Ring and rotor) as variables. She performed ravel strip uniaxial tensile tests on the samples using an Instron at constant rate of displacement. She captured the images of the fabric with the help of high magnification video camera. By this way the changes in the yarn and fabric geometry within the plane of the cloth was observed. In order to observe the changes in the curvature and cross section of the yarns during fabric deformation, she used an encapsulation technique similar to that used by Zageil [23]. Figure 2.18 shows a typical stress-strain curve for 36 in^{-1} x 30 in^{-1} fabric constructed with a 16.7 tex rotor spun yarns.

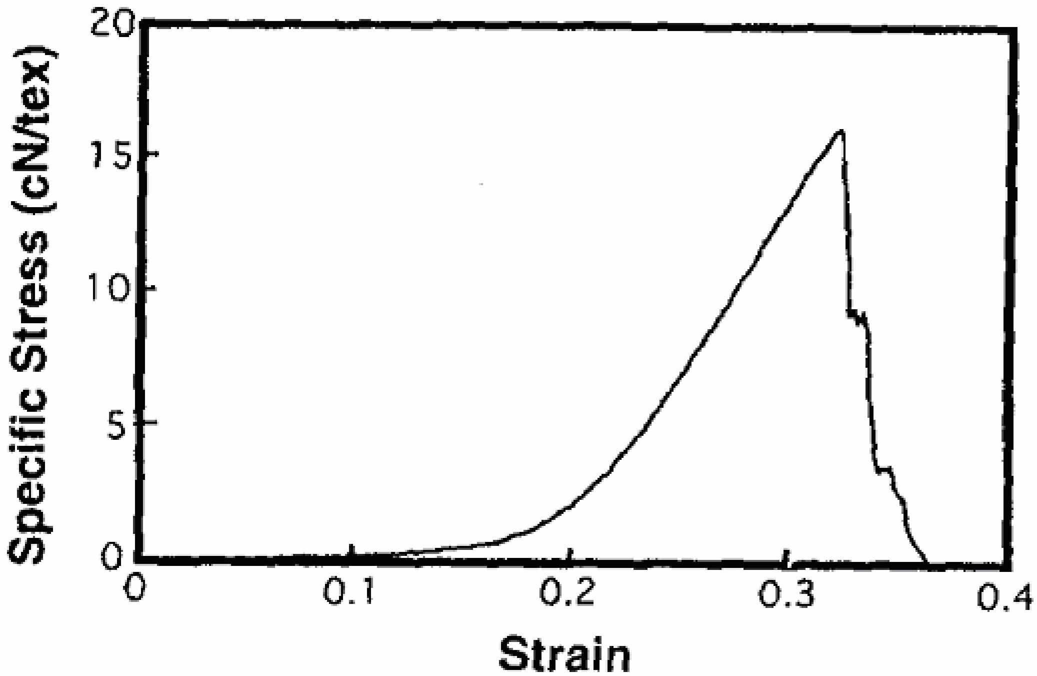

Figure 2. 18: Stress-strain curve of fabrics from rotor spun yarns [24]

The initial low modulus region in the curve is due to the crimp removal in the test direction and as the test progresses the amount of crimp decreases and the fiber themselves begin to extend. This can be seen in the final region of the curve. In the final region of the curve the load extension properties of the cloth is determined by the load extension property of the yarns used in the fabric [24].

Based on the experimental results Realff [24] identified yarn consolidation (diameter decrease), yarn flattening, yarn bending and fabric shearing as potentially important factors in influencing the fabric deformation and failure. Realff [24] mentioned that the shearing behavior of the fabric depends on the yarn frictional properties and normal forces at the yarn cross over points and the fabric made with yarns having high friction coefficient or high forces at the cross over points will undergo less shearing than the one made with yarns having low friction coefficient or low forces at cross over points.

Yarn consolidation and crimp interchange:

Realff [24] explained the changes in the yarn geometry when the fabric is subjected to uniaxial tensile loading with the help of series of fabric cross sectional images taken at various strain levels as shown in Figure 2. 19.

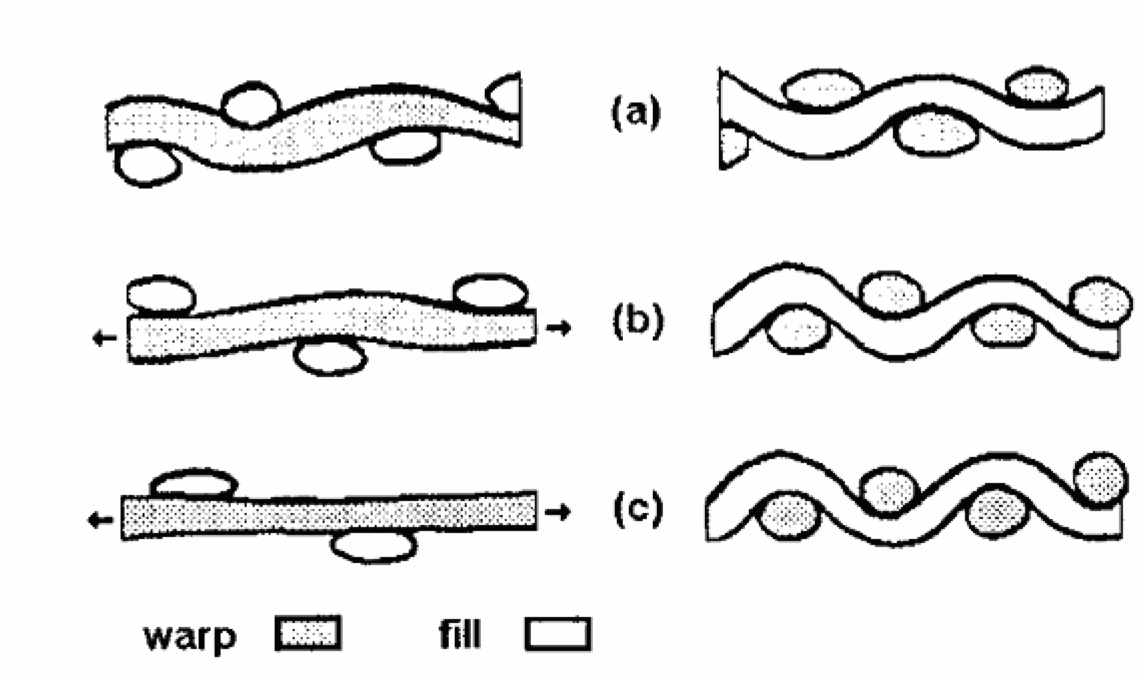

Figure 2. 19: Fabric cross sectional images taken at various strain levels (a) 0%, (b) 6.6% (c) 11% of a plain weave fabric (72 in^{-1} X 60 in^{-1}) constructed of 16.7 rotor spun yarns [24]

When uniaxial load is applied to the fabric, crimp interchange occurs. During the crimp interchange the amount of crimp decreases in the loaded direction and increases in the cross direction. The crimp interchange is responsible for the initial low resistance portion of the fabric stress-strain curve, extension of this region and hence fabric elongation to failure depends on the original amount of original crimp in the fabric. Thus by altering the original crimp in the fabric, the duration of crimp interchange mechanism can be changed. When the amount of uniaxial stress is increased the yarns in the loading direction straightens further and the diameter of the yarns decreases (consolidation) and become more circular in cross section. The yarns in the cross direction undergo more flattening and the amount of crimp increases. This can be seen in Figure 2.19 and 2.20.

Figure 2.20 shows the changes in the cross section of the yarn and the changes in the relative crimp in a woven fabric.

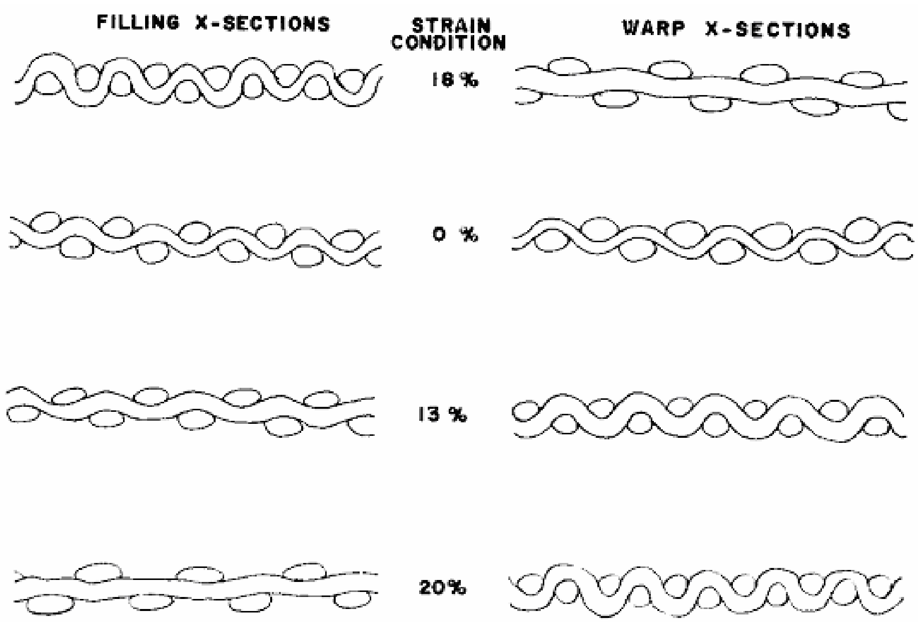

Figure 2. 20: Changes in the yarn cross-section and relative crimp in different strained condition [23]

At zero percent strain the fabric represents the original fabric configuration. The top section shows the geometrical changes taking place in the fabric when stress is applied the filling direction causing 18% strain. The third section from the top indicated a 13% strain in the warp direction. The bottom section represents the geometrical changes taking place in the fabric when the fabric is subjected to stress in the warp direction causing a strain of 20%. In case of the original fabric configuration the warp and the filling yarns have a fairly round cross section. In case of fabric with 18% filling strain, we can see that there is consolidation of filling yarns, which increases the roundness of yarn in the filling direction and have been brought in to the center plane of the fabric. The yarns in the warp direction tend to flatten out and assume a position of maximum crimp. In case of fabric with 13 and 20 % strain in the warp direction, the warp yarns consolidate and become round, while the filling yarn gets flattened out and assume a position of maximum crimp. In case of the figures in the bottom row of sections we can see that the warp yarns have not fully moved down to the center plane of the fabric, this is because of the jamming of the filling yarns which interlace around them.

When the fabric is subjected to a biaxial stress such that the tension applied on the warp and the filling are same, both the warp and the filling will be subjected simultaneously to forces tending to increase roundness and flatten the yarn. In case of biaxial loading it is difficult to predict which tendency will dominate. When the fabric is stretched biaxially, the load is buildup on one direction (either the warp or the filling direction) before it is put up on the other. The yarns in the direction in which the load will build up first will become round and compact while the yarns in the other direction which are loaded at a later time will start from a flattened configuration to reach an equilibrium cross section to reach a balance between the axial tensile effects and lateral compressive effects. The influence of the biaxial loading on the fabric geometry can be seen in Figure 2. 21.

Figure 2. 21 shows the geometry of the fabric under different levels of biaxial and uniaxial stresses, which are actually traced from photographs taken of materials stressed or strained and then surrounded by hard embedding plastic.

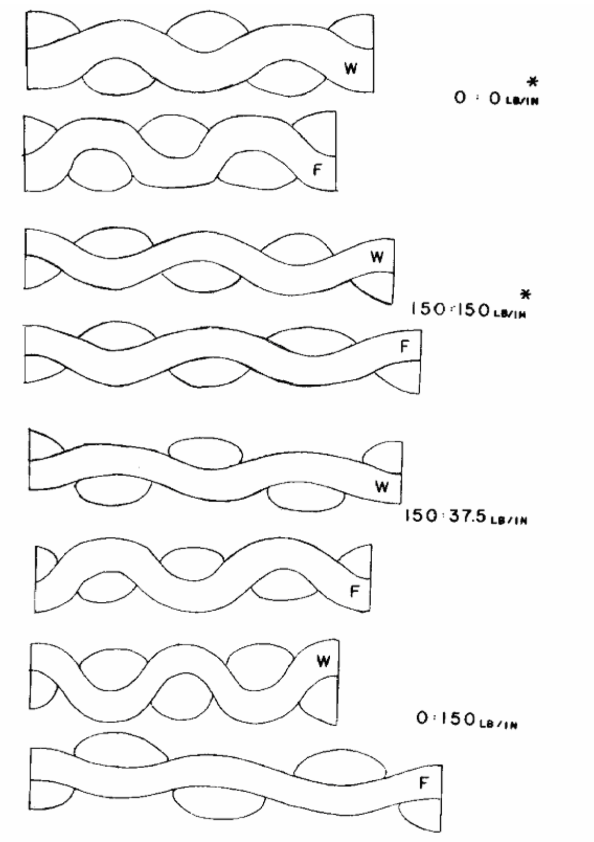

Figure 2. 21: Changes in the geometry of the fabric under different level of biaxial and uniaxial stresses [23]

In the zero stress condition, the warp yarn and the filling yarns assumes positions of maximum crimp, with filling yarns having slightly higher crimp than the warp yarn. When stress of 150 lb/in is applied in both warp and the filling direction, the cross section of both warp and filling yarns flatten out and at the same time the yarn elongates in both warp and the filling directions. We can see that the filling yarn whose crimp level is slightly more than the warp yarn elongates slightly more than the warp yarn.

When the fabric is subjected to different level of stress (150 lb/in in the warp direction and 37.5 lb/in in the filling direction) , the extension of the warp yarn dominates over the filling yarn and the warp yarn cross section becomes round while the filling yarn cross section becomes slightly flatter.

When the fabric is subjected to a uniaxial stress of 150 lb/in in the filling direction, the filling yarn elongates to a great extent and becomes rounder in cross section and the warp yarn gets flattened out.

Yarn flattening:

The yarns get flattened under the influence of uniaxial and biaxial strain applied on the fabric. The assumption that the yarn is round will not hold under these circumstances. The normal force between the yarns during the weaving process results in yarn flattening and distortion of yarn cross-section in the resulting fabric. The cross section of the yarn is also greatly influenced by the surrounding fabric matrix.

The flattening effect on the yarn is influenced by the amount of twist in the yarn. When the amount of twist is increased the yarns will form harder, rounder bundles of fibers, and these yarns will have fewer tendencies to flattening and distortion resulting from pressures in the fabric matrix. On the other hand the lower twisted yarns where the fibers are loose will act more in fluid manner and will try to fill the space in the fabric matrix.

Figure 2.22 shows the forces acting on a plain weave fabric.

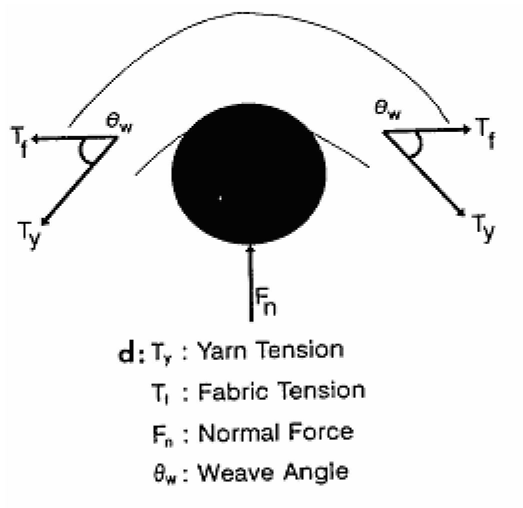

Figure 2. 22: Forces acting on a plain weave fabric [24]

The normal pressure exerted by the warp yarn on the filling yarn and vice versa will be increased significantly when the fabric is subjected to uniaxial or biaxial stress. This increase in normal pressure will lead to distortion of the yarn cross section. When the stress is increased further the normal pressure exerted by one set of orthogonal yarns over the other set increases and the individual yarn section will tend to flatten further, simultaneously the added tension in the yarn will tend to form it into a rounder section.

The pore shape of the fabric changes when it is subjected to uniaxial and biaxial stress. Figure 2.20 shows that when uniaxial strain is applied on the fabric yarns get elongated, which tends to open up the structure of the fabric and thereby increasing the pore size. This phenomenon of increasing pore size is very important in case of fabrics for the parachutes or filters.

Figures 2.23 and 2.24 show the sliced serial sections of a biaxially stressed parachute fabric before and after subjection to a stress of 100 lb/in in both warp and the filling directions.

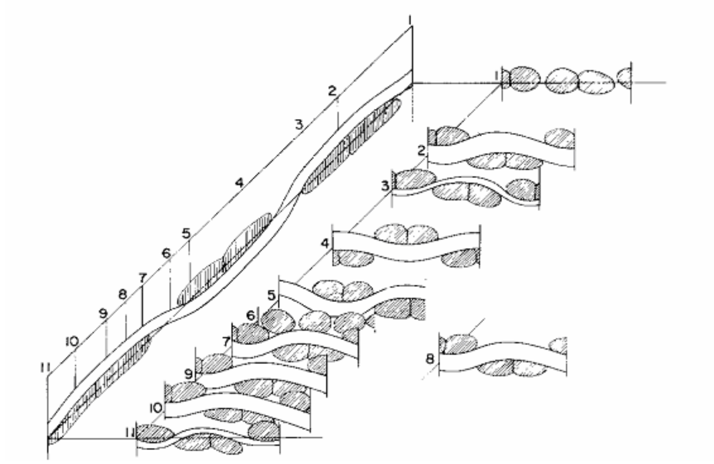

Figure 2. 23: Sliced cross sections of a parachute fabric before subjected to a biaxial stress of 100lb/in [23]

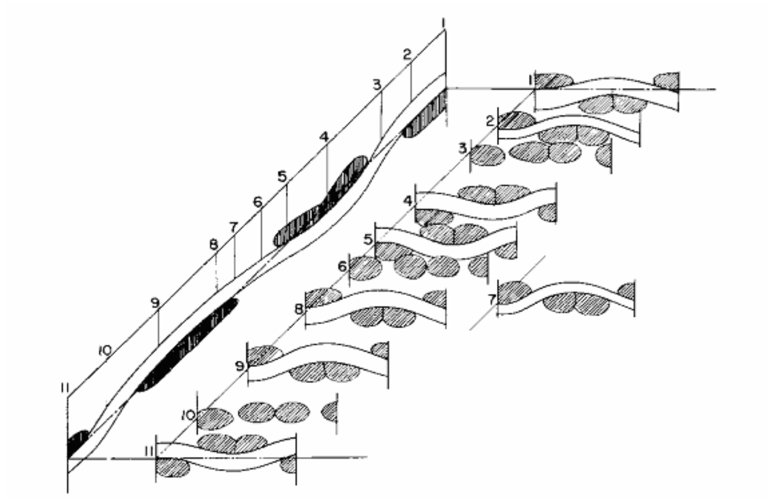

Figure 2. 24: Sliced cross sections of a parachute fabric after subjected to a biaxial stress of 100lb/in [23]

The changes in the yarn geometry and the pore geometry can be analyzed with the help of these sections, which is very important in the mechanical applications for parachute fabrics [27].

Fabric jamming:

In some cases, when the fabric is subjected to uniaxial strain application, the yarns in the loading direction do not straighten fully and will not come to the center of the fabric as

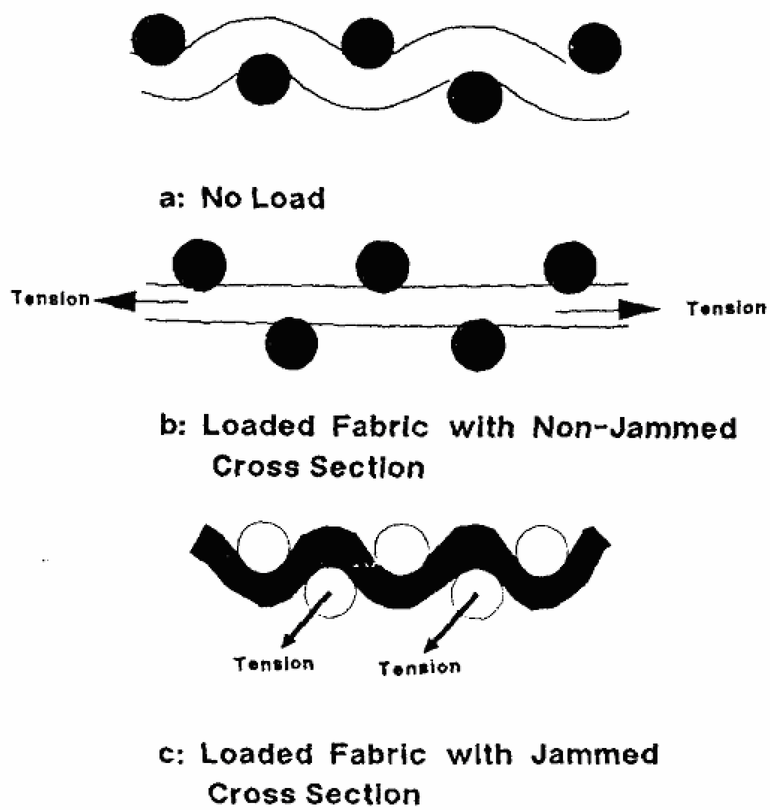

Figure 2. 25: Yarn deformation process in the plain weave fabric structures during uniaxial tensioning [25]

shown in Figure 2.25 (c). This is because of the insufficient cross yarn length per unit cell of the weave. The loaded yarn becomes straight as shown in Figure 2.25 (b) in case of fabrics having the sufficient cross yarn length per unit structure [25].

The behaviors of the fabric woven with ring and rotor spun yarns when subjected to uniaxial fabric strain were different. The fabric woven with ring yarn, which when subjected to uniaxial stress has more isolated breaks and larger disruption zone than the fabric woven with rotor spun yarn. The difference in the friction coefficient between the ring and the rotor yarn is responsible for the above-mentioned trend. The friction coefficient of the ring spun yarn is lower than the rotor spun yarn. The difference in yarn strength distribution for these two types (ring and rotor) of yarns is also a reason for the above-mentioned trend. The rotor yarns have lower variance than the ring yarns [24].

The type of the yarn used also influences the amount of crimp in the fabric. The fabrics woven with ring spun yarn have higher crimps than the fabrics made with rotor spun yarn. This is because of the bending behavior of the tow types of yarn. Because of the higher crimps, the stress strain response of the ring-spun fabrics has a larger crimp interchange regime [26].

The geometry of the fabric is also influenced by the weave texture and number of yarns per unit length in each direction [24]. Figure 2.26 shows the cross section of two sets of fabric having different pick density but with same warp.

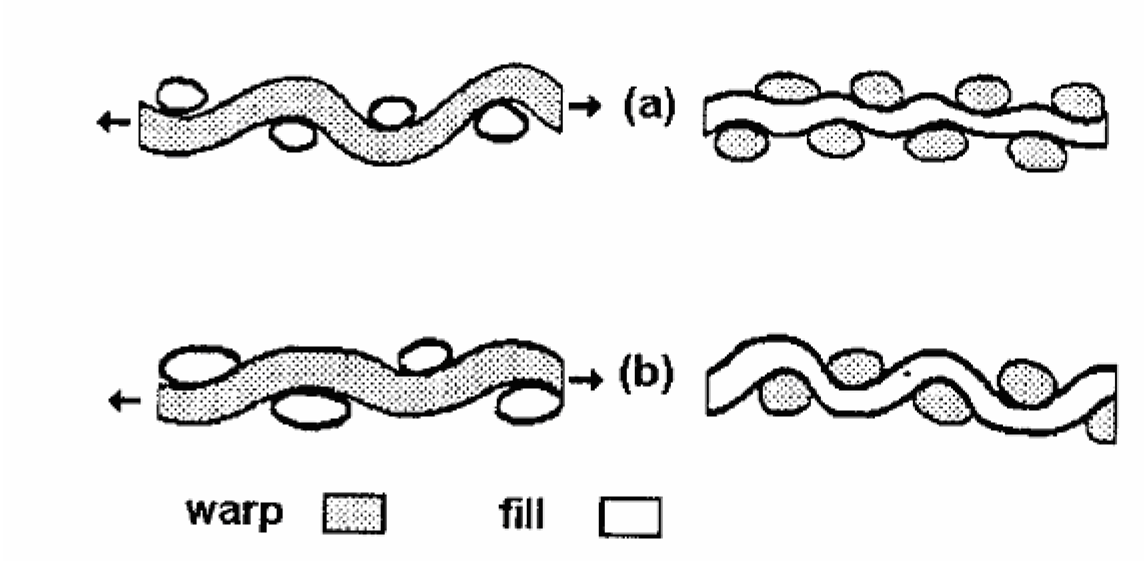

Figure 2.26: Geometry of fabrics (before loading) woven with 61.3 tex ring spun yarns (a) 72 in^{-1}x $30in^{-1}$ and (b) $36in^{-1}$x$30in^{-1}$ [24]

From Figure 2.26 shows the change in geometry of the fabric. As the geometry of the fabric changes the stress strain behavior of the fabric also changes. Figure 2.27 illustrate this. The fabric with the highest pick density (72 in^{-1}x 30 in^{-1}) (i.e. the fabric which has largest amount of initial crimp) has the largest crimp interchange region and highest elongation to failure and vice versa.

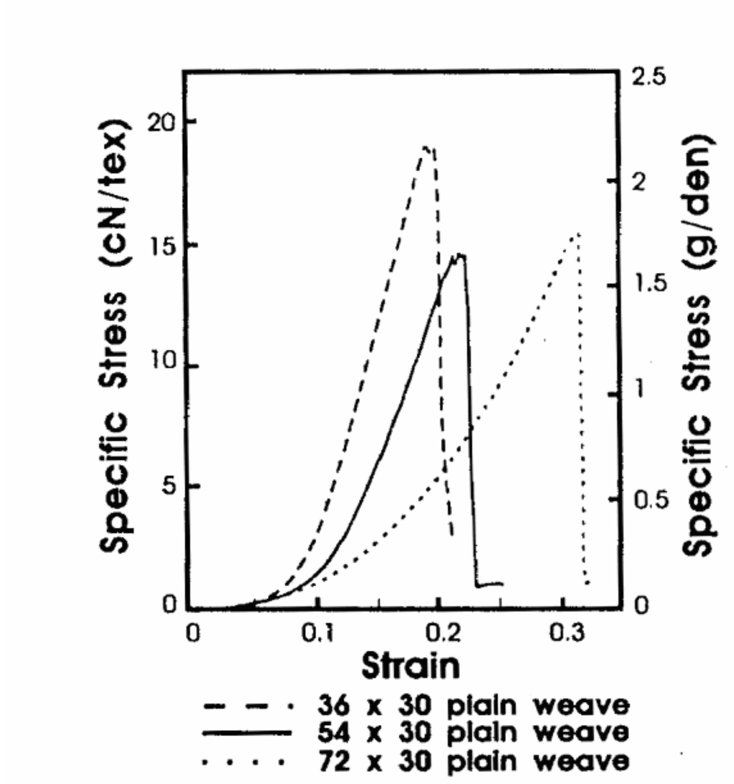

Figure 2. 27: Stress strain behavior of fabrics with different pick densities [24]

3 RESEARCH OBJECTIVE

Studies have been conducted separately on the two topics "the behavior of fabric air permeability in terms of fabric construction parameters" and "the influence of tensile strain on the fabrics geometry." But influence of strain on the air permeability of the fabrics has not been studied so far. The objective of this research is to provide basic understanding of the air permeability behavior of fabrics with elastomeric constituents when subjected to different levels of strain. The research also helps in understanding the effect of fabric parameters on the air permeability behavior of the fabrics. These studies will lead to better understanding and designing of active functional fabrics for technical applications such as parachute, sailcloth, and windscreens. One way to activate fabrics is the use of electroactive materials. Activating such material by electric volt (or current) causes fabric geometrical change and hence the porosity of the material can be changed actively. The Electroactive material may be shape memory alloy (SMA), electro active polymers (EAP) etc. Elastomeric fabrics (Fabrics employed with elastomeric material either in the warp or the filling or both directions) are ideal for the electro active fabrics because those fabrics can be activated with minimum force when compared to standard fabrics. Thus with a small force/large strain electroactive material incorporated in the woven fabrics of elastomeric components could be easily strained and consequently fabric air permeability could be widely varied as a result of fabric geometrical changes.

4 EXPERIMENTAL

In order to study the air permeability behavior of the fabric under strained conditions a device, which can impart desired level of strain in the fabric, and hold it in such state is greatly needed.

4.1 Design and construction of fabric straining device

The device consists of two platforms (fixed and movable) and a threaded rod, which passes through the grooves in the fixed and movable platforms as shown in Figure 4.1. When the handle, which is attached to one end of the threaded rod is rotated the movable platform moves away from the fixed platform. Guide rods, which are fixed to the movable platform, pass through the slots in the fixed platform. These guide rods helps in avoiding lateral movements of the moveable platform. Four bolts are attached to the fixed platform and two to the movable platform as shown in Figure 4. 1. The purpose of the bolts is to support the top and bottom clamps (Figure 4. 2), which holds the fabric to be strained in between them.

The fabric to be tested is placed over the frames of the fixed and the movable platform Figure 4.3b. Then top clamps are placed over the bottom clamp in the fixed platform and in the movable platform. Wing nuts are used to hold the clamps together. By this way the fabric is gripped between the clamps in the fixed and the movable platform Figure 4.3c. After gripping the fabric in between the two frames the handle, which is attached to the threaded rod is rotated causing the movable platform to slide in the horizontal axis there by causing uniaxial strain in the fabric Figure 4. 3d. Based on the rotation given to the handle the distance moved by the movable platform and hence the amount of uniaxial strain applied to the fabric can be varied. After the fabric is strained to the required level another set of top clamps are placed over the bottom clamps in the fixed platform to hold the fabric in the strained state as shown in Figure 4.3e. Then the top clamps are removed from the movable platform (Figure 4.3f) so that the fabric in the strained state can be taken from the device. Now the frame holding the strained fabric can be taken out from the fabric-straining device for fabric air permeability testing Figure 4. 4. Thus the fabric-straining device helps in straining to fabrics to the required level and holds it at that state until tested.

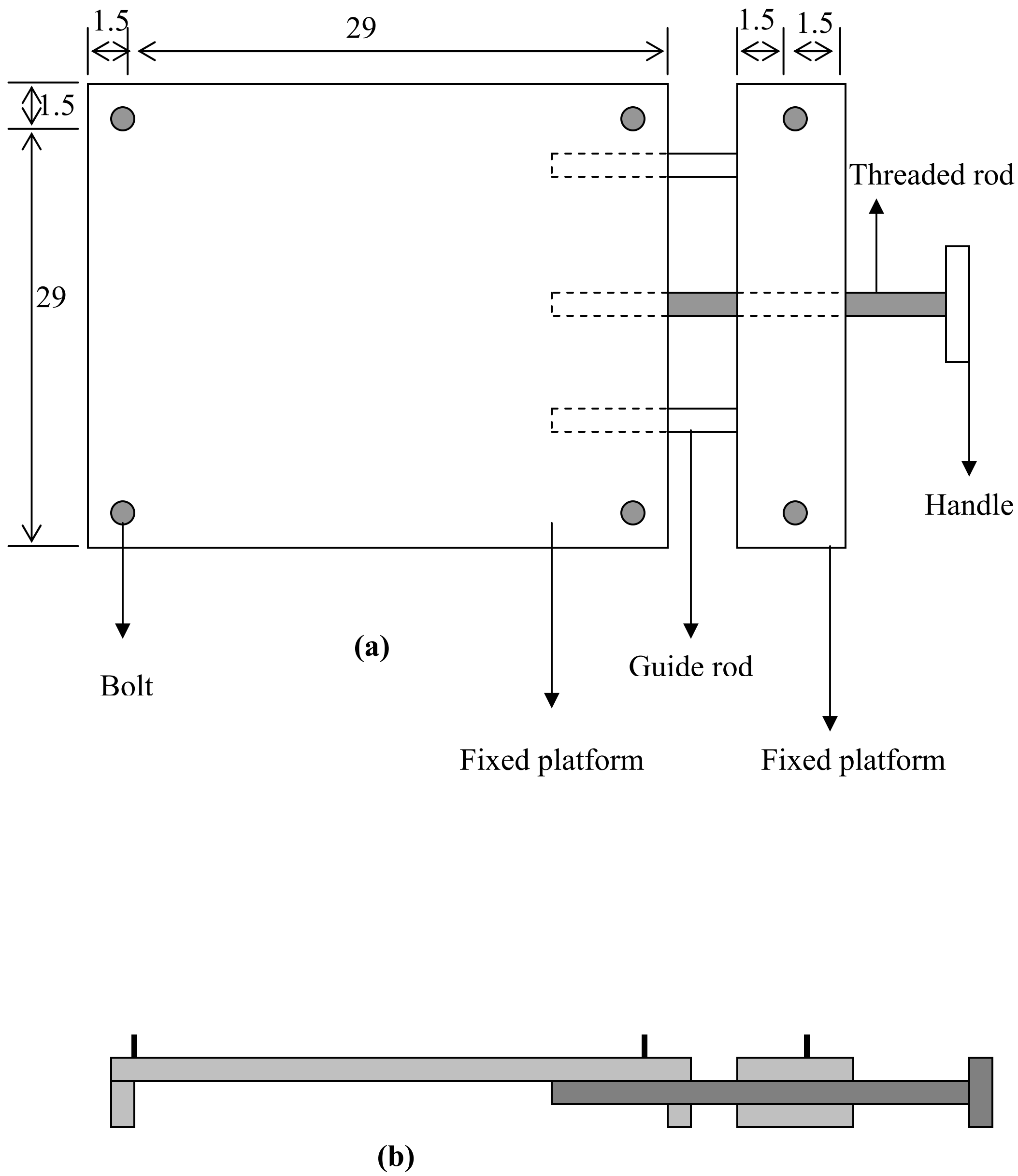

All Dimensions in cm

Figure 4. 1: Fabric-straining device (Without frame) (a) PLAN (b) CROSS SECTIONAL ELEVATION

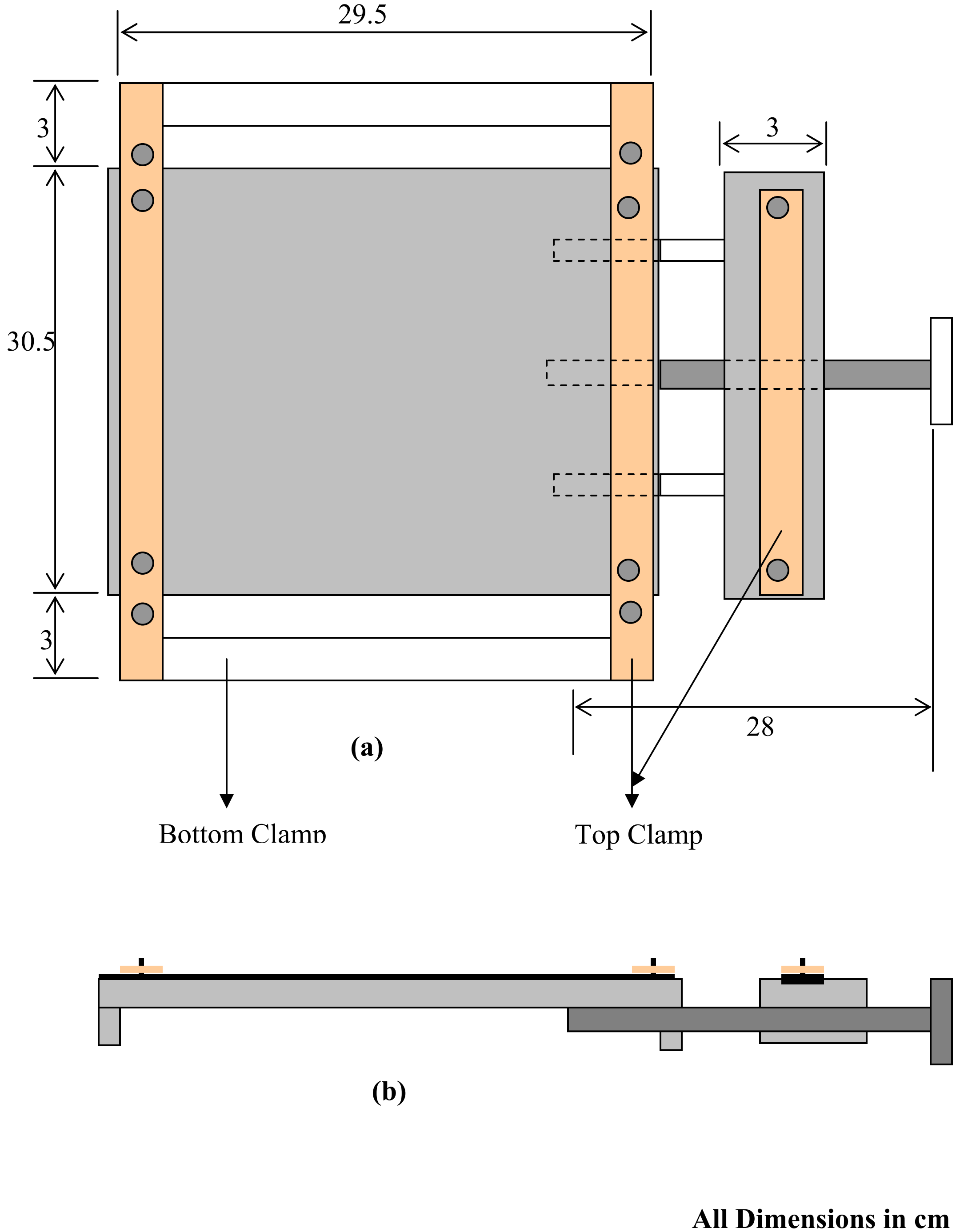

Figure 4. 2: Fabric-straining device (With frame) (a) PLAN (b) CROSS SECTIONAL ELEVATION

4.3a) Fabric sample and Straining Device

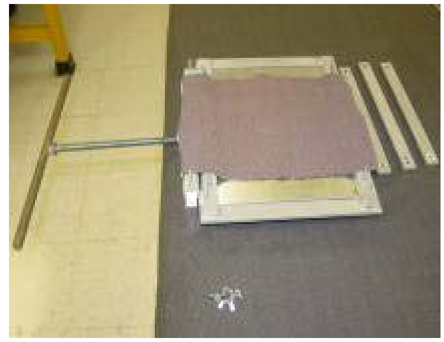

4.3b) Fabric sample placed on frames of platform

4.3c) Fabric sample gripped by clamps

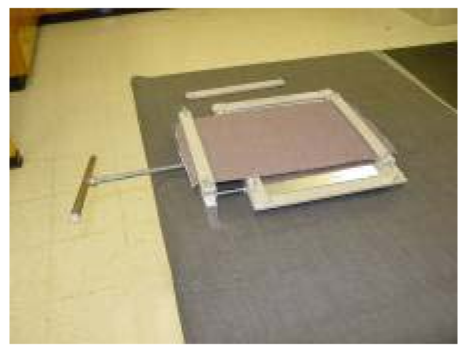

4.3d) Fabric sample strained by turning the handle

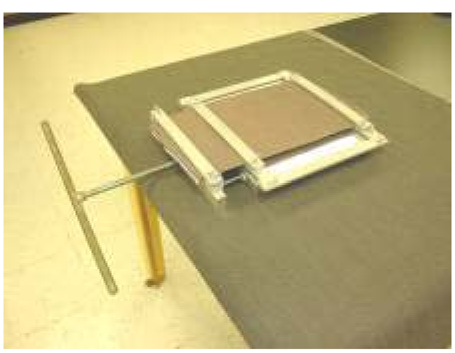

4.3e) Fabric sample held in strained state

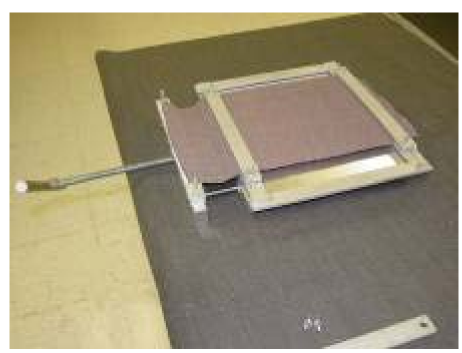

4.3f) Top clamp in the movable platform is removed

Figure 4. 3: Procedure of straining fabric in the fabric straining equipment

Figure 4. 4: Fabric in strained state ready to be taken to air permeability testing

4.2 Materials

The warp yarn used in this experiment is 253 Denier (g/9km) 100 % cotton yarn. The warp density is 104 EPI. The filling yarn used in this experiment was the Type 400 elastomeric yarn from DuPont.

Type 400 elastomeric yarn:

Dupont has come up with a new class of elastomeric yarn specially designed for applications that require stretch characteristic. The type 400 yarns are composed of a new kind of melt spun elastomeric fiber based on bicomponent technology in which two different polymers (PET and PTT) are joined together side by side as shown in Figure 4.5.

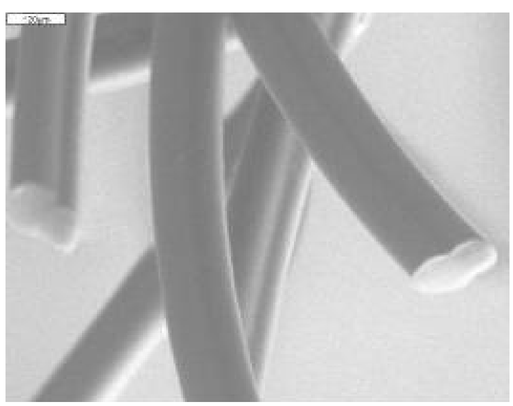

Figure 4. 5: Cross sectional image of Type 400 elastomeric yarn (Magnification of 400 x)

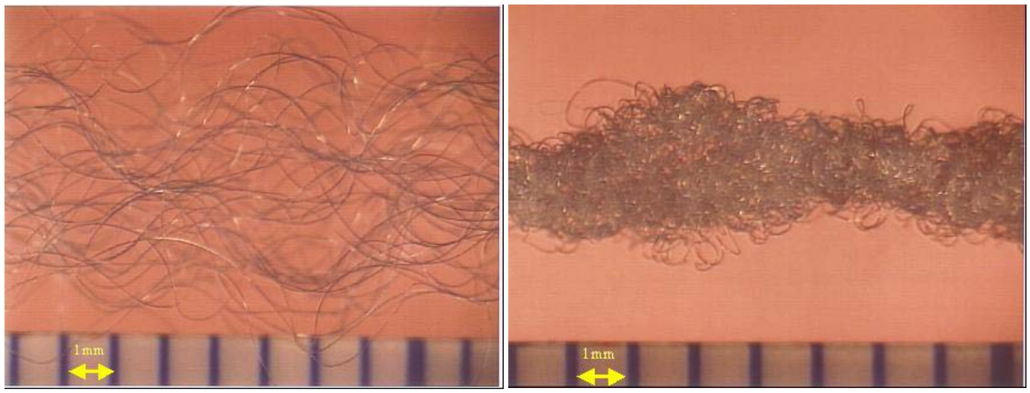

Figure 4. 6: optical Images of the Type 400 elastomeric yarn without heat setting (L) and with heat setting (R) at a magnification of 10x

The two polymers in each filament have differential shrinkage properties. Since the shrinkage properties are different, the filaments when exposed to heat produce a smooth helical crimp in it (Figure 4.6(R)). These naturally imparted crimp improves the stretch recovery property of this type of yarn when compared to the yarns in which crimps are introduced mechanically. The durability of these crimps are also better than those which are introduced mechanically. The regularity of these naturally formed crimps improves the aesthetic property of the fabric in which these yarns are used. The type 400 can be used either as a warp or filling and can be combined in a fabric with any natural or synthetic yarn available in the market.

4.3 Experimental Variables

The following four variables were used for the experimental design.

1) Yarn count

2) Type of weave

3) Fabric tightness

4) Uniaxial tensile strain applied during testing

Yarn Count:

Count of a yarn indicates the relationship between the weight and length of the yarn. Three different linear densities of the Type 400 yarns were used as filling yarns. They are

Table 1: Yarn count and number of filaments

Count (Denier)	Number of filaments	Denier per filament
152	68	2.235
303	68	4.456
615	136	4.522

Type of weave:

Three different types of weaves were used in this experimental design – Plain, 2x2 Twill, and 2x2 Basket as shown in Figure 4.6.

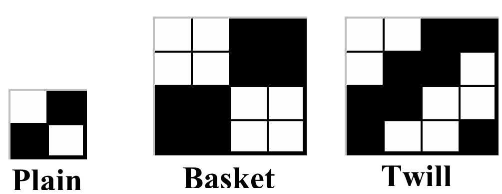

Figure 4. 7: Weave design of plain, 2x2 basket and 2x2 twill

Fabric Tightness:

The degree of tightness for a given fabric is a measure of how the warp and the filling yarn are closely woven. Five levels of tightness were used in this experimental design. Basically tightness is defined as the ratio of cloth parameters to the corresponding parameters of a reference fabric. The fabric properties can be related to the tightness level in the fabric, which helps the designers to develop fabrics with certain performance. The fabric tightness also helps in constructing similar fabrics whose construction parameters may not be same.

In this experimental design Russell's tightness method is used. Definition of Russell tightness is given by Seyam [19]. Russell's tightness calculation involves the use of Ashenhurst's ends plus intersections theory for the calculation of the reference fabric. The tightness calculations are shown in Appendix 8.1.

Fabric Tightness calculation:

Two parameters are needed to calculate the fabric tightness: yarn diameter and weave factor.

Weave Factor:

Weave factor is a numerical value, which expresses the amount of interlacing of the warp and the filling yarns [19]. The warp and the filling weave factors can be calculated from the following equations.

$$M_1 = \frac{N_1}{i_1}$$

$$M_2 = \frac{N_2}{i_2}$$

Where

M_1 = Warp weave factor

M_2 = Filling weave factor

N_1 = No of warp ends per weave repeat

i_1 = No of filling intersections per weave repeat

N_2 = No of picks per weave repeat

i_2 = No of warp intersections per weave repeat

Yarn Diameter:

The diameter of the yarn is calculated with the help of the following formula [19]

Diameter of the yarn in inches = $\dfrac{1}{29.3\sqrt{\phi P_f N_{cc}}}$

ϕ = Packing factor

P_f = Fiber density

N_{cc} = Yarn count in cotton system

Russell's Fabric Tightness:

The maximum warp ends per unit fabric width and maximum picks per unit fabric length can be calculated with the help of Ashenhurst's ends plus intersections theory [19].

$$t_{1max} = \frac{M_1}{M_1 d_1 + d_2}$$

$$t_{2max} = \frac{M_2}{M_2 d_2 + d_1}$$

t_{1max} = Maximum warp ends per unit fabric width

t_{2max} = Maximum picks per unit fabric width

d_1 = Diameter of the warp yarn

d_2 = Diameter of the filling yarn

Fabric tightness can be calculated using the Russell's tightness [19]

$$C_f = \frac{t_1 + t_2}{t_{1max} + t_{2max}}$$

C_f = Construction factor

t_1 = End density t_2 = Pick density

Additional tightness can be used to express the warp and the filling tightness. These are

$$C_1 = \frac{t_1}{t_{1max}} \quad \text{and} \quad C_2 = \frac{t_2}{t_{2max}}$$

where C_1=Warp Construction factor and C_2= Filling construction factor

Uniaxial fabric strain:

About five levels of uniaxial strain were applied on each fabric. The uniaxial strain is applied with the help of specially designed fabric straining device, which was explained earlier.

Summary of the structures constructed:

The matrix shown in the Table 2 illustrates the 42 different structures produced. The three different weaves (Plain, Twill and basket) were employed. In each weave 14 samples were constructed with 5 different levels of tightness values for filling yarn counts 303 denier & 152 denier and 4 different level of tightness for filling yarn count 615 Denier. Because of the limitations in the weaving machine it was not able to weave fabrics with low tightness values with yarns having high denier, indicated by the blank spaces in the Table 2.

Table 2: Summary of structures constructed

Weave	Tightness		
	Filling yarn count (Denier)		
	152	303	615
Plain	0.566	0.567	
	0.614	0.608	0.611
	0.642	0.640	0.650
	0.676	0.697	0.690
	0.745	0.721	0.739
Twill	0.424	0.425	
	0.480	0.486	0.485
	0.506	0.516	0.515
	0.568	0.541	0.550
	0.650	0.668	0.654
Basket	0.423	0.424	
	0.481	0.480	0.485
	0.547	0.541	0.551
	0.620	0.614	0.625
	0.733	0.741	0.743

4.4 Processing:

Weaving:

Weaving was done on a PICANOL flexible rapier loom. The weavers beam contains a total of 7072 warp yarns and has a width of 68". Sixteen harnesses were used and the warp yarns were drawn in straight draft. The reed used was 26- dent reed (26 Dents per inch).

Weave Design:

Unstitched double cloth construction was used for weaving the three weaves (Plain, twill (2x2) and basket (2x2)). The reason why double cloth was constructed is because of the high thread density (104 Threads per inch) in the warp direction, which could limit the range of pick density that is required to cause the fabrics to possess significant shrinkage and stretchability. The preliminary trials conducted proved this. Splitting the fabric into two layers helps in increasing the % of elastomeric components in each layer of the fabric by increasing the space available between the warp yarns in each layer and the space available for the shrinkage of the filling yarns. Figures 4.8, 4.9 and 4.10 shows the design, chain plan and draw for the weaving of plain, twill and basket unstitched double cloth.

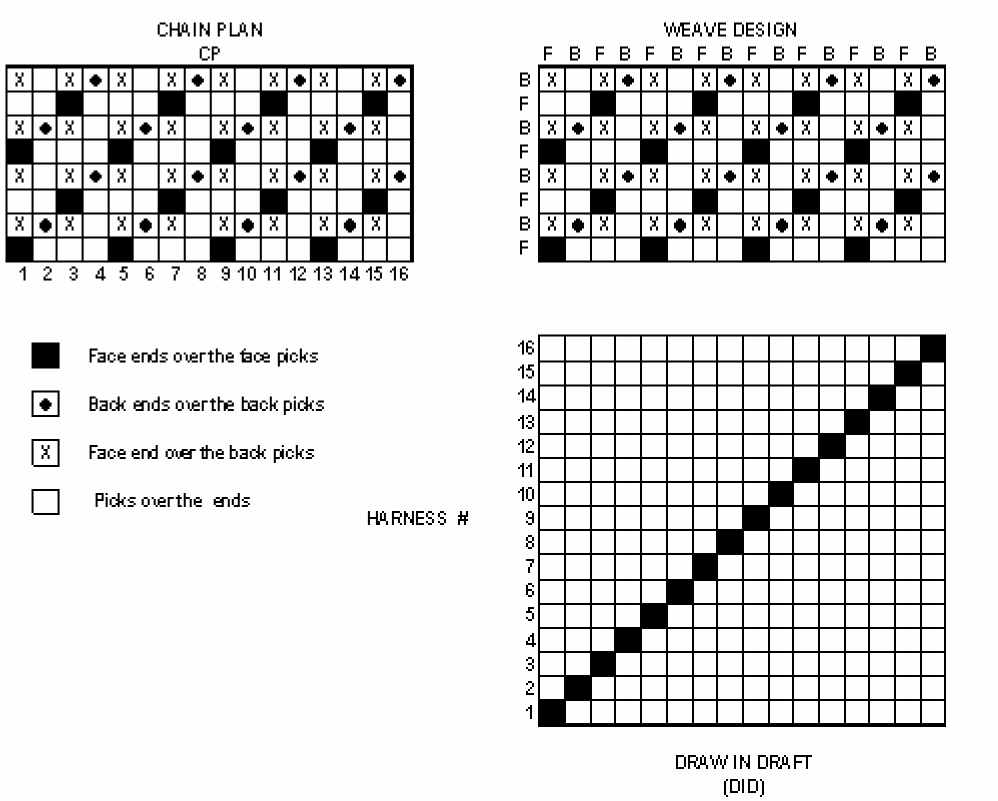

Figure 4. 8: Design, Chain Plan and draft for weaving double plain cloth

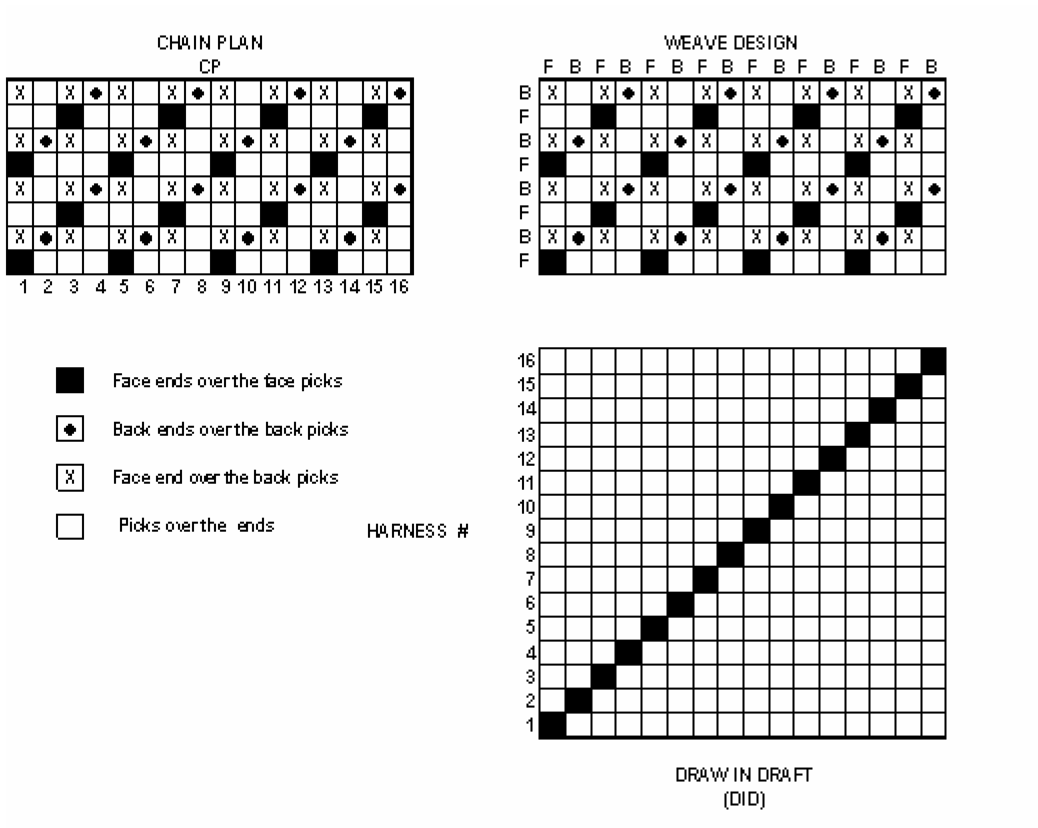

Figure 4. 9: Design, Chain Plan and draft for weaving double 2x2 twill cloth

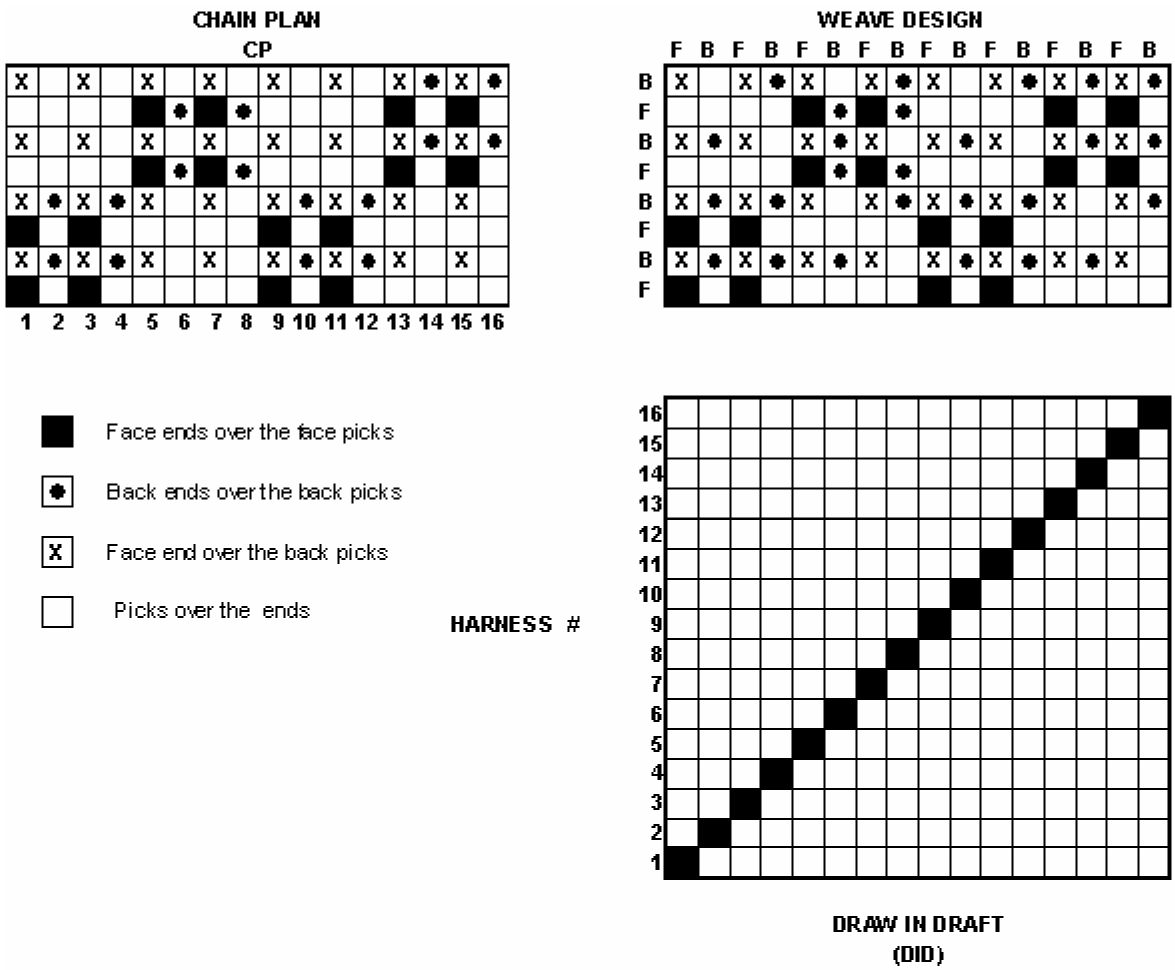

Figure 4. 10: Design, Chain Plan and draft for weaving double 2x2 basket cloth

Heat setting:

The purpose of heat setting is to develop stretchability to fabric in the filling direction. Swatches of woven fabrics were heat set by using a W. Mathis AG heat setting machine. The fabrics with suitable dimensions for air permeability test were pinned in the frames as shown in Figure 4. 11.

Figure 4. 11: Fabric pinned to the frame enters the heat-setting unit

The circulating rails attached to the machine helps in carrying the frames through the machine. The powerful circulating fans inside the machine helps in maintaining uniform temperature throughout. The temperature inside can be varied from 0 to 1000°C. The heat setting for these fabrics are done at 160° to 165 °C for 30 to 40 seconds as recommended by the yarn manufacturer (Dupont).

4.5 Testing and Evaluation

Air-permeability testing was done using a Frazier air permeability tester according to ASTM D737-99 test procedure. The fabric to be tested is strained with the help of the fabric straining device explained earlier and is taken to the Frazier air permeability tester (Figure 4. 12a).

The testing procedure in the Frazier air permeability tester is explained as follows

Mounting the fabric

The fabric in the strained state is placed over the test area and locked as shown in Figures 4.12b & 4.12c.

Selecting the right nozzle

Before starting the actual experiment the selection of right nozzle for a particular type of fabric is important. This is done by trial and error method. With machine switched on adjust the rheostat until the inclined monometer reads 0.5. The vertical monometer must reed between 3 and 13. If the reading is not between 3 and 13 open door to suction chamber replace present nozzle if necessary with proper size and close the door. Figure 4.13a shows the different sizes of nozzles and scales.

Air Permeability Measurement

After placing the fabric in the test area, the differential air pressure is created by adjusting the rheostat. When the required differential pressure is maintained, in our case it is 0.5 inches of water column, the reading in the right-hand monometer column is noted. Figure 4.13 b shows the position of inclined monometer, vertical monometer and reservoir. The noted value can be converted into air permeability reading (cubic feet per square foot per minute) with the help of conversion chart. Five tests are made for each fabric sample. Figure 4.13c shows the position of rheostat and suction chamber. Thus the air permeability of the strained fabric is measured. The tests can be repeated for other fabric samples with different strain levels imparted with the help of fabric straining device.

Figure 4. 12: a) Fabric in strained taken to Air permeability testing

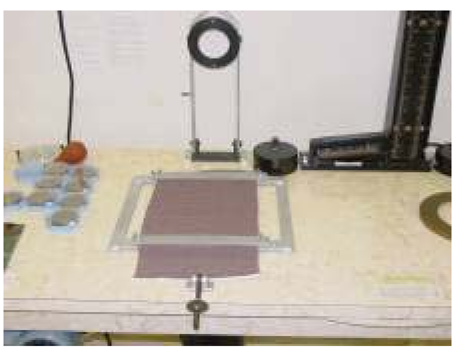

Figure 4. 12: b) Fabric sample in strained state is placed over the test area

Figure 4. 12: c) Fabric sample is held in position and locked

Figure 4. 12: Air permeability measurement procedure

Figure 4. 13a: Nozzles with different diameter

Figure 4. 13b: Position of rheostat and suction chamber

Figure 4. 13c: Position of reservoir, Inclined Monometer and reservoir

Figure 4. 13: Construction of air permeability tester

5 RESULTS AND DISCUSSION

5.1 Influence of strain on the air permeability of fabrics

Figures 5.1 to 5.9 show the air permeability behavior of the finished elastomeric fabrics under the influence of strain. We can observe from Figures 5.1 to 5.9 that for a finished elastomeric fabric woven with particular weave, warp and filling yarns and having particular in-loom fabric tightness, the air permeability increases with increasing strain with exceptions in Figure 5.2 marked by the oval. The reasons for these exceptions (initial decrease in air permeability with increasing strain) will be explained after explaining the behavior of the normal curves (increase in air permeability with increasing strain). The increase in air permeability of the finished elastomeric fabrics with increasing strain can be explained with changes occurring in the geometry of the elastomeric fabric structure with respect to strain.

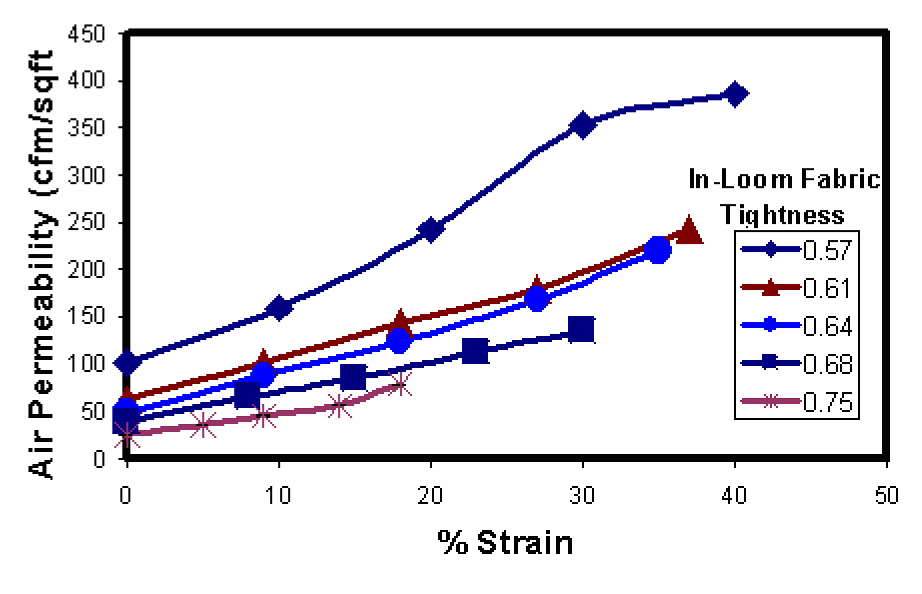

Figure 5. 1: Influence of strain on the air permeability of finished elastomeric fabrics (Plain weave, 152 D filling) woven with different in-loom fabric tightness

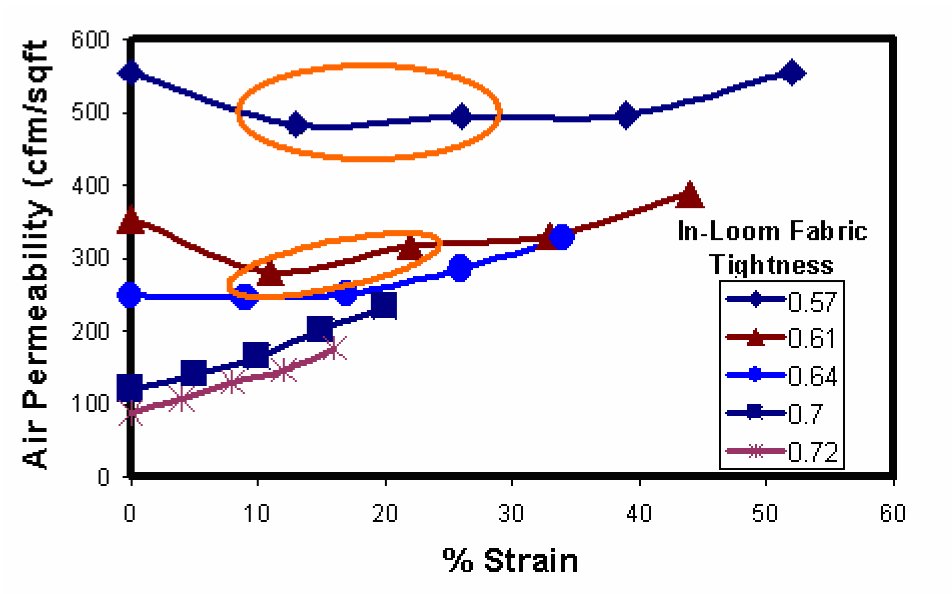

Figure 5. 2: Influence of strain on the air permeability of finished elastomeric fabrics (Plain weave, 303 D filling) woven with different in-loom fabric tightness

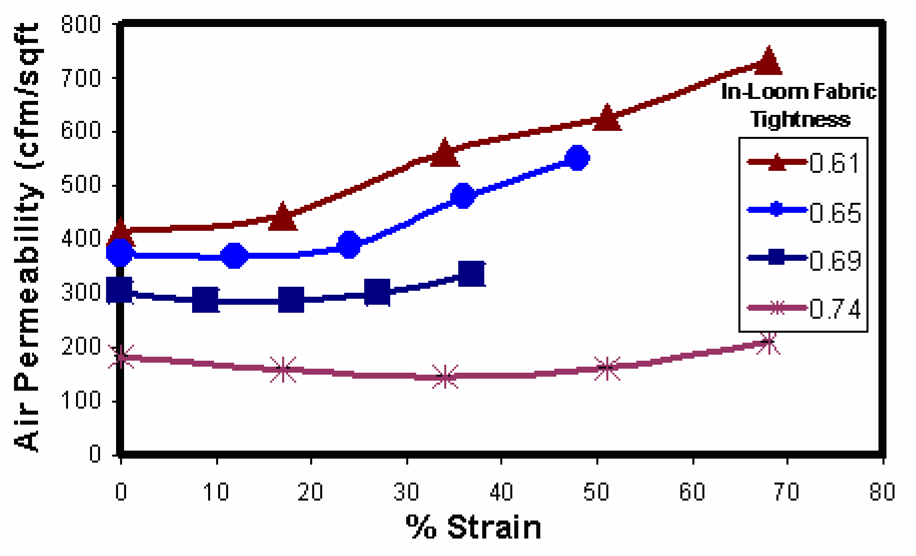

Figure 5. 3: Influence of strain on the air permeability of finished elastomeric fabrics (Plain weave, 615 D filling) woven with different tightness

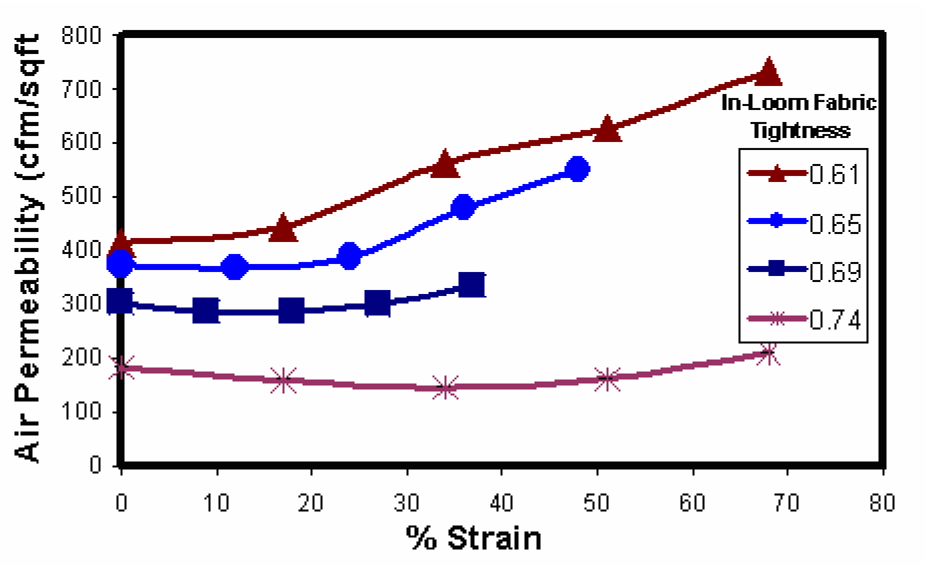

Figure 5. 4: Influence of strain on the air permeability of finished elastomeric fabrics (Twill (2x2) weave, 152 D filling) woven with different tightness

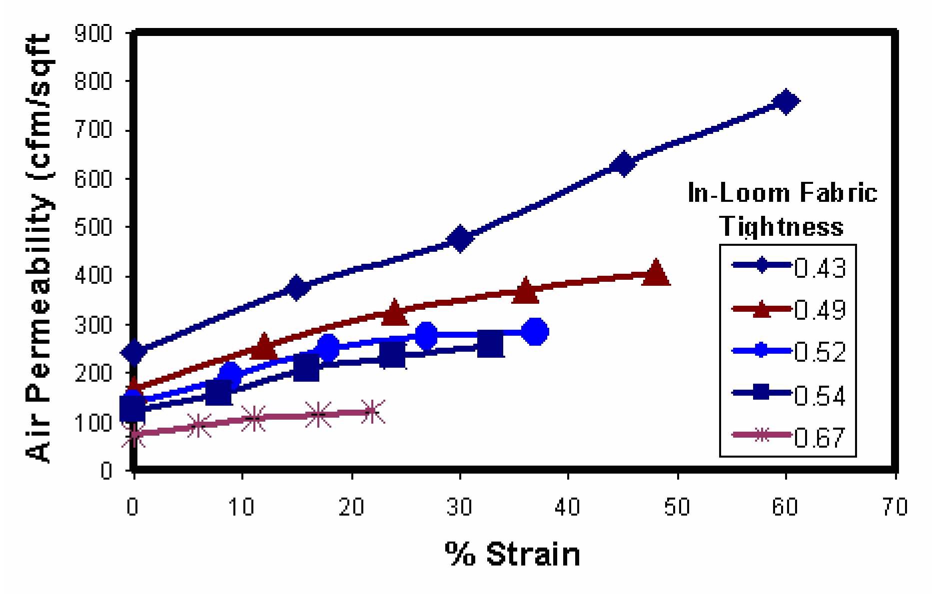

Figure 5. 5: Influence of strain on the air permeability of finished elastomeric fabrics (Twill (2x2) weave, 303 D filling) woven with different tightness

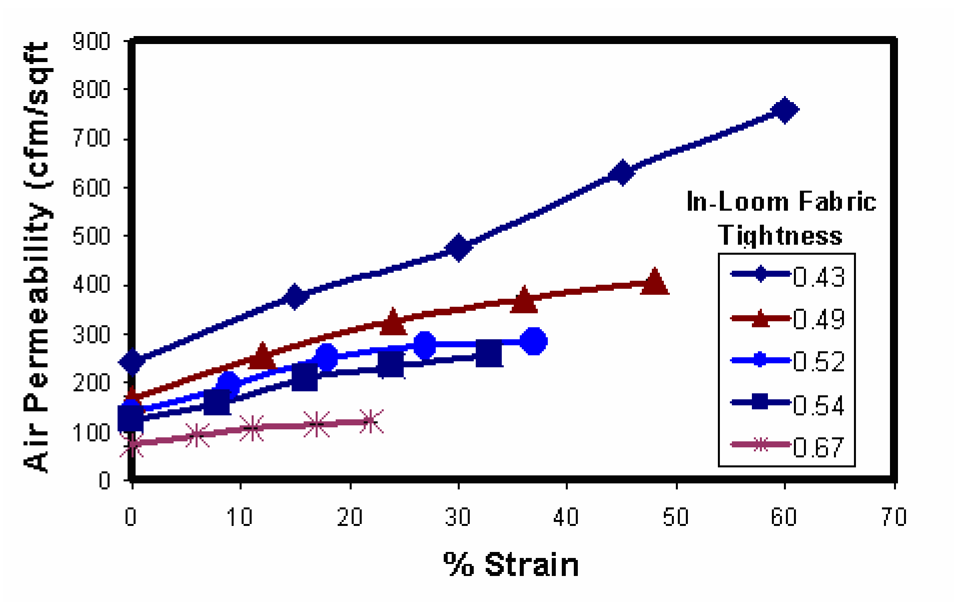

Figure 5. 6: Influence of strain on the air permeability of finished elastomeric fabrics (Twill (2x2) weave, 615 D filling) woven with different tightness

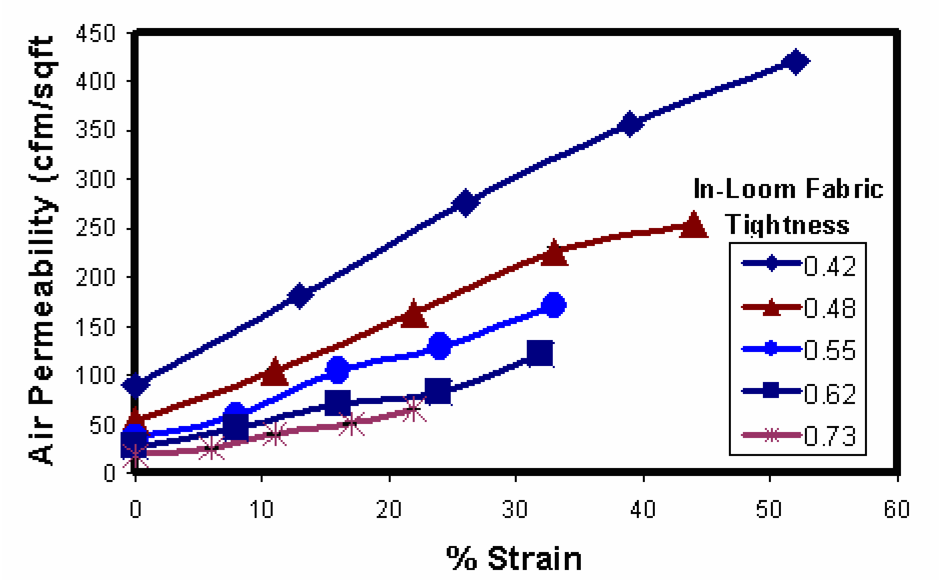

Figure 5. 7: Influence of strain on the air permeability of finished elastomeric fabrics (Basket (2x2) weave, 152 D filling) woven with different tightness

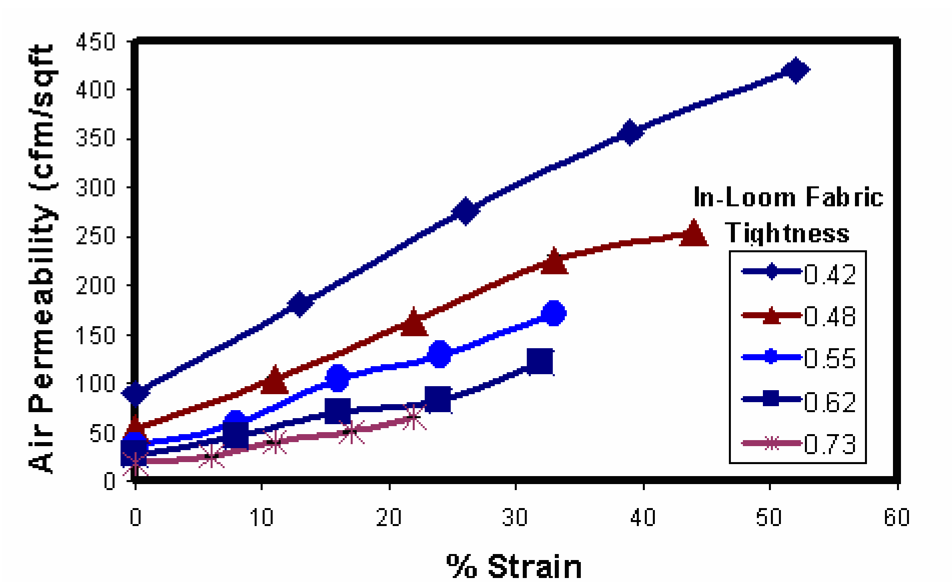

Figure 5. 8: Influence of strain on the air permeability of finished elastomeric fabrics (Basket (2x2) weave, 303 D filling) woven with different tightness

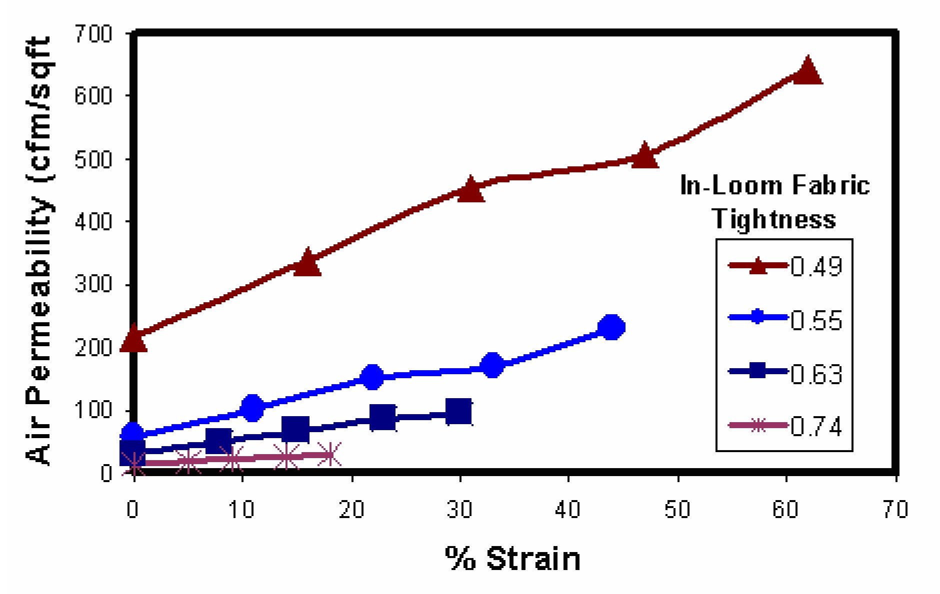

Figure 5. 9: Influence of strain on the air permeability of finished elastomeric fabrics (Basket (2x2) weave, 615 D filling) woven with different in-loom fabric tightness

Figures 5.10 to 5.13 show the changes in the geometry of the finished elastomeric fabrics under the influence of strain. Figure 5.10 shows the optical image of the finished elastomeric fabric at 0% strain. We can see from Figure 5. 10 that at 0% strain the warp and the filling yarns are closely packed and the degree of openness in the fabric is very low. When strain of 12% is applied to the fabric in the filling direction, the elastic yarns expand which causes the warp spacing (distance between the warp yarns) to increase and consolidated the yarn in the loading direction (filling yarn). This can be seen in Figure 5. 11. When strain level is increased to 36% and then to 48%, the distance between the warp yarns increases further and also the filling yarn consolidates further which increases the degree of openness in the fabric with respect to strain. This can be seen in Figure 5.12 and 5.13. The increase in fabric openness leads to increase in air permeability in the fabric. This is the reason why for a finished elastomeric fabric woven with particular weave, warp and filling yarns the air permeability of the fabric increases with increase in strain.

In case of Figure 5.2 the curves with in-loom fabric tightness levels (0.57 and 0.61) behave in a different manner than the other curves i.e. the curves indicate that the air permeability of the finished elastomeric fabric decreases initially (points inside the oval) with increasing strain and then increases. The reason for this decrease in air permeability is because of the wrinkles formed in the finished elastomeric fabric at such low tightness. This effect is explained with the help of Figures 5.14 to 5.17.

Figure 5. 10: Optical image of finished elastomeric fabric at 0% strain [Fabric construction detail: 89 EPI x 30 PPI) with 152 D filling] Magnification 25x

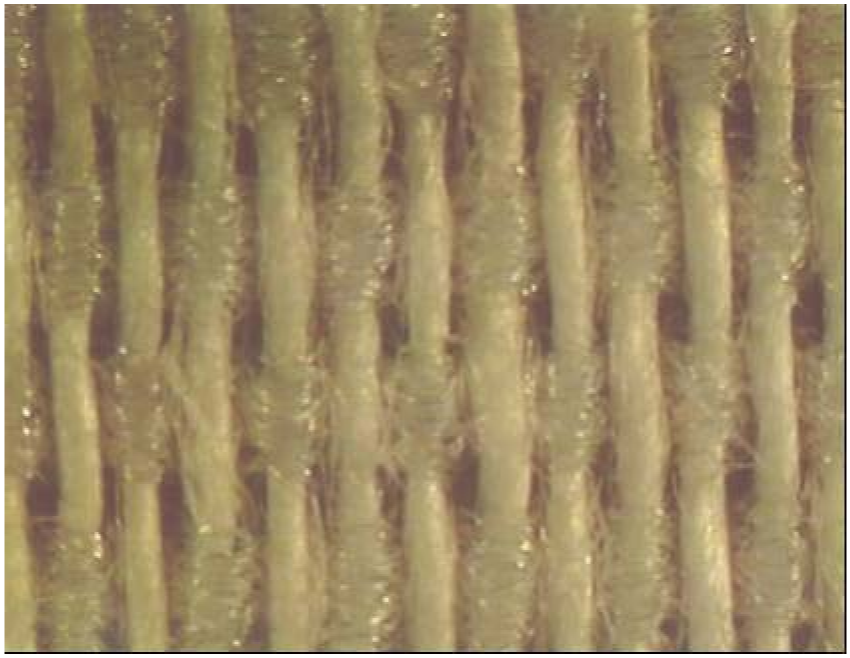

Figure 5. 11: Optical image of finished elastomeric fabric at 12% strain [Fabric construction detail: 89 EPI x 30 PPI) with 152 D filling] Magnification 25x

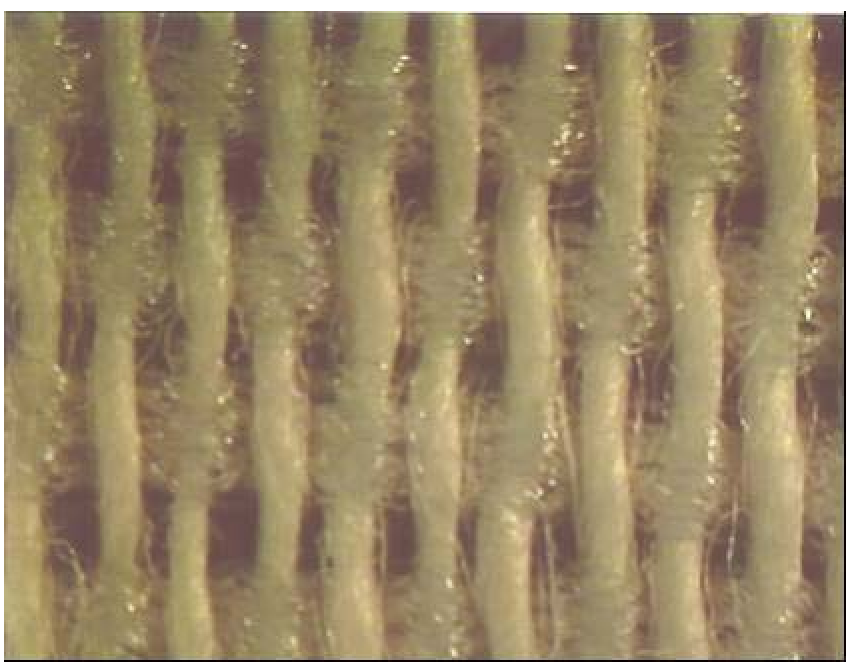

Figure 5. 12: Optical image of finished elastomeric fabric at 36% strain [Fabric construction detail: 89 EPI x 30 PPI) with 152 D filling] Magnification 25x

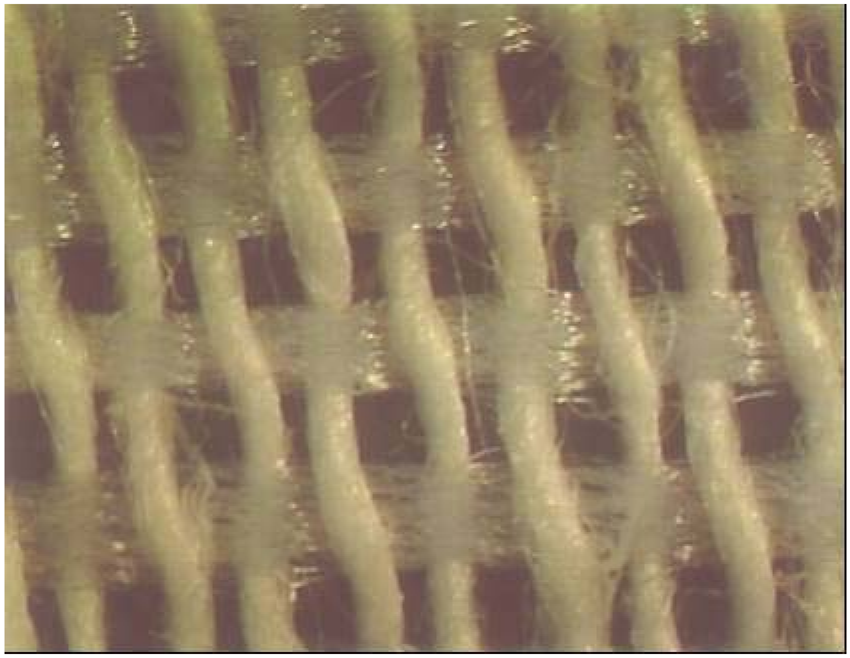

Figure 5. 13: Optical image of finished elastomeric fabric at 48% strain [Fabric construction detail: 89 EPI x 30 PPI) with 152 D filling] Magnification 25x

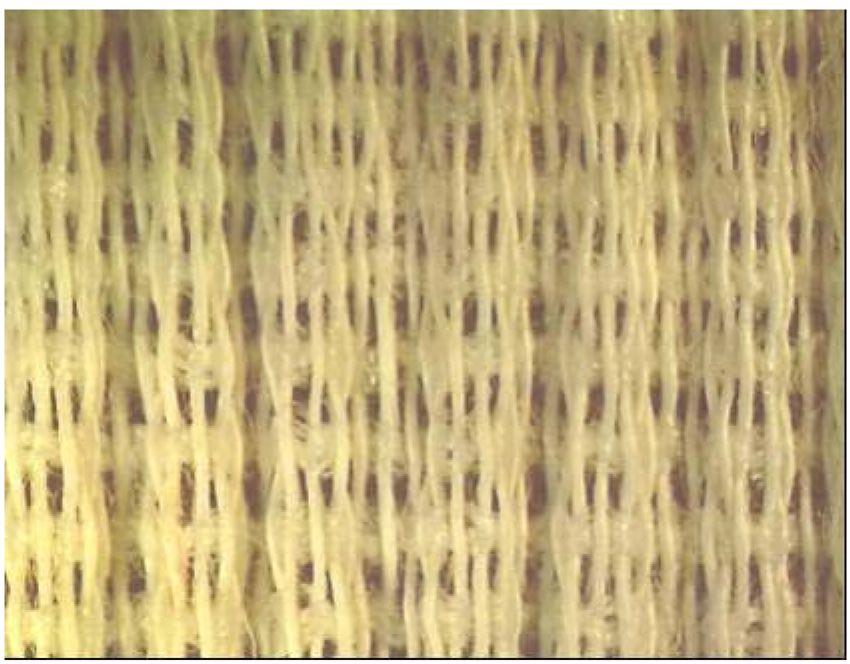

Figure 5. 14: Optical image of finished elastomeric fabric at 0% strain [Fabric construction detail: (Plain weave, 99 EPI x 37 PPI) with 303 D filling] Magnification 8x

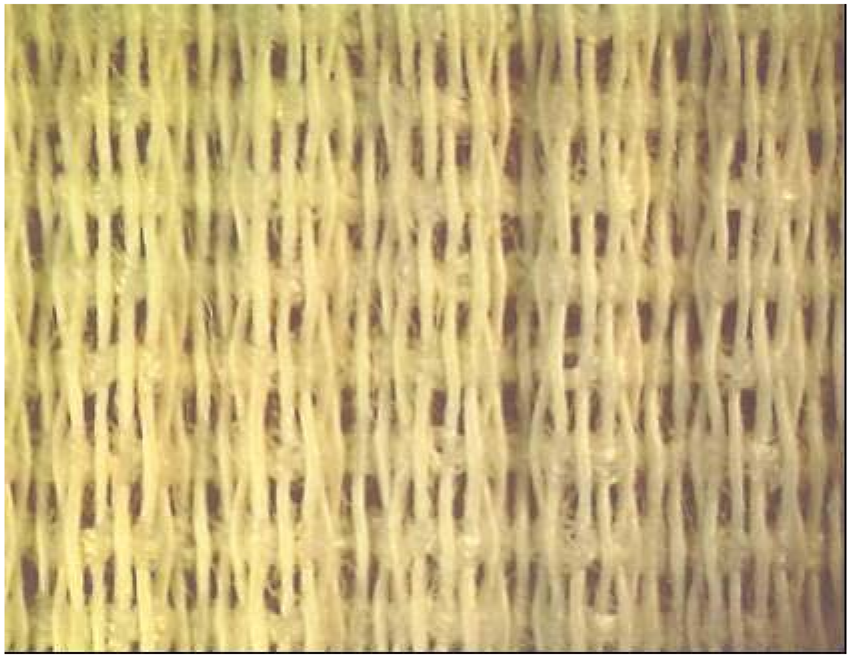

Figure 5. 15: Optical image of finished elastomeric fabric at 13% strain [Fabric construction detail: Plain weave, 99 EPI x 37 PPI with 303 D filling] Magnification 8x

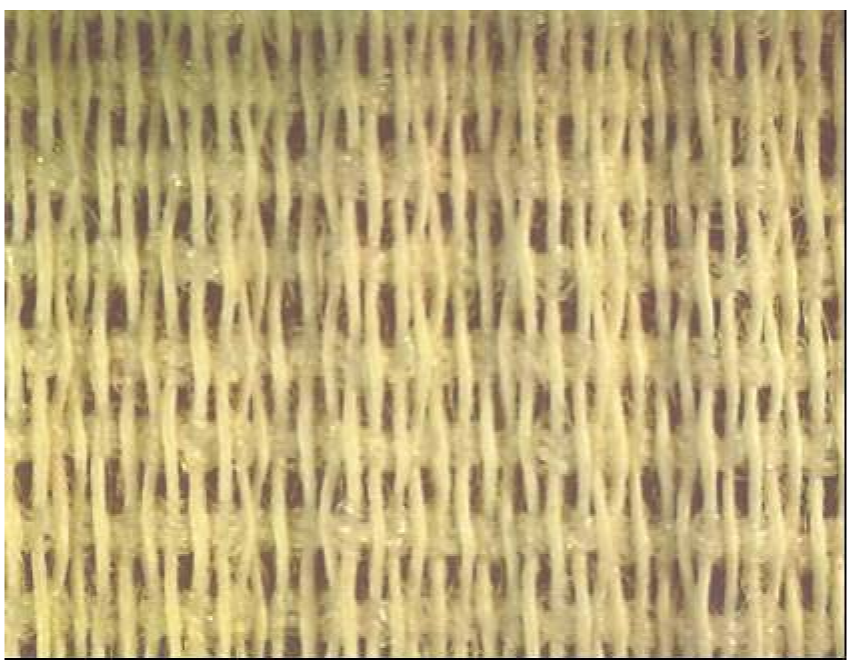

Figure 5. 16: Optical image of finished elastomeric fabric at 26% strain [Fabric construction detail: (Plain weave, 99 EPI x 37 PPI) with 303 D filling] Magnification 8x

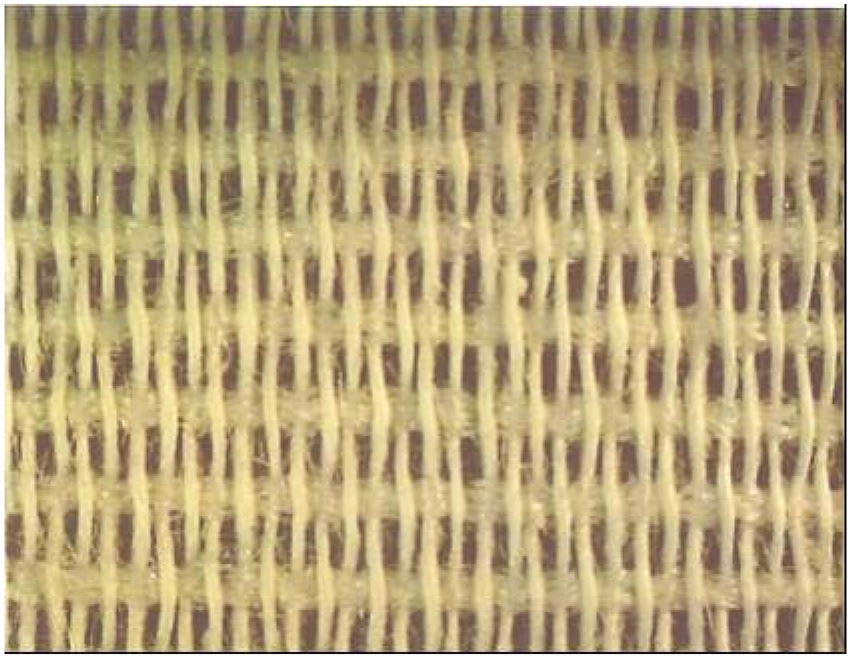

Figure 5. 17: Optical image of finished elastomeric fabric at 52% strain [Fabric construction detail: (Plain weave, 99 EPI x 37 PPI) with 303 D filling] Magnification 8x

Figures 5.14 to 5.17 show the optical images of the finished elastomeric fabric (with wrinkles) under the influence of different levels of strain. Figure 5.14 shows the optical image of the fabric at 0% strain. We can see from Figure 5.14 that the fabrics are wrinkled and also the elastomeric filling yarn is not strained. At this stage the air permeability of the fabric is about 550 cfm/sqft (curve 1 having an in-loom fabric tightness 0.57 in Figure 5.2). When strain is applied to the fabric (0 to 13%) the wrinkles in the fabric reduces, but the distance between the warp yarns are not altered (Figure 5.15). Because of this the number of interstices in the fabric over the test area reduces without alteration in the distance between the warp yarns, which reduces the air permeability of the fabrics to 483 cfm/sqft. This can be observed in curve 1 Figure 5.2.

When the strain level is increased from 13% to 26% the wrinkles in the fabric reduces further and the elastomeric filling yarn begins to expand (Figure 5.16). The reduction in wrinkles reduces the number of interstice in the fabric over the test area; at the same time the expansion of the elastomeric filling yarns causes the distance between the warp yarns to increase, which increases the size of the interstice. This increases the air permeability of the fabrics to 494 cfm/sqft (curve 1 having an in-loom fabric tightness 0.57 in Figure 5.2). When the strain is increased further (26% to 52%), the wrinkles in the fabric are completely removed and also the elastomeric filling yarns are strained further. This reduces the number of the interstices over the test area simultaneously increasing the size of the interstice. This increases the air permeability of the fabrics to 554 cfm/sqft (curve 1 having a in-loom fabric tightness 0.57 in Figure 5.2). Thus in a finished elastomeric fabric (with wrinkles) upon the application of strain the air permeability reduces initially and then increases. The same trend can be observed in another wrinkled fabric (curve 2 having an in-loom fabric tightness of 0.61 in Figure 5.2).

5.2 Influence of fabric construction on the air permeability of finished elastomeric fabrics

Influence of In-loom fabric tightness

Air permeability of the finished elastomeric fabrics also depends on the in-loom fabric tightness. Figures 5.18 to 5.20 show the influence of in-loom fabric tightness on the air permeability of the finished elastomeric fabrics woven with three different weaves with specific set of warp and filling yarns for different level of in-loom fabric tightness values. We can see from Figures 5.18 to 5.20 that the air permeability of the fabric decreases with increasing in-loom fabric tightness. The reason for the reduction in air permeability with increasing in-loom fabric tightness can be attributed to the changes in geometry of the finished elastomeric fabric with different in-loom fabric tightness levels. The degree of in-loom fabric tightness is a measure of how close the warp and the filling yarns are woven

We can observe from these Figures (5.21 to 5.23) that when the in-loom fabric tightness levels increases from 0.57 to 0.74, the closeness between the warp and the filling yarn increases and thus the amount of free space for the passage of air decreases. Thus the air permeability of the finished elastomeric fabric decreases with increasing in-loom fabric tightness levels. We can see this effect (decreasing air permeability with increasing in-loom fabric tightness) from Figures 5.18 to 5.20. This effect can also be observed in Figures 5.1 to 5.9.

The oval in Figures 5.19 and 5.20 indicate the finished elastomeric fabric samples having wrinkles in it. These fabrics even though behave like the normal fabric (i.e. air permeability decreases with increasing in-loom fabric tightness), the air permeability values with respect to particular in-loom fabric tightness are much higher. As mentioned earlier it is very difficult to predict the behavior of the finished elastomeric fabrics having wrinkles because of the non-uniformity of the structure as a result of the wrinkles.

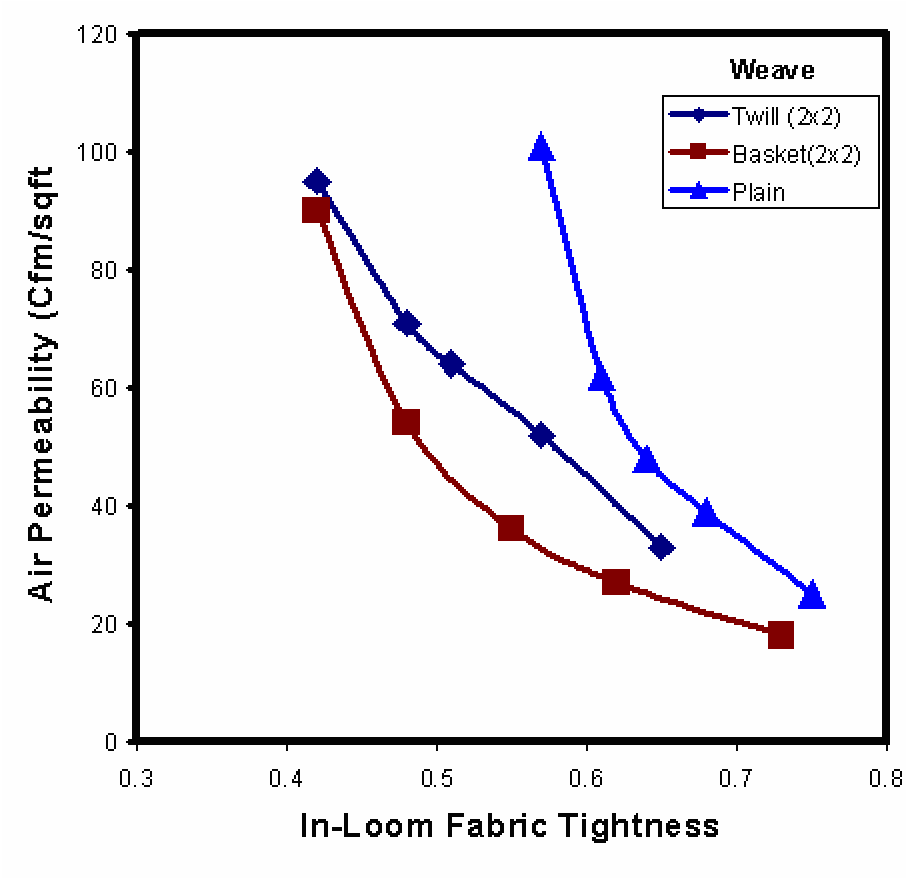

Figure 5. 18: Air permeability of finished elastomeric fabrics as a function of in-loom fabric tightness for three different weaves woven with 152D filling

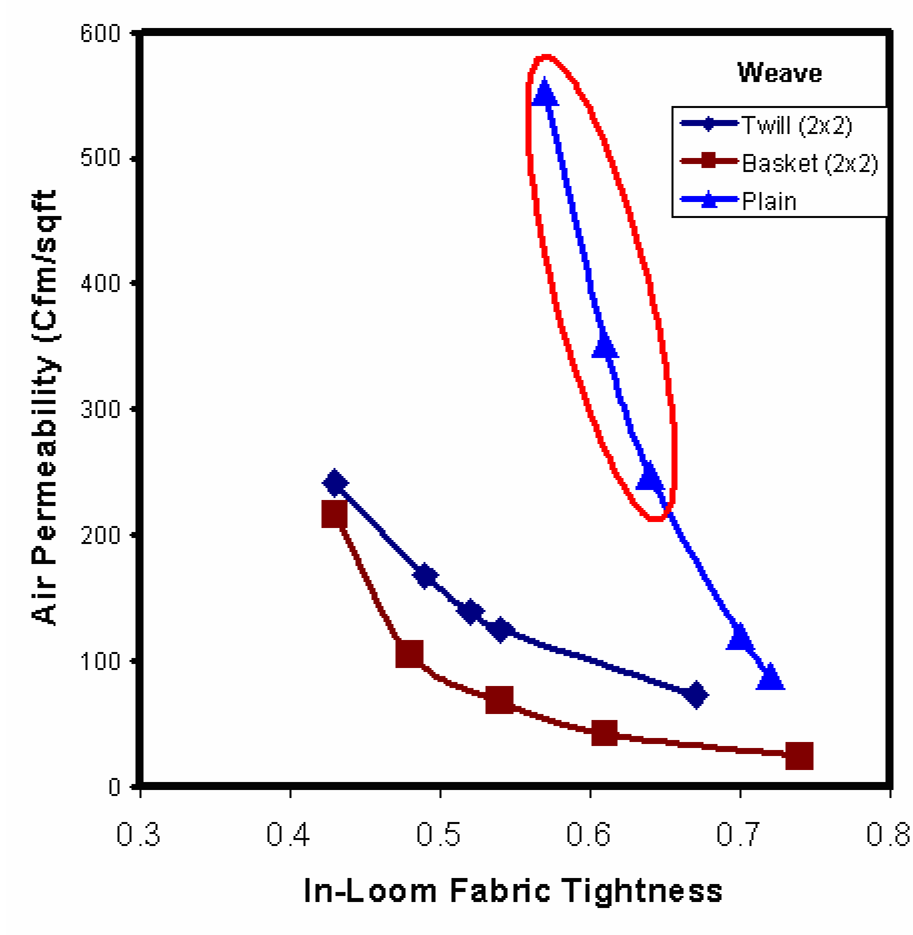

Figure 5. 19: Air permeability of finished elastomeric fabrics as a function of in-loom fabric tightness for three different weaves woven with 303D filling

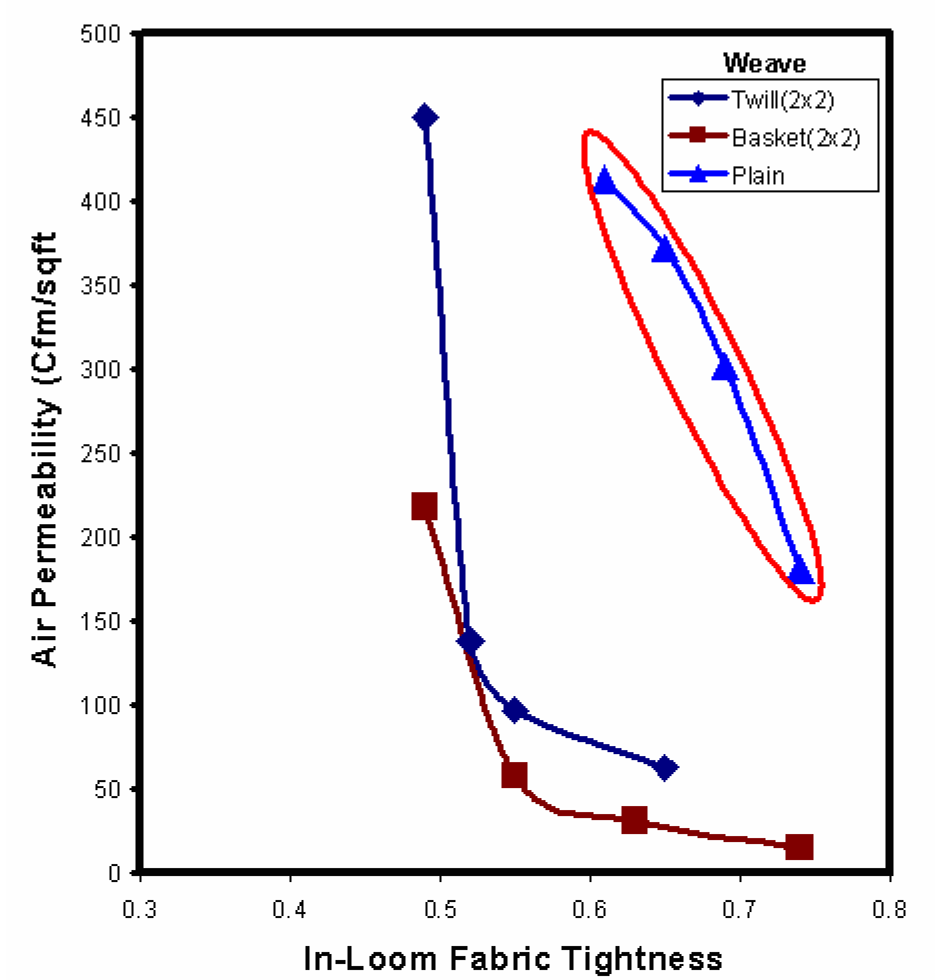

Figure 5. 20: Air permeability of finished elastomeric fabrics at 0% strain as a function of in-loom fabric tightness for three different weaves woven with 615D filling

Figure 5. 21: Optical image of woven finished elastomeric fabric (In-loom fabric tightness: 0.57, 89 EPI x30 PPI) with 152D filling) Magnification 25x

Figure 5. 22: Optical image of woven finished elastomeric fabric (In-loom fabric tightness: 0.64, 89 EPI x 42 PPI) with 152D filling) Magnification 25x

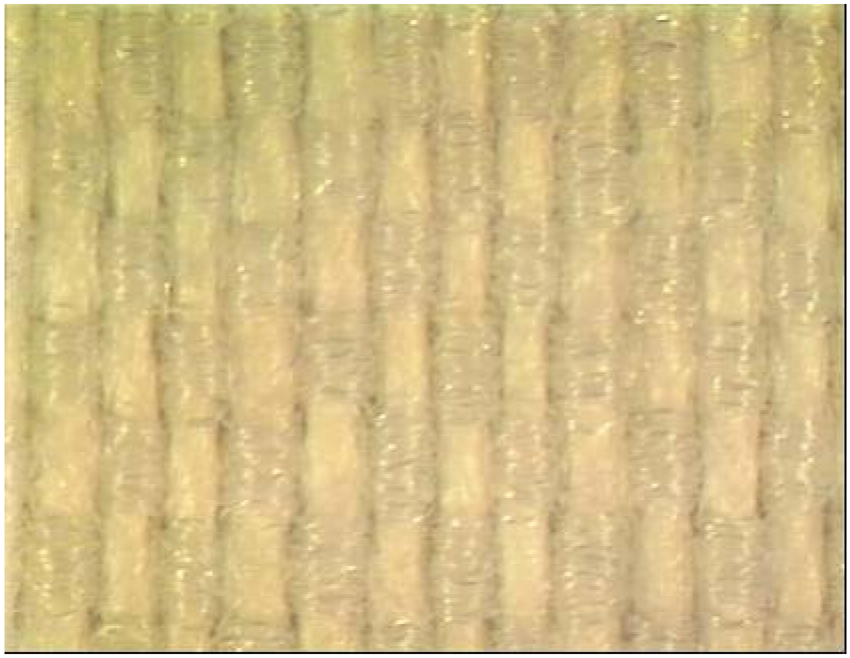

Figure 5. 23: Optical image of woven finished elastomeric fabric (In-loom fabric Tightness: 0.74, 84 EPI x 55 PPI) with 152D filling) Magnification 25x

Influence of weave type

Type of weave employed in the finished elastomeric fabric also has an influence on the air permeability behavior of the fabric. Figures 5.18 to 5.20 show the influence of in-loom fabric tightness on the air permeability of the finished elastomeric fabrics woven with three different weave with specific set of warp and filling yarns. We can see from these Figures (5.18 to 5.20) that the air permeability of plain weave is higher than the twill, and the air permeability of the twill fabric is higher than the basket. This order (plain followed by twill and basket) may seem to be contradicting the literature [10, 13] but in reality it is not. If we compare the finished fabric tightness of the three types of fabric (plain, twill (2x2), basket (2x2)) having same in-loom fabric tightness (Table 3), we can see that the basket weave has the highest tightness and lowest air permeability and plain weave has the lowest tightness and highest air permeability. Thus the order (plain followed by twill and basket) when we are comparing the air permeability value to the in-loom fabric tightness is not contradictory.

Table 3: Finished fabric tightness

Weave	In-Loom Fabric Tightness	Finished fabric Tightness	Air permeability (Finished fabric)	Fabric thickness (Finished fabric)
Plain	0.566	0.918	101	0.35
Twill*	0.548	0.936	52	0.43
Basket	0.548	0.952	36	0.46

The method of calculation of the finished fabric tightness in Table 3 involves making adjustment based on Brierley's experimental findings [19]. Appendix 8.2 shows the calculations in detail.

5.3 Influence of in-loom fabric tightness on the shrinkage % in the filling direction

We can see from Figures 5.24 to 5.26 the relationship between the fabric shrinkage % in the filling direction (direction in which the elastomeric threads are employed) and the in-loom fabric tightness. For a fabric woven with particular set of warp and filling yarns and with particular type of weave the fabric shrinkage % decreases with increasing in-loom fabric tightness with exceptions in Figure 5.25 and 5.26 marked by the ovals. The reason for the decrease in fabric shrinkage with increasing in-loom fabric tightness will be explained first, followed by the reasons for the exceptions in Figure 5.25. When the in-loom fabric tightness level increases the closeness between the adjacent warp and the filling yarn increases which restricts the movement of the yarns (warp and the filling) there by reducing the fabric shrinkage. The exceptions (increasing shrinkage % with increasing in-loom fabric tightness) are encircled by the oval in Figure 5.25. The reason for this exception is because of the wrinkles formed in the fabric samples during heat setting.

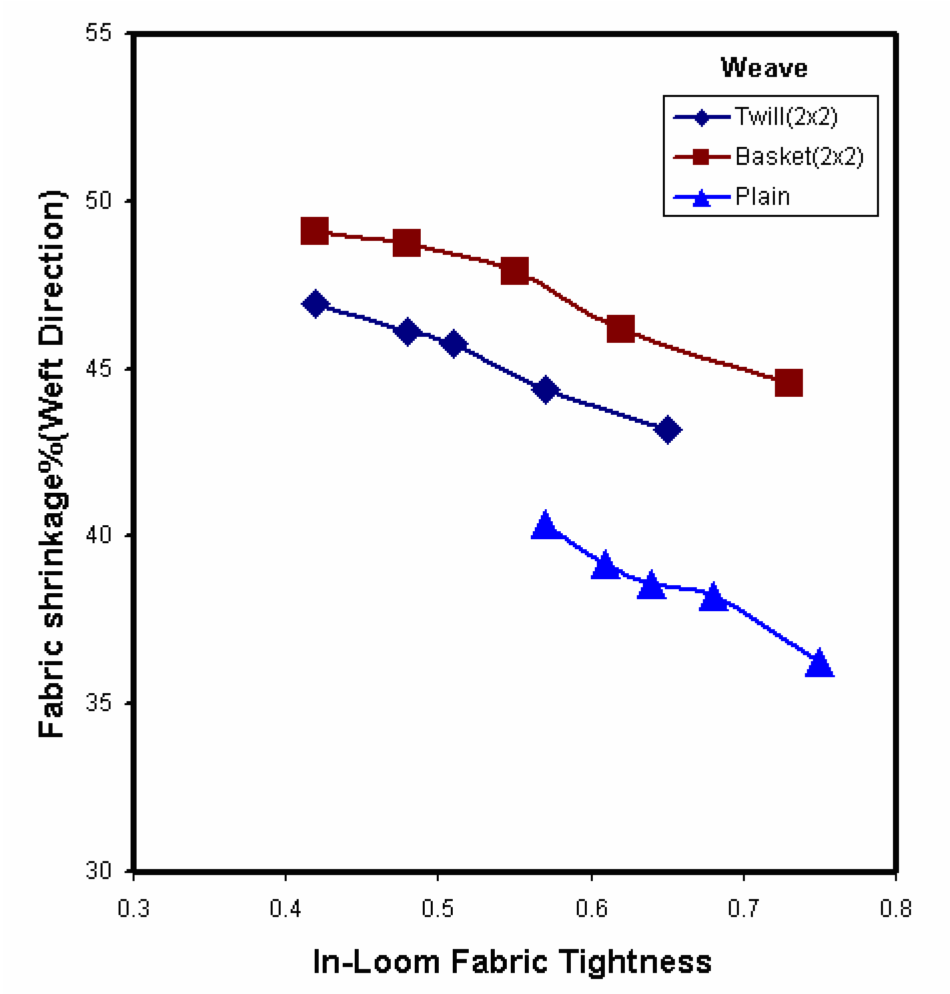

Figure 5. 24: Fabric shrinkage in the filling direction as a function of in-loom fabric tightness for three different types of weaves woven with 152D filling

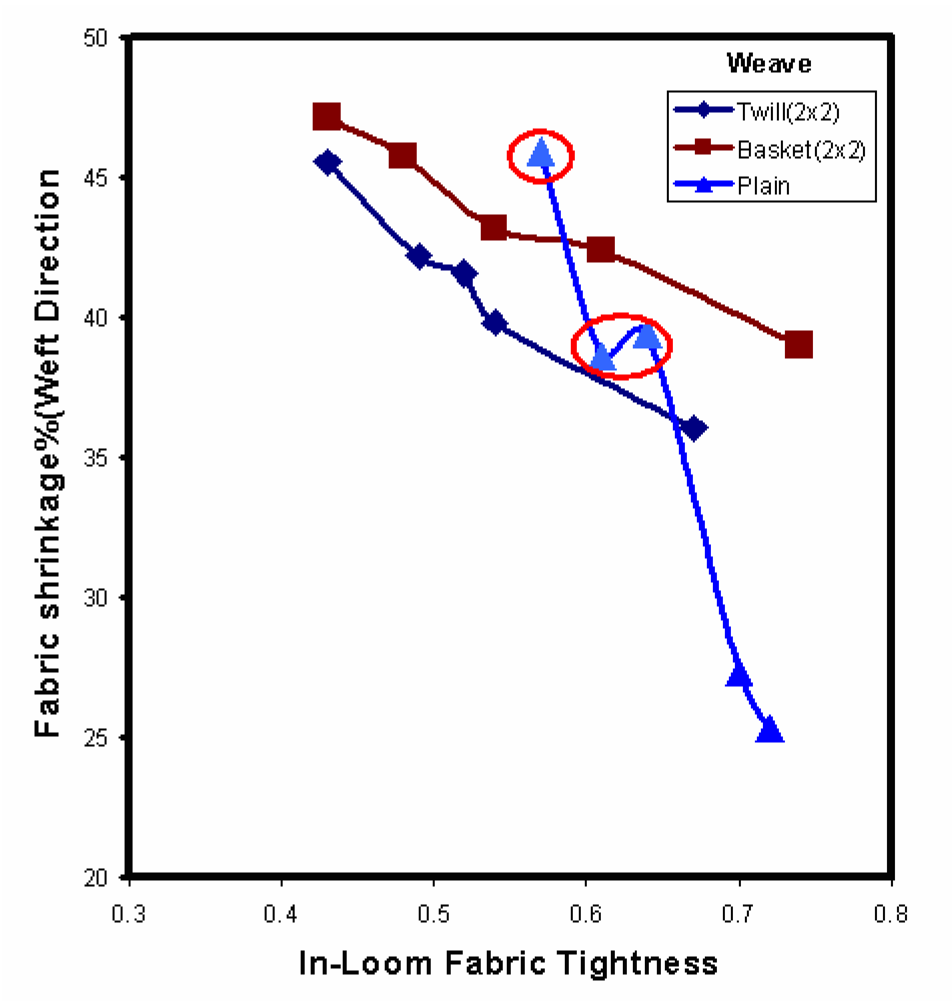

Figure 5. 25: Fabric shrinkage in the filling direction as a function of in-loom fabric tightness for three different types of weaves woven with 303D filling

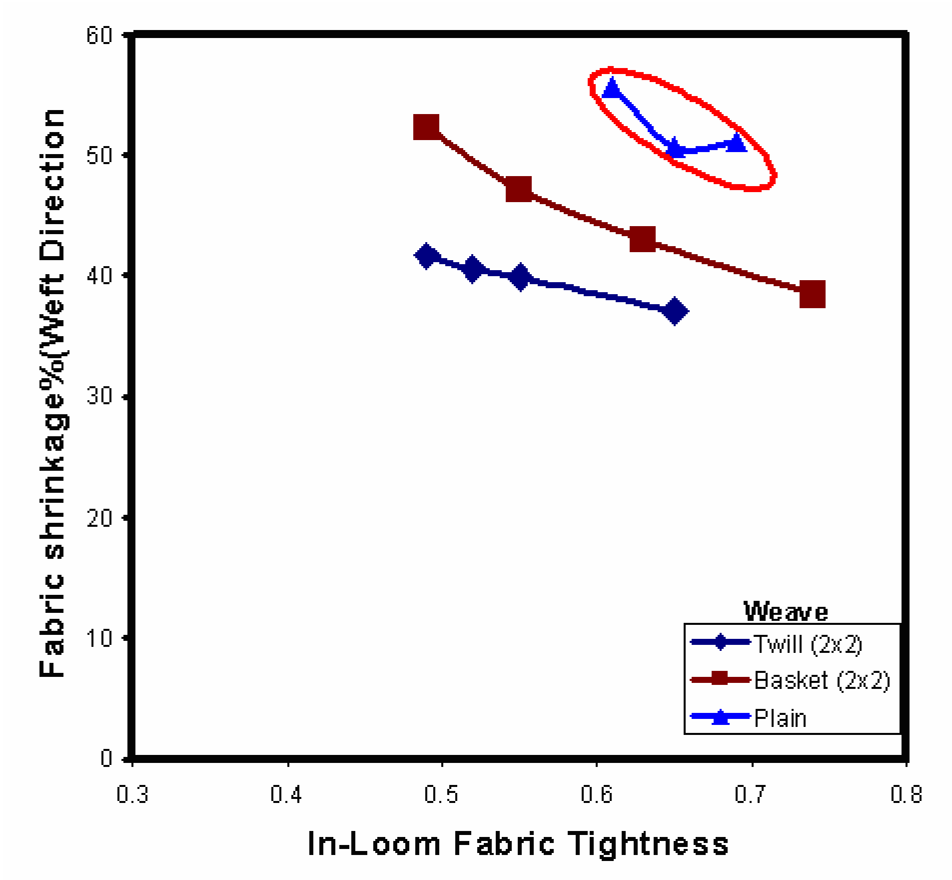

Figure 5. 26: Fabric shrinkage in the filling direction as a function of in-loom fabric tightness for three different types of weaves woven with 615D filling

5.4 Influence of weave on the shrinkage % in the filling direction

Figures 5.24 to 5.26 show the relationship between the fabric shrinkage % and in-loom fabric tightness for fabrics employed with plain, twill (2x2) and basket (2x2) weaves. We can see from these Figures (5.24 to 5.26) that for a fabric with similar in-loom fabric tightness woven with particular set of warp and filling yarns, the shrinkage level of basket weave is higher than the twill and the plain with exceptions in Figures 5.25 and 5.26 marked by the ovals. The reasons for the higher shrinkage level in basket when compared to the twill and plain will be explained first followed by the exceptions in Figures 5.25 and 5.26. The reason for the higher shrinkage level in the fabrics having basket weave when compared to the fabric having twill and the plain weave can be associated with the nature of interlacement between the warp and the filling yarns in a weave repeat of a basket weave. In basket weave the warp and the filling yarns are interlaced in pairs, in which case there are more chances that the yarns get over lapped which is not the case in the twill and plain weaves where each yarn is individually separated by interlacing within a repeat. This is the reason for higher shrinkage % of the basket weave when compared to the twill weave and plain weave. Similarly when we compare fabrics employed with twill weave with plain weave, the number of warp and the filling interlacements per square cm is low in case of fabrics having twill weave when compared to the fabrics having plain weave. So when the fabric is heat set, there will be less restriction for the warp or the filling yarns or both (depending on the direction in which the elastomeric yarns are employed) to come closer in the fabrics employed with twill weave when compared to the fabrics employed with plain weave. This is the reason for the increase in shrinkage level in the fabrics having twill weave when compared to the fabrics having plain weave.

The exceptions (Shrinkage % of plain weave is higher than the twill and the basket) are encircled by the ovals in Figure 5.25 and 5.26. The reason for this exception is because of the wrinkles formed in those finished elastomeric fabric samples during heat setting.

5.5 Influence of in-loom fabric tightness on the finished fabric elongation % in the filling direction (due to the removal of crimps)

Finished fabric elongation at the removal of crimp is determined in the same manner as it is done to determine the yarn crimp or yarn take-up in woven fabrics. ASTM D3883-90 suggests a method of using the stress strain curve of the material whose elongation at the removal crimp and initial stretch need to be found out.

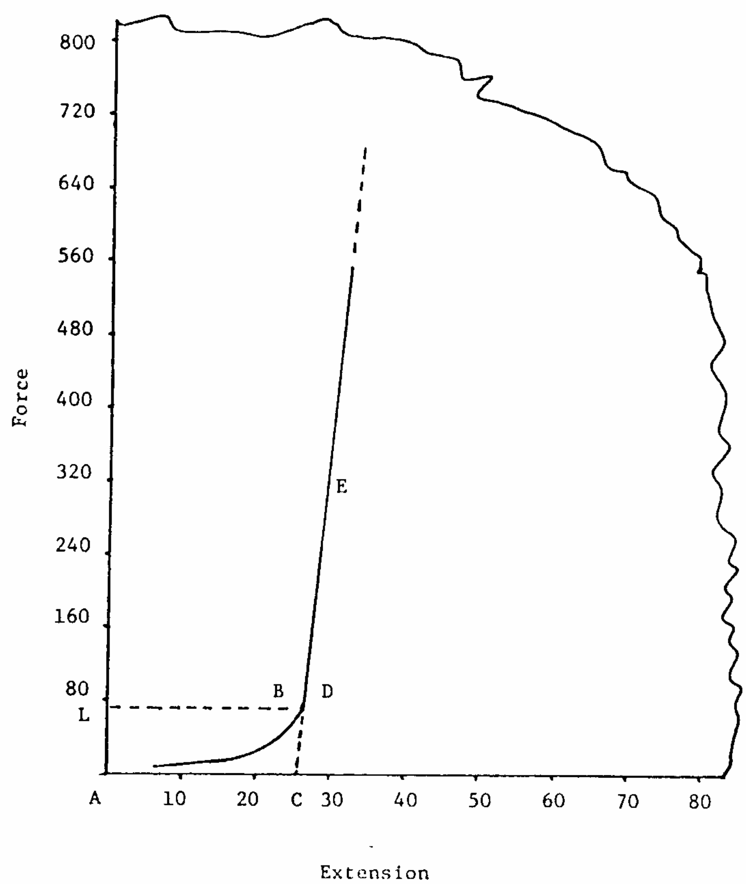

Figure 5. 27: Load extension curve of the test material [28]

The method suggests extrapolating the straight-line portion DE of the load elongation curve to point C as shown in Figure 5.27. The portion of the curve AD represents the portion of the curve, which represents the removal of the crimp and initial stretch. The distance AC indicated the extension at which this is achieved. Similarly we can determine the fabric elongation at the removal of the crimp and initial stretch from the load extension curve of the fabric. Typical stress strain evaluation results of the elastomeric fabrics woven with three different filling yarn counts, weave types and pick densities are shown in Appendix 8.3. The fabric elongation % in the filling direction at the removal of crimps (weave and fabric crimp) can be determined from these curves in the way described earlier.

5.6 Influence of in-loom fabric tightness and linear density of elastomeric filling yarn on the finished fabric elongation % in the filling direction (at the removal of crimps)

The elongation of the finished fabrics in the filling direction (direction in which the elastomeric threads are employed) at the removal of the crimps can be associated with the in-loom fabric tightness. Figures 5.28 to 5.30 show the relationship between the finished fabric elongation (at the removal of crimps) in the filling direction and in-loom fabric tightness. We can see from these Figures (5.28 to 5.30) that the elongation % decreases with increasing in-loom fabric tightness with exceptions in Figure 5. 30 marked by oval. The behavior (decrease in fabric elongation with increasing in-loom fabric tightness) can be explained with the fact that closeness between the warp and the filling yarn increases with increasing in-loom fabric tightness. This increase in closeness between the warp and the filling yarn restricts the elongation of the yarn reduce the fabric elongation. Thus the finished fabric elongation decreases with increasing in-loom fabric tightness. The odd behavior (increase in finished fabric elongation with in-loom fabric tightness) is encircled by oval in Figures 5.29 & 5.30. The reason for this odd behavior is because of the non-uniform wrinkles (formed due to the difference in shrinkage between the warp and the weft yarns) formed in the fabric during heat setting. Behavior of this wrinkled fabric is very difficult to predict because of the non-uniformity in the formation of wrinkles.

We can also see from Figures 5.28 to 5.30 the influence of yarn size on the fabric elongation % at the removal of crimps (Filling direction). When we compare fabrics made out of filling yarns with different counts, having a particular in-loom fabric tightness in the range between 0.4 to 0.5, it is found out that fabrics made out of elastomeric yarns with yarn count of 600 Denier have higher elongation %, than the fabrics made out of elastomeric yarns with yarn count of 150 Denier which has higher elongation %, than the fabrics made out of elastomeric yarns with yarn count of 300 Denier with exceptions in Figure 5.30 marked by ovals. The behavior of fabrics with respect to the count of the yarns used in the fabrics can be associated with the stress strain behavior of the elastomeric yarns (heat set) used in the fabric. The stress strain behavior of the heat set and non-heat set elastomeric yarns of different counts can be found in the Appendix 8.3 & 8.4. It can be seen from these stress strain behavior of the heat set elastomeric yarns that maximum elongation % of the 600 Denier yarn (136 filaments) is higher than the 150 Denier yarn (68 filaments) which has higher elongation % than the 300 Denier yarn (68 filaments). The same order (600 Denier followed by 150 Denier followed by 300 Denier) can be observed in Figures 5.28 to 5.30 for fabrics having in-loom fabric tightness levels ranging from 0.4 to 0.55 with exceptions in Figures 5.30. The reason for the exceptions in Figure 5.30 is because of the uneven wrinkles formed in the finished fabric during heat setting.

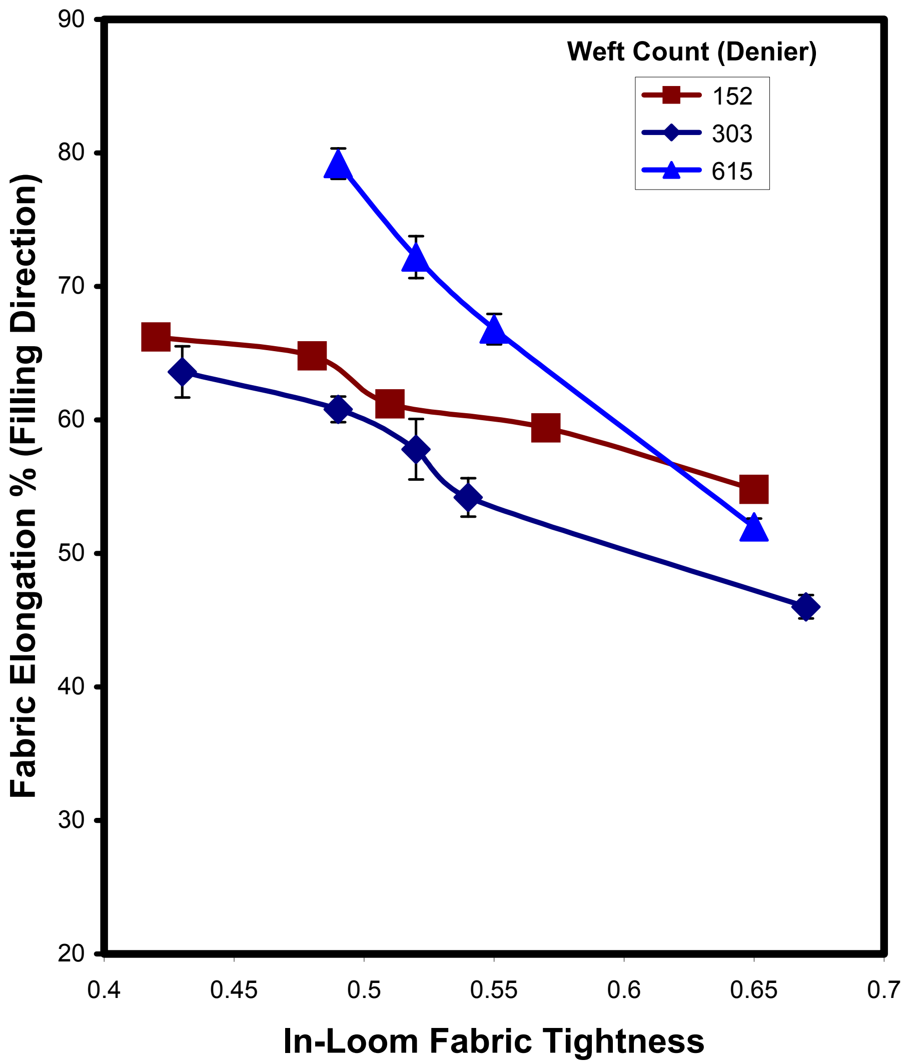

Figure 5. 28: Finished fabric Elongation % at the removal of crimps (Filling direction) as a function of in-loom fabric tightness for Twill fabrics woven with three different filling counts

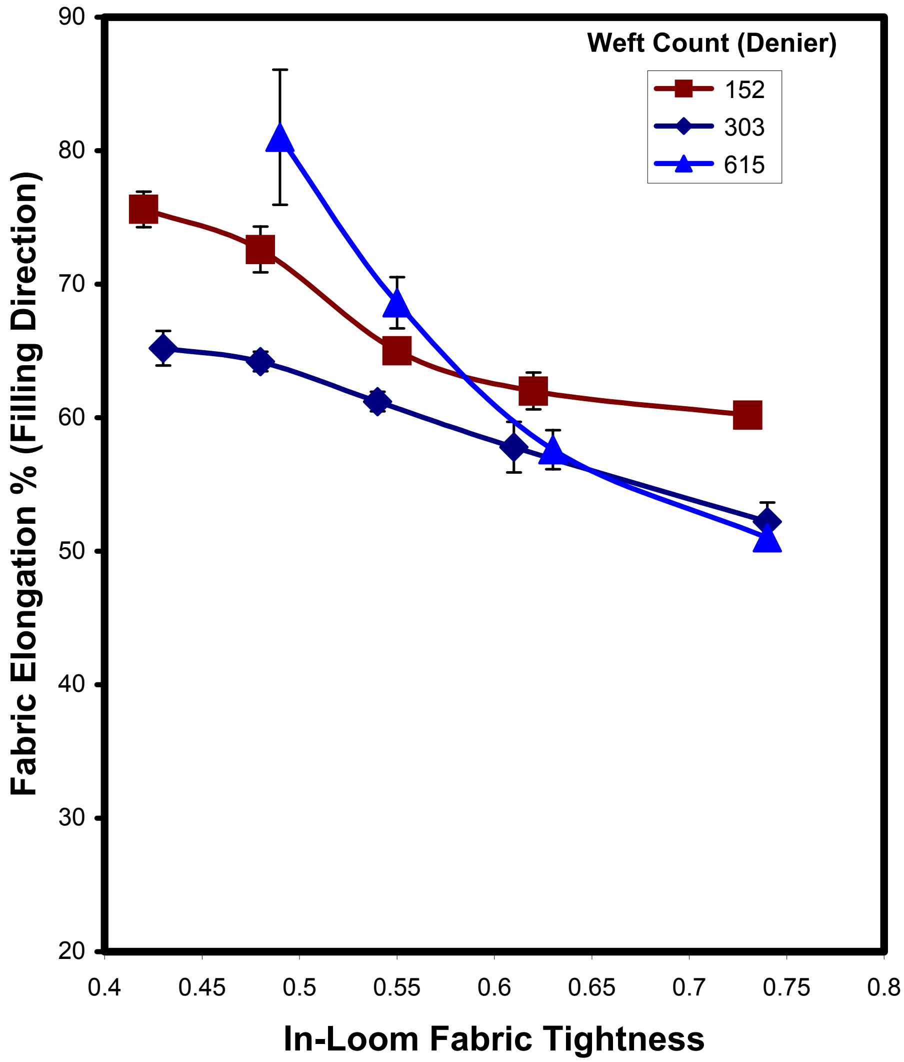

Figure 5. 29: Finished fabric Elongation % at the removal of crimps (Filling direction) as a function of in-loom fabric tightness for basket fabrics woven with three different filling counts

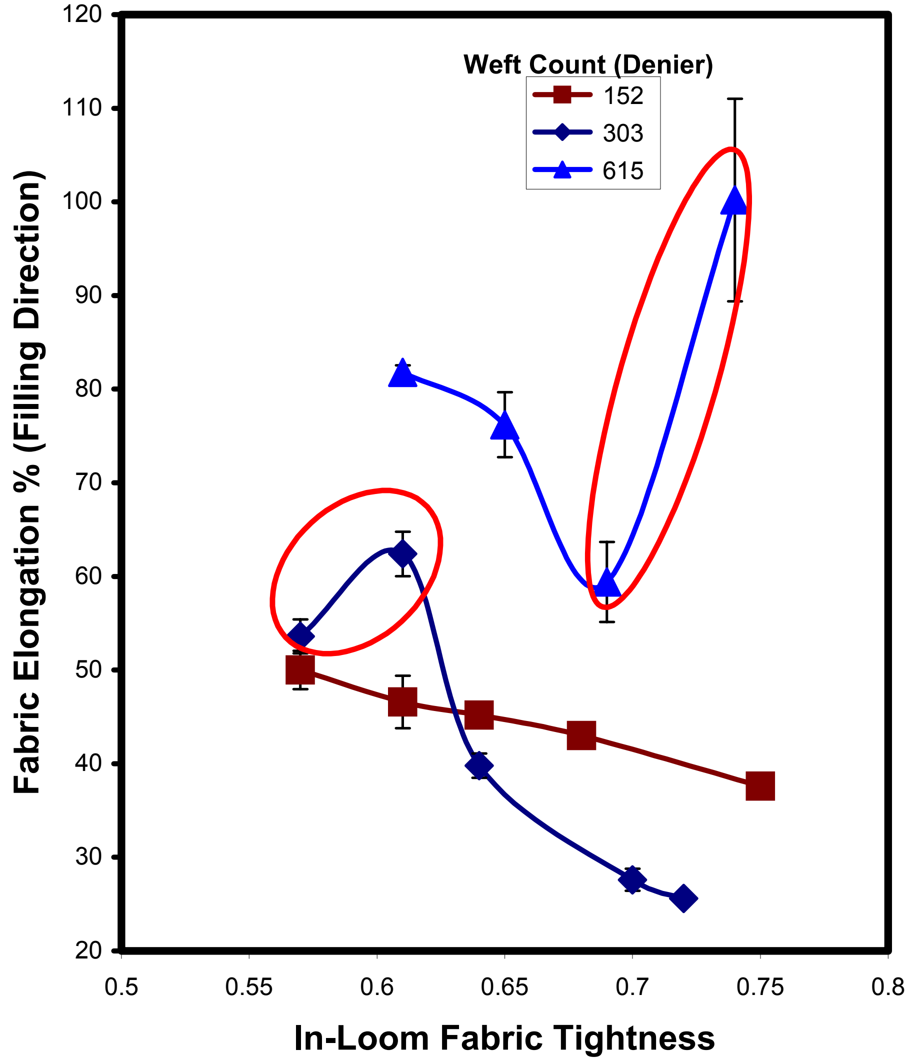

Figure 5. 30: Finished fabric Elongation % at the removal of crimps (Filling direction) as a function of in-loom fabric tightness for plain weave fabrics woven with three different filling counts

5.7 Influence of type of weave on the finished fabric elongation % in the filling direction (at the removal of crimps)

Elongation of finished elastomeric fabric at the removal of crimps also depends on the type of the weave employed in the fabric. Figures 5.31 to 5.33 show the influence of in-loom fabric tightness on the finished fabric elongation %. The finished fabric elongation % of basket weave is higher than the twill, and the finished fabric elongation % of the twill fabric is higher than the plain, with exceptions in Figures 5.32 and 5.33 marked by oval. The reason for the higher elongation % of the basket weave when compared to the twill and plain can be associated with the shrinkage % in the filling direction during the fabric heat setting. Figures 5.24 to 5.27, shows that for a fabric with particular in-loom fabric tightness level, the shrinkage % of the basket weave is higher than the twill, and the shrinkage % of the twill fabric is higher than the plain. We can notice that the order of curves in Figures 5.24 to 5.27 is same as that is figures 5.31 to 5.33. Higher the fabric shrinkage (in the filling direction) more will be the amount of crimp formed in the yarns (elastomeric filling), and more the fabric has to be extended to remove these crimps. The reason for the exceptions marked by red oval in Figures 5.32 and 5.33 is because of the non-uniform wrinkles formed in the finished fabric during heat setting. The wrinkles are formed due to the difference in shrinkage between the warp and the weft yarns during the heatsetting. Behaviors of these wrinkled fabrics are very difficult to predict because of the non-uniformity in the formation of wrinkles.

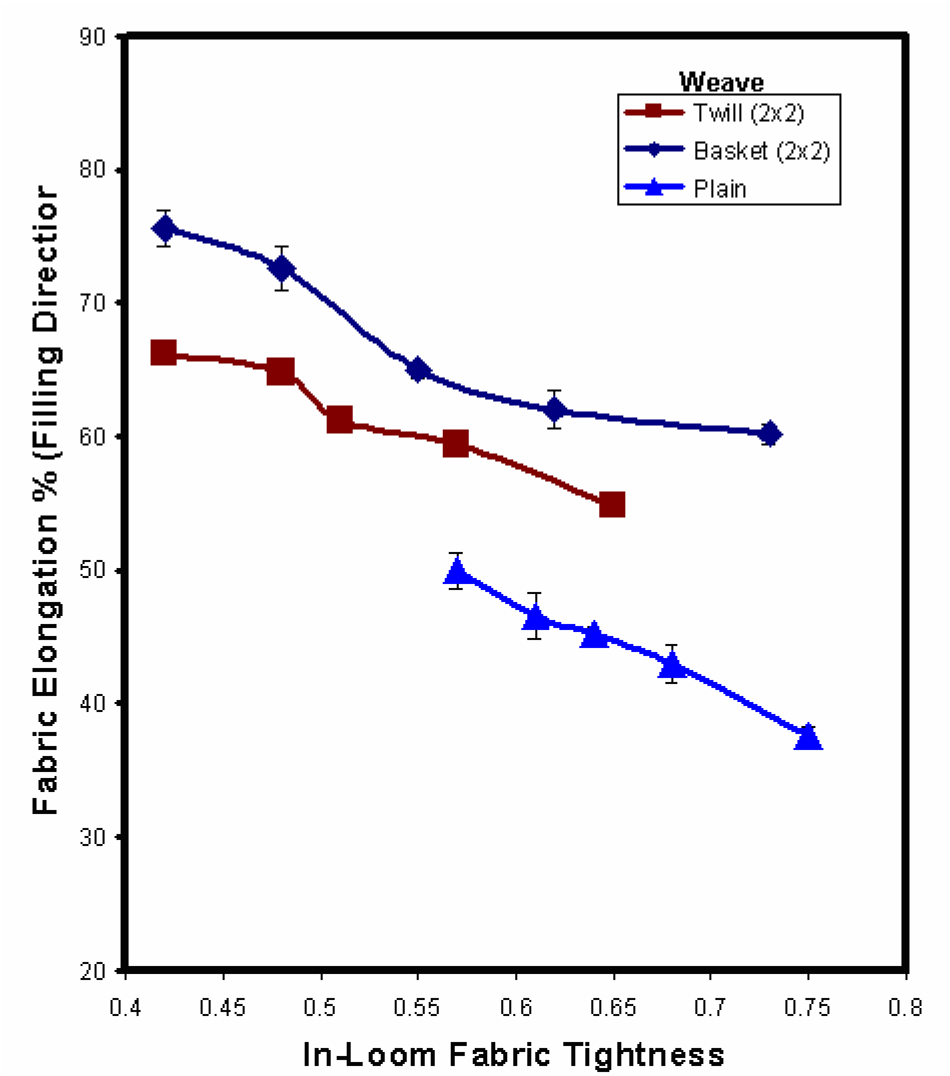

Figure 5. 31: Finished fabric Elongation % at the removal of crimp (Filling direction) as a function of in-loom fabric tightness for three different types of weaves woven with filling yarn linear density of 152Denier

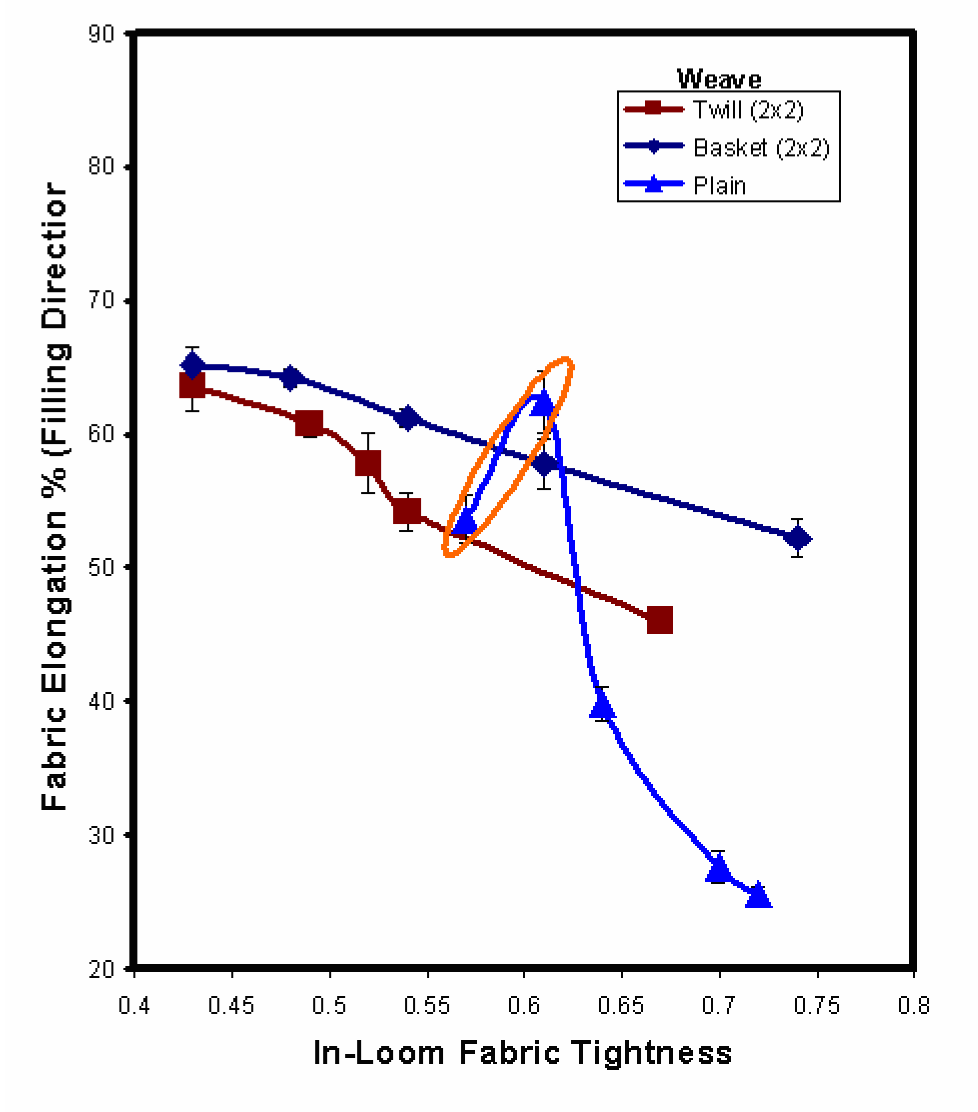

Figure 5. 32: Finished fabric Elongation % at the removal of crimp (Filling direction) as a function of in-loom fabric tightness for three different types of weaves woven with filling yarn linear density of 303Denier

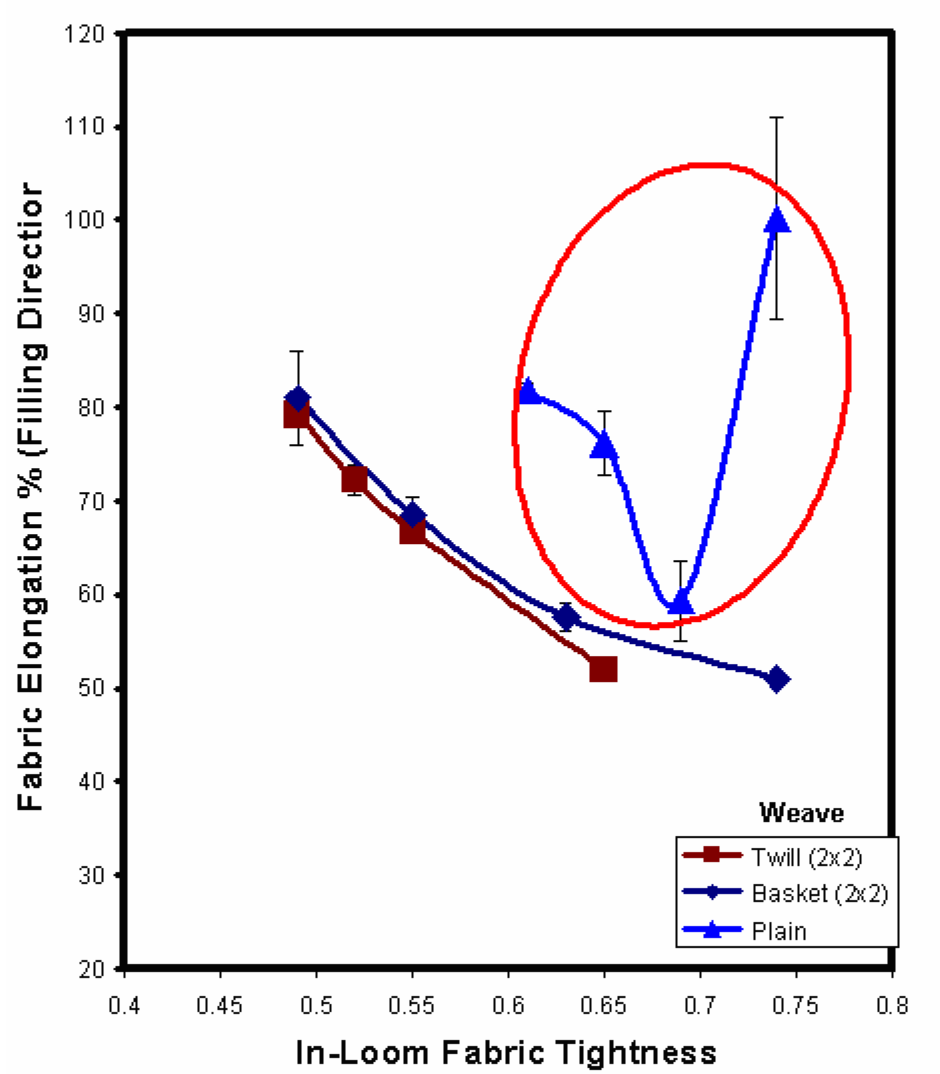

Figure 5. 33: Finished fabric Elongation % at the removal of crimp (Filling direction) as a function of in-loom fabric tightness for three different types of weaves woven with filling yarn linear density of 615Denier

5.8 Influence of in-loom fabric tightness on the volumetric porosity of the finished elastomeric fabrics

In-loom fabric tightness also influences the volumetric porosity of the finished elastomeric fabric. The method of calculating the volumetric porosity is shown in Appendix 8.6. Figures 5.34 to 5.36 show the relationship between the volumetric porosity and in-loom fabric tightness. Porosity of the finished fabrics decreases with increasing in-loom fabric tightness with exceptions in Figures 5.35 and 5.36, (indicated by oval). The reason for the decreasing volumetric porosity with increasing in-loom fabric tightness is because as the in-loom fabric tightness increases the closeness between the warp and the filling yarn increase, which reduces the unoccupied space in the fabric and also increases the fabric weight and thickness, there by reducing the volumetric porosity of the finished fabric. The increasing fabric weight and fabric thickness with increasing in-loom fabric tightness can be seen in sections (5.10 & 5.12).

5.9 Influence of weave type on the volumetric porosity of the finished elastomeric fabrics

Figures 5.34 to 5.36 show the influence of weave on the volumetric porosity of the finished elastomeric fabrics. We can see from the Figures that fabric employed with basket weave have higher volumetric porosity than the fabrics employed with twill and plain with exceptions in figures 5.35 and 5.36. The reason for the higher volumetric porosity of the basket weave when compared to the twill weave, and higher volumetric porosity of the twill weave in comparison to the plain weave can be associated with the higher fabric thickness and fabric weight of the basket weave in comparison with the twill weave (Figures 5.37 to 5.42) and the higher fabric thickness and fabric weight of the twill weave (Figures 5.37 to 5.42) in comparison with the plain weave.

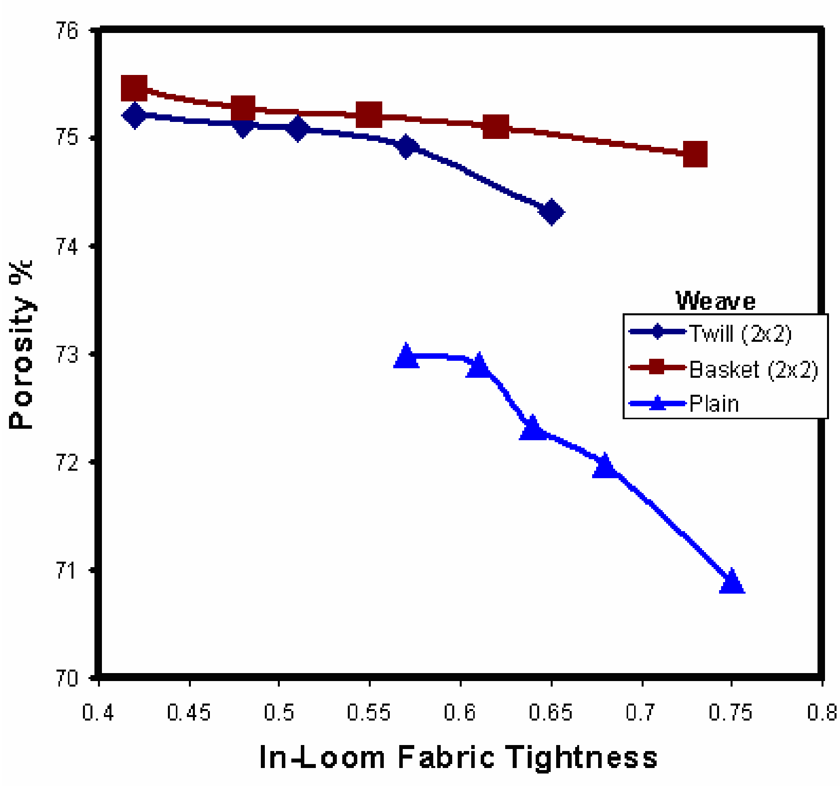

Figure 5. 34: Volumetric porosity as a function of in-loom fabric tightness for three different types of weaves woven with 152D filling

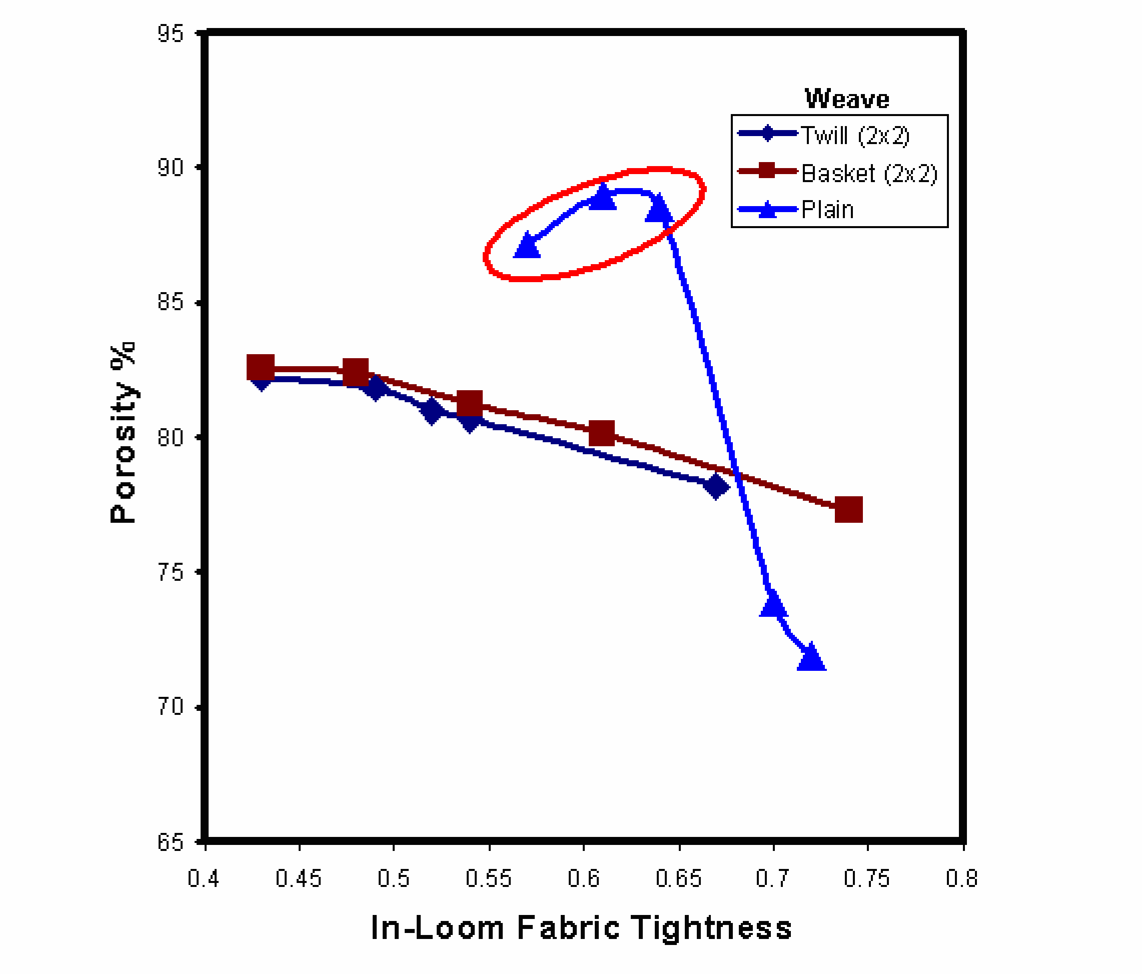

Figure 5. 35: Volumetric porosity as a function of in-loom fabric tightness for three different types of weaves woven with 303D filling yarn

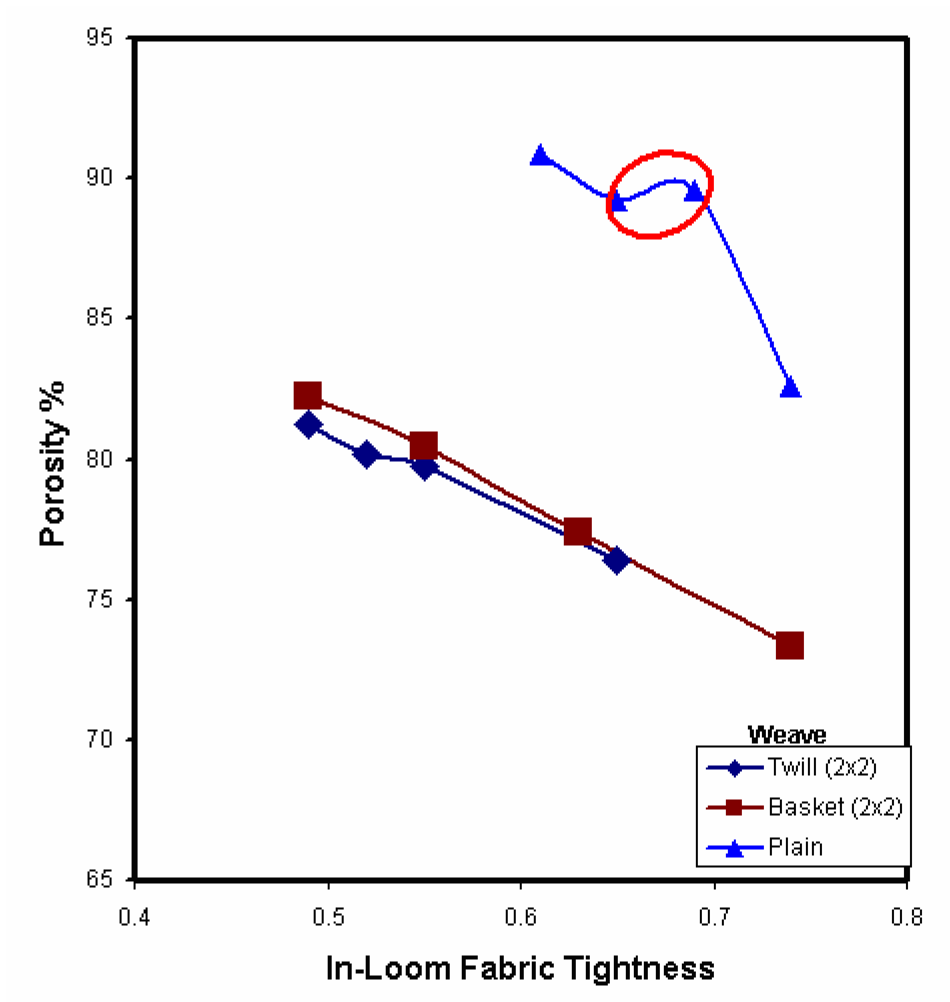

Figure 5. 36: Volumetric porosity as a function of in-loom fabric tightness for three different types of weaves woven with 615D filling

5.10 Influence of in-loom fabric tightness on finished elastomeric fabric weight (gms/cm^2)

Finished elastomeric fabric weight (g/cm^2) can be associated with the in-loom fabric tightness. Figures 5.37 to 5.39 indicate the relationship between finished elastomeric fabric weight (g/cm^2) and in-loom fabric tightness for fabrics woven with different types of weaves and with particular set of warp and filling yarns. We can see from these Figures (5.37 to 5.39) for a particular weave fabric woven with certain set of warp and filling yarns with different in-loom fabric tightness levels, the finished elastomeric fabric weight /cm^2 increases with increasing in-loom fabric tightness levels with exceptions in Figures 5.38 to 5.39 encircled with ovals. The reason for the increase in fabric weight (g/cm^2) with increasing in-loom fabric tightness will be explained first, followed by the reasons for the exceptions in Figure 5.38 and 5.39. The reason for this behavior (the increase in fabric weight g/cm^2 with increasing in-loom fabric tightness) is that when the in-loom fabric tightness level increases the closeness between the warp and the weft yarns and thus the number of warp or weft or both threads per cm^2 increases, which increases the finished elastomeric fabric weight/cm^2. The exceptions (decrease in fabric weight (g/cm^2) with increasing in-loom fabric tightness) are encircled by ovals in Figure 5.38 and 5.39. The reason for this behavior is because of the non-uniform wrinkles formed in the finished elastomeric fabric.

5.11 Influence of weave on the finished elastomeric fabric weight (g/cm^2)

From Figures 5.37 to 5.39 we can also study the influence of weave on the relationship between finished elastomeric fabric weight (g/cm^2) and in-loom fabric tightness. We can see from the Figures (5.37 to 5.39), among finished elastomeric fabrics woven with different kinds of weaves (plain, twill and basket) with particular set of warp and filling yarns and having certain in-loom fabric tightness levels, fabric employed with basket weave have more weight per cm^2 than the fabrics employed with twill and plain. This can be associated with the higher shrinkage % of the basket weave woven with particular set of warp and filling yarns and having certain in-loom fabric tightness levels in comparison with the shrinkage % of the twill and basket woven with similar set of warp and filling yarns and in-loom fabric tightness levels which can be observed in Figures 5.24 to 5.26. Now the exceptions (decrease in finished fabric weight (g/cm^2) with increasing in-loom fabric tightness) are encircled by ovals in Figure 5.38 and 5.39. The reason for this curve behavior is because of the non-uniform wrinkles formed in the finished elastomeric fabric.

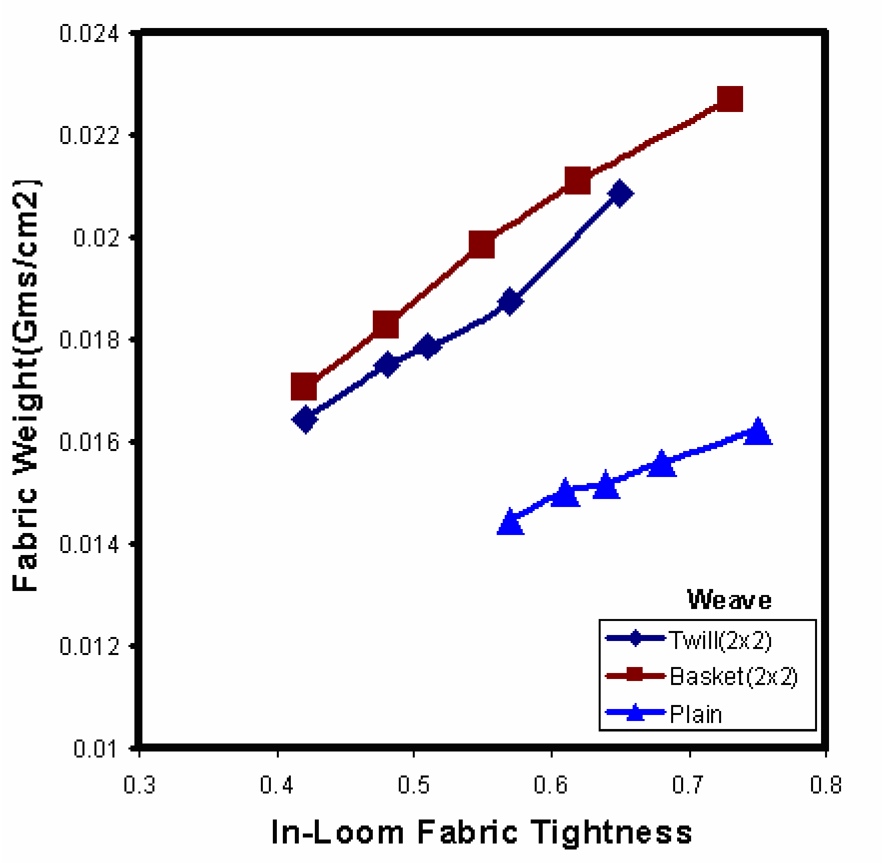

Figure 5. 37: Finished elastomeric fabric weight (gms/cm^2) as a function of in-loom fabric tightness for three different types of weaves woven with 152D filling

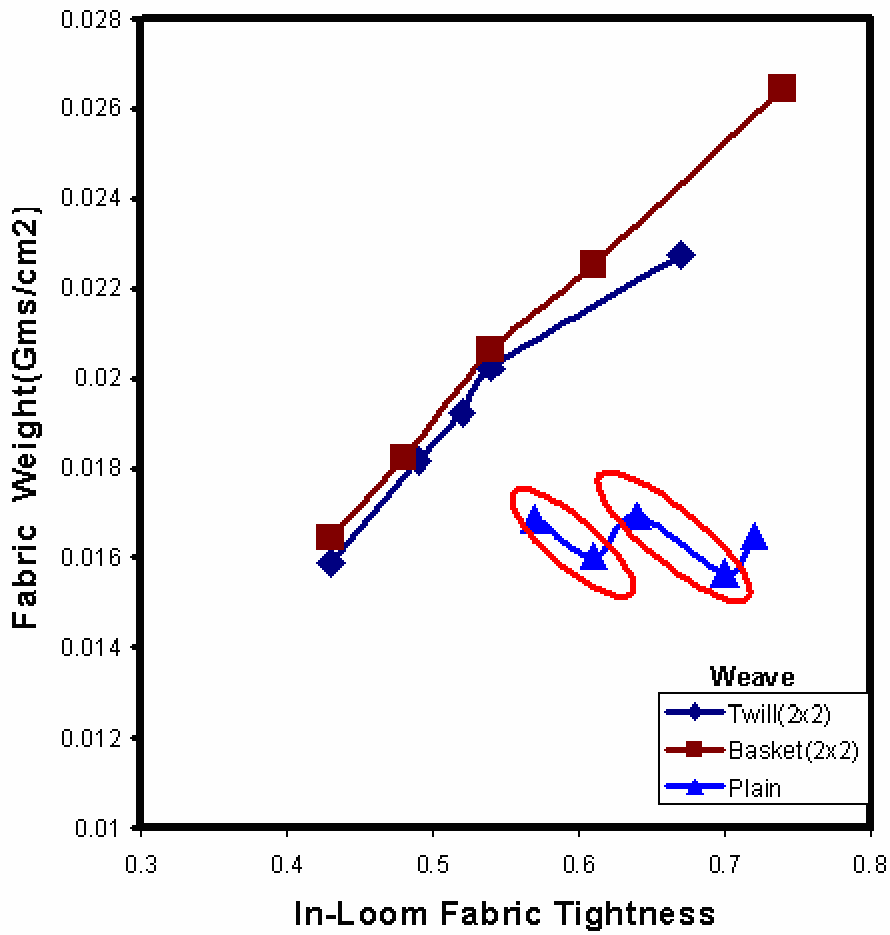

Figure 5. 38: Finished elastomeric fabric weight (gms/cm^2) as a function of in-loom fabric tightness for three different types of weaves woven with 303D filling

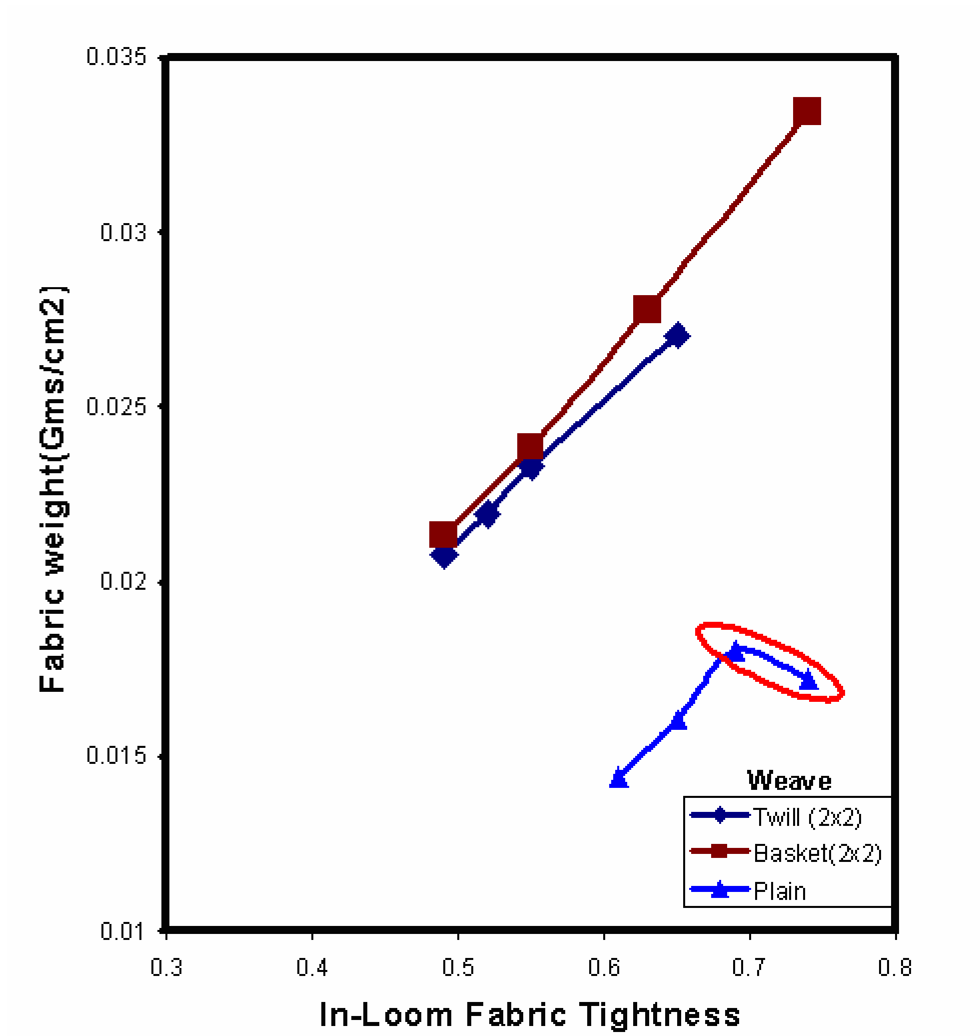

Figure 5. 39: Finished elastomeric fabric weight (gms/cm^2) as a function of in-loom fabric tightness for three different types of weaves woven with 615D filling

5.12 Influence of in-loom fabric tightness on the thickness of the finished elastomeric fabric

Finished elastomeric fabric thickness can also be associated with the in-loom fabric tightness. Figures 5.40 to 5.42 indicate the relationship between finished elastomeric fabric thickness (cm) and in-loom fabric tightness for fabrics woven with different types of weaves and with particular set of warp and filling yarns. We can see from these Figures (5.40 to 5.42) for a particular weave fabric woven with certain set of warp and filling yarns with different in-loom fabric tightness levels, the finished elastomeric fabric thickness increases with increasing in-loom fabric tightness levels with exceptions in Figures 5.41 & 5.42 encircled with red colored ovals. The reason for this behavior (increase in fabric thickness with increasing in-loom fabric tightness) is that when the in-loom fabric tightness level increases the closeness between the warp and the weft yarns and thus the number of warp or weft or both threads per cm^2 increases which there by increases the volume of filling threads and crimp of warp and filling yarns also increase. This increase in volume increases the fabric thickness. The exceptions (decrease in fabric thickness with increasing in-loom fabric tightness) are encircled by ovals in Figure 5.41 and 5.42. The reason for this curve behavior is because of the non-uniform wrinkles formed in the finished elastomeric fabric during heat setting. The formation of non-uniform wrinkles in the fabric causes the thickness of fabric to vary across the fabric which hinders the measurement of actual thickness of the fabric.

5.13 Influence of weave on the thickness of the finished elastomeric fabric

Figures 5.40 to 5.42 show the relationship between finished elastomeric fabric thickness (mm) and in-loom fabric tightness. We can see from the Figures (5.40 to 5.42), among fabrics woven with different kinds of weaves (plain, twill and basket) with particular set of warp and filling yarns and having certain in-loom fabric tightness levels, finished elastomeric fabric employed with basket weave have more thickness than the finished elastomeric fabrics employed with twill and plain. This can be associated with the higher shrinkage % of the basket weaves in comparison with the shrinkage % of the twill and plain fabrics which can be observed in Figures 5.24 to 5.26. More the shrinkage more bulkier the fabric gets and more thicker the fabric is. The exceptions (decrease in fabric thickness with increasing in-loom fabric tightness) because of the non-uniform wrinkles formed in the finished elastomeric fabric during heat setting are encircled by ovals in Figure 5.41 and 5.42.

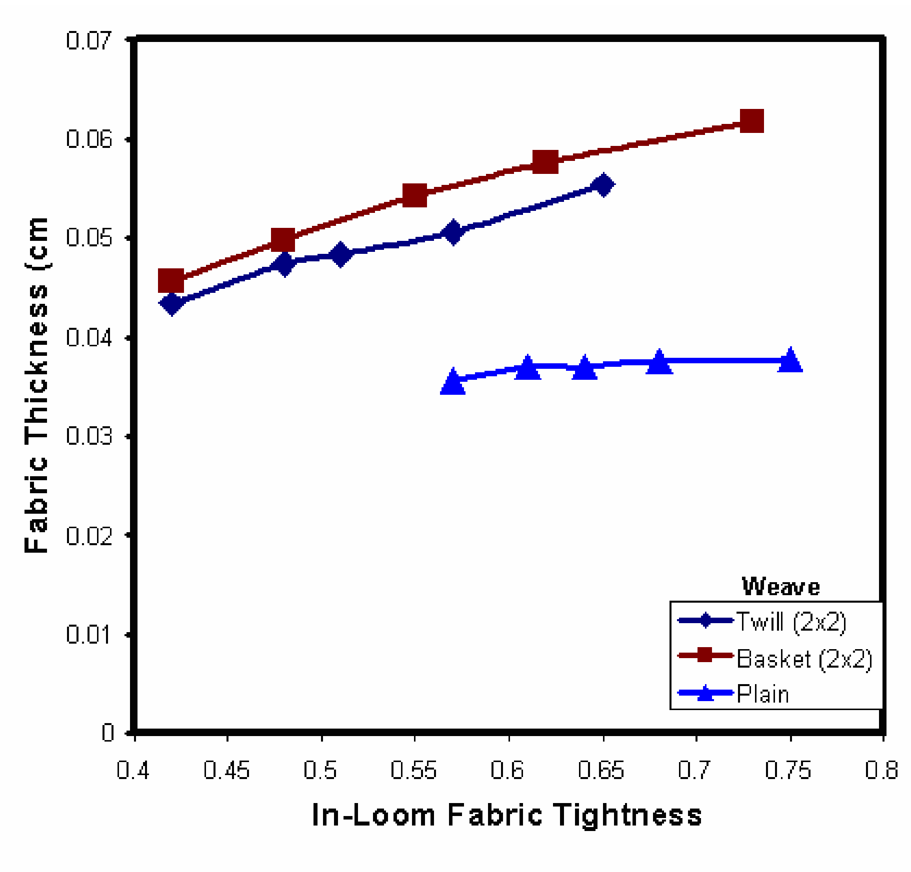

Figure 5. 40: Finished fabric thickness as a function of in-loom fabric tightness for three different types of weaves woven with 152D filling

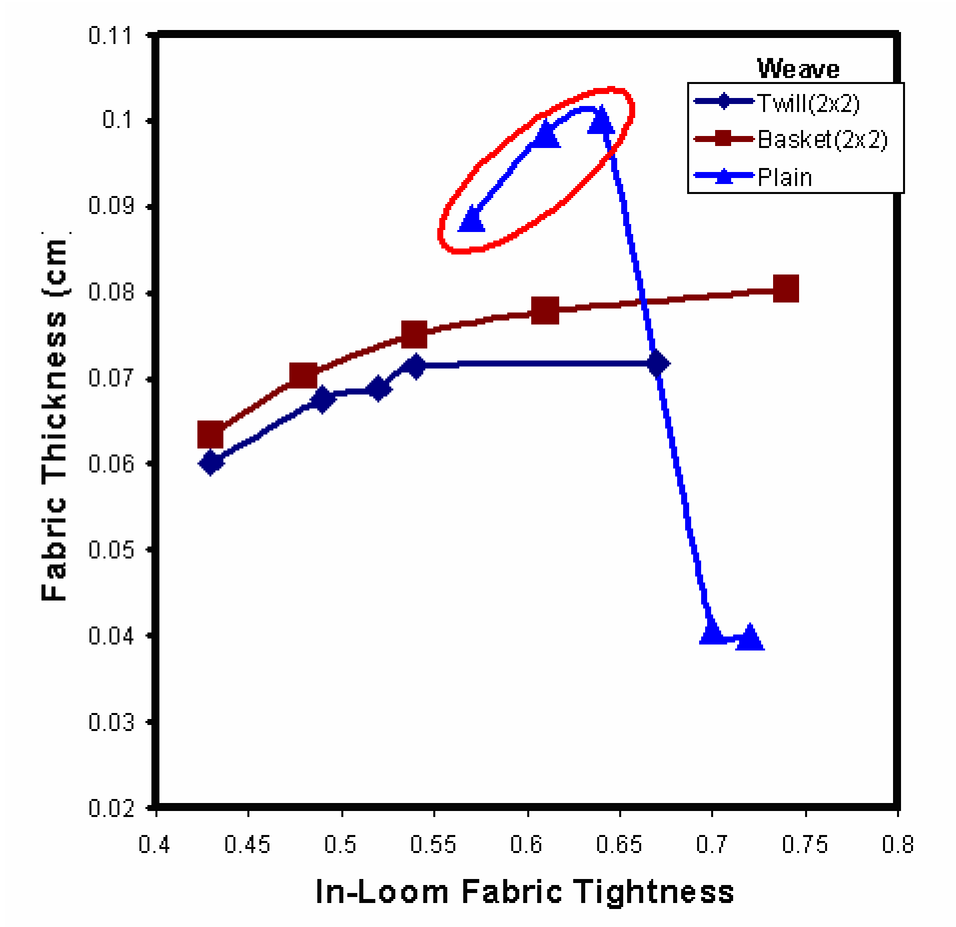

Figure 5. 41: Finished fabric thickness as a function of in-loom fabric tightness for three different types of weaves woven with 303D filling

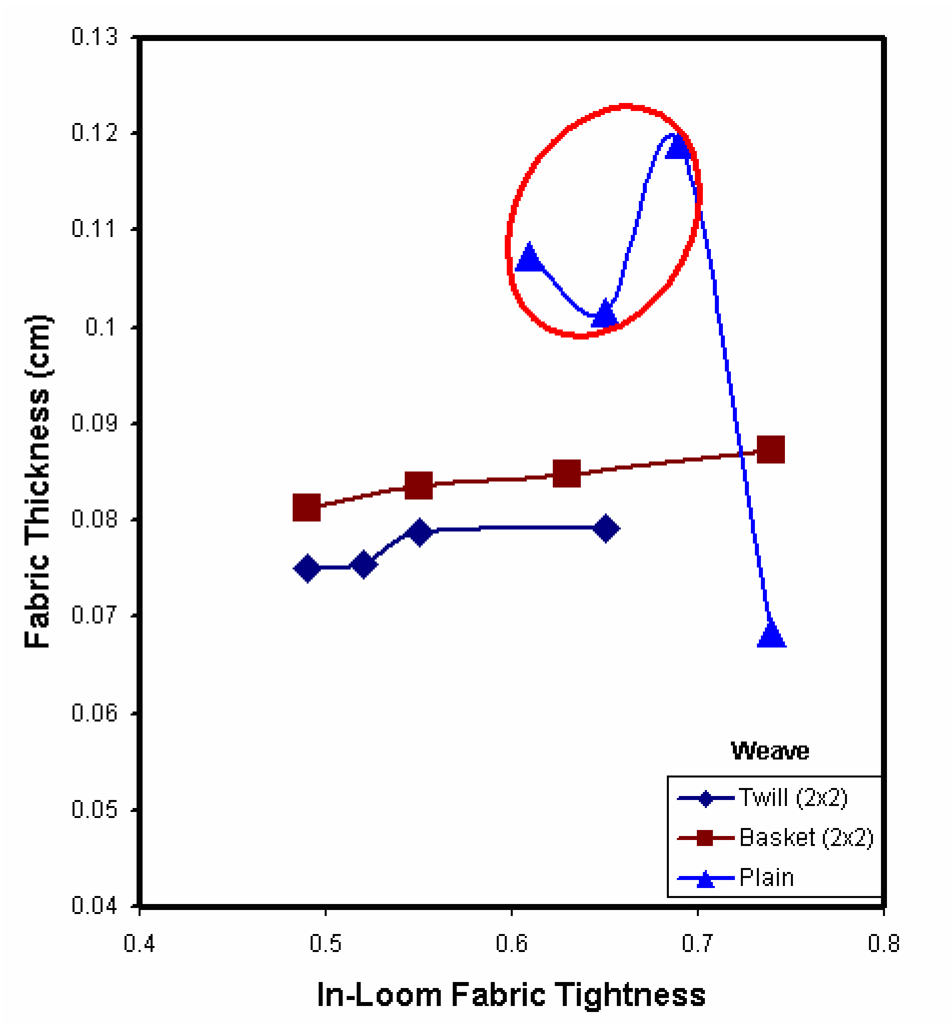

Figure 5. 42: Finished fabric thickness as a function of in-loom fabric tightness for three different types of weaves woven with 615D filling

6 SUMMARY AND CONCLUSIONS

It has been found out from the experimental results that the air permeability of the finished elastomeric fabric (made out of type 400 elastomeric yarns) is influenced by the amount of uniaxial strain applied on it. For a fabric woven with particular set of warp & filling yarns and type of weave the air permeability increases with increasing uniaxial strain (In the direction in which the elastomeric thread is employed).

The air permeability of a finished elastomeric fabric depends on in-loom fabric tightness level. For a fabric employed with particular weave and warp and filling yarns the air permeability decreases with increasing in-loom fabric tightness value.

The air permeability of finished elastomeric fabric also depends on the type of weave employed in the fabric. When we compare finished fabrics woven with three kinds of weaves with a particular set of warp and filling yarns, for a particular level of in-loom fabric tightness, fabric having plain weave have higher air permeability than fabrics employed with twill and basket weave.

This research helped in achieving the objective of this research “To provide basic understanding of the air permeability behavior of the fabrics with elastomeric constituents when subjected to different levels of strain”. The research also helped in understanding the effect of fabric parameters on the air permeability behavior of the fabrics.

This study will lead to better understanding and designing of active functional fabrics for technical applications such as parachute, sail cloth and wind screens. This research will also help in developing better elastomeric fabrics (fabrics employed with elastomeric material either if the warp or filling or both directions) that are ideal for the construction of electroactive fabrics, since those fabrics can be activated with minimum force compared to standard fabrics. This research can be extended towards the development of active fabrics by employing electroactive materials such as shape memory alloy (SMA), electro active polymers (EAP) in the boundaries of elastomeric fabric and activating them by electric volt (or current). Activating such materials causes fabric geometrical change and hence the porosity of the material can be changed actively.

7 REFERENCES

1 Clayton, F.H., The Measurement of the Air permeability of Fabrics, *Journal of the Textile Institute*. 26, TT71-TT86 (1935).

2 Brown, J.J., and Rusca, R.A., Effect of Fabric Structure on Fabric properties, *Textile Res. J*. 25, 472-476 (1955).

3 Mohamed, M.H., and Lord, P.R., Comparison of Physical Properties of fabrics Woven from Open-End and Ring Spun Yarns, *Textile Res. J*. 43, 154-166 (1973).

4 Lord, P.R., and Mohamed, M.H., Twistless Yarns and Woven fabrics, *Textile Res. J*. (x), 96-102 (197?).

5 Paek, S.L., Effect of Yarn Type and Twist Factor on Air permeability, Absorbency, and Hand Properties of Open-end and Ring-Spun yarn Fabrics, *Journal.Textile.Institute.* 86 (x), 581-589 (1995).

6 Lord, J., The Determination of the Air Permeability of Fabrics, *Journal Textile Institute.* 50, T569-T582 (1959).

7 Backer, S., The relationship Between the Structural Geometry of a textile Fabric and its Physical Properties, *Textile Res. J*. 18 (x), 650-658 (1948).

8 Rainard, L.W., Air Permeability of fabrics, *Textile Res. J*. **16** (10), 473-480 (1946).

9 Seyam, A.M., and El-Shiekh, A., Mechanics of Woven Fabrics: Part V: Impact of Weavability Limit Parameters on Properties of Fabrics from Yarns With Thickness Variation, *Textile Res. J*. 65 (1), 14-25 (1995).

10 Backer, S., The Relationship Between the Structural Geometry of a Textile Fabric and Its Physical Properties, Part 4: Interstice Geometry and Air Permeability, *Textile Res. J*. 21, 703-714 (1951).

11 Bailey, Jr., T.L.W., Longitudinal Sectioning of Cords and fabrics, *Textile Res. J*. **18** (12), 655-663 (1947).

12 Peirce, F.T., Geometry of Cloth structure, J. *Textile Inst*. 28, T45 (1937).

13 Penner, S.E., and Robertson, A.F., Flow Through Fabric-Like structures, *Textile Res. J*. 21, 775-788 (1951).

14 Lu, W.M., Tung, K.L., and Hwang, K.J., Fluid Flow Through Basic Weaves of Monofilament Filter Cloth, *Textile Res. J*. **66** (5), 311-323 (1996).

15 Hoerner, S.F., Aerodynamic Properties of Screen fabrics, *Textile Res. J*. **22** (4), 274-280 (1952).

16 Robertson, A.F., Air porosity of Open -Weave fabrics, *Textile Res. J*. **20** (12), 838-857 (1950).

17 Hsieh, Y.L., Liquid Transport in Fabric Structures, *Textile Res. J*. **65** (5), 299-307 (1995).

18 Skinkle, J.H., "Textile testing: Physical, chemical and Microscopical," Chemical publishing Co, New York, 90-91 (1949).

19 Seyam, A. M., Structural Design of Woven Fabric: Theory and Practice, the Textile Progress Journal **31**, No. 3 (2002).

20 Sieminski, M.A., and Hotte, G.H., The Porosity of the Textile materials, *Rayon Text.Mo*. **25**(12), 608-610 (1944).

21 Burleigh, E.G., Wakeham, H., Honold, E., and Skau, E.L., Pore Size Distribution in Textiles, *Textile Res. J*. **xx** (x), 547-555 (1949).

22 Kullman, R.M.H., Graham, C.O., and Ruppenicker, G.F., Air permeability of Fabrics made from unique and Conventional yarns, *Textile Res. J*. **51** (12), 781-786 (1981).

23 Hearle, J. W. S., Grosberg, P., and Backer, S., "Structural Mechanics of Fibers, yarns, and Fabrics," Wiley-Inter-science, New York, 1969.

24 Realff, M.L., Identifying Local Deformation Phenomena During Woven Fabric Uniaxial Tensile Loading, *Textile Res. J*. **64**(3), 135-141 (1994).

25 Seo, M.H., Realff, M.L., Pan, N., Boyce, M., Schwartz, P., and Backer, S., Mechanical Properties of Fabric Woven from Yarns Produced by Different Spinning Technologies: Yarn failure in Woven fabric, *Textile Res. J*.63(3) , 123-134 (1993).

26 Realff, M.L., Boyce, M.C., and Backer, S., A Micro mechanical Model of the Tensile Behavior of Woven Fabric, *Textile Res. J.* , 445-459 (1997).

27 Ericksen, R.H., Davis, A.C., and Warren, W.E., Deflection-Force Measurements and Observations on Kevlar 29 Parachute Fabrics, *Textile*

28 American Society for Testing Materials, 1990 Annual Book of ASTM Standards, D 3883-90, Philadelphia, PA, 1990.

8 APPENDICES

8.1 Fabric Tightness calculation:

Two parameters are needed to calculate fabric tightness. These are yarn diameter and weave factor..

Yarn Diameter calculation:

The diameter of the yarn is calculated with the help of the following formula [19]

Diameter of the yarn in inches = $\dfrac{1}{29.3\sqrt{\phi P_f N_{cc}}}$

ϕ = Packing factor

P_f = Fiber density

N_{cc} = Yarn count in cotton system

We have used two kinds of yarn in this experiment, 100% cotton ring spun warp and T-400 bi-component filling. The packing factor of the ring spun yarn is 0.6 and filament yarn is 0.65 [19]. The density of warp yarn (Cotton) is 1.52 g/cm^3 and density of weft yarn (T-400) is 1.4 g/cm^3. Table 4 indicates the diameter of weft yarns used in this experiment and table 5 indicates the diameter of warp yarn calculated using the formula mentioned above.

Table 4: Weft Yarn Diameter:

Count (Denier)	Count (cotton count)	Diameter (inch)
152	35	0.006047525
303	18	0.00843287
615	9	0.01192588

Table 5: Warp Yarn Diameter:

Count (Denier)	Count (cotton count)	Diameter (inch)
253	21	0.007798756

Weave Factor calculation:

Weave factor is numerical value which express the amount of interlacing of the warp and the filling yarns [19].

$$M_1 = \frac{N_1}{i_1}$$

$$M_2 = \frac{N_2}{i_2}$$

M_1 = Warp weave factor

M_2 = Filling weave factor

N_1 = No of warp ends per weave repeat

i_1 = No of filling intersections per weave repeat

N_2 = No of filling ends per weave repeat

i_2 = No of warp intersections per weave repeat

Table 6: Weave factor of plain twill and basket weaves:

Weave	N_1	i_1	N_2	i_2	M_1	M_2
Plain	2	2	2	2	1	1
Twill (2x2)	4	2	4	2	2	2
Basket (2x2)	4	2	4	2	2	2

Thread density calculation of the reference fabric:

Thread density of the reference fabric can be calculated with the help of Ashenhurst's Ends plus Intersections Theory [19]. Figure 8.1 shows the geometry of Ashenhurst's

Ends plus Intersections theory. Table 7 indicates the reference warp and filling yarns per unit fabric width for fabrics woven with different weaves and filling yarns.

$$t_{1Max} = \frac{M_2}{M_2 d_2 + d_1}$$

$$t_{2Max} = \frac{M_2}{M_2 d_2 + d_1}$$

t_{1Max} = Reference warp density (ends/unit fabric width)

t_{2Max} = Reference pick density (picks/unit fabric length)

d_1 = Diameter of the warp yarn

d_2 = Diameter of the filling yarn

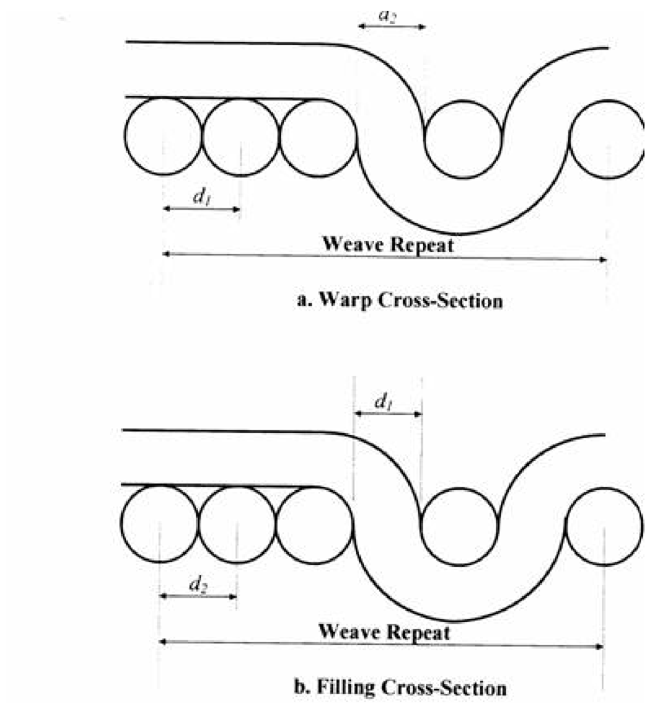

Figure 8. 1: Ashenhurst's geometry of ends plus intersections theory [19]

Table 7: Reference warp and pick densities

weave	Filling Yarn Count (Denier)	t_{1Max}	t_{2Max}
Plain	152	72.46	72.46
	303	61.73	61.73
	615	50.76	50.76
Twill (2x2)	152	92.59	101.01
	303	83.33	81.30
	615	72.72	63.29
Basket (2x2)	152	92.59	101.01
	303	83.33	81.30
	615	72.72	63.29

Russell's Fabric Tightness calculation:

Fabric tightness was calculated using Russell's tightness [19]. Table 8-16 shows the filling, warp and fabric construction factors of the plain, basket and twill fabrics woven from 152 D, 303 D and 615 D filling yarns. The warp, filling and fabric construction factors were calculated using the formula mentioned below

$$C_{Fabric} = \frac{t_1 + t_2}{t_{1Max} + t_{2Max}} \;,\; C_{Warp} = \frac{t_1}{t_{1Max}} \text{, and } C_{Weft} = \frac{t_2}{t_{2Max}}$$

Where

C_{Warp} = Warp construction factor

C_{Weft} = Filling construction factor

C_{Fabric} = Fabric construction factor

t_1 = Warp density t_2 = Pick density

Table 8: Warp, filling and fabric construction factor of plain weave fabrics made out of 152 D filling

Warp Density (t_1), Ends/inch	Pick Density (t_2), Picks/inch	Filling Construction Factor (C_{Weft})	Warp Construction Factor (C_{Warp})	Fabric Construction factor (C_{Fabric})
52	30	0.414	0.7176	0.5658
52	37	0.5106	0.7176	0.6141
52	41	0.5658	0.7176	0.6417
52	46	0.6348	0.7176	0.6762
52	56	0.7728	0.7176	0.7452

Table 9: Warp, filling and fabric construction factor of plain weave fabrics made of 303D filling

Warp Density (t_1), Ends/inch	Pick Density (t_2), Picks/inch	Filling Construction Factor(C_{Weft})	Warp Construction Factor (C_{Warp})	Fabric Construction factor(C_{Fabric})
52	18	0.2916	0.8424	0.567
52	23	0.3726	0.8424	0.6075
52	27	0.4374	0.8424	0.6399
52	34	0.5508	0.8424	0.6966
52	37	0.5994	0.8424	0.7209

Table 10: Warp, filling and fabric construction factor of plain weave fabrics made out of 615 D filling yarn

Warp Density (t_1), Ends/inch	Pick Density (t_2), Picks/inch	Filling Construction Factor(C_{Weft})	Warp Construction Factor (C_{Warp})	Fabric Construction factor(C_{Fabric})
52	10	0.197	1.0244	0.6107
52	14	0.2758	1.0244	0.6501
52	18	0.3546	1.0244	0.6895
52	23	0.4531	1.0244	0.73875

Table 11: Warp, filling and fabric construction factor of basket weave made out of 152 D filling

Warp Density (t_1), Ends/inch	Pick Density (t_2), Picks/inch	Filling Construction Factor(C_{Weft})	Warp Construction Factor (C_{Warp})	Fabric Construction factor(C_{Fabric})
52	30	0.297	0.5616	0.423547826
52	41	0.4059	0.5616	0.480365217
52	54	0.5346	0.5616	0.547513043
52	68	0.6732	0.5616	0.619826087
52	90	0.891	0.5616	0.73346087

Table 12: Warp, filling and fabric construction factor of basket weave fabrics made out of 303D filling yarn

Warp Density (t_1), Ends/inch	Pick Density (t_2), Picks/inch	Filling Construction Factor (C_{Weft})	Warp Construction Factor (C_{Warp})	Fabric Construction factor (C_{Fabric})
52	18	0.2214	0.624	0.425185185
52	27	0.3321	0.624	0.479851852
52	37	0.4551	0.624	0.540592593
52	49	0.6027	0.624	0.613481481
52	70	0.861	0.624	0.741037037

Table 13: Warp, filling and fabric construction factor of basket weave fabrics made out of 615D filling yarn

Warp Density (t_1), Ends/inch	Pick Density (t_2), Picks/inch	Filling Construction Factor (C_{Weft})	Warp Construction Factor (C_{Warp})	Fabric Construction factor (C_{Fabric})
52	14	0.2212	0.715	0.485228426
52	23	0.3634	0.715	0.551395939
52	33	0.5214	0.715	0.624915398
52	49	0.7742	0.715	0.742546531

Table 14: Warp, filling and fabric construction factor of twill weave fabrics made out of 152 D filling

Warp Density (t_1), Ends/inch	Pick Density (t_2), Picks/inch	Filling Construction Factor (C_{Weft})	Warp Construction Factor (C_{Warp})	Fabric Construction Factor (C_{Fabric})
52	30	0.297	0.5616	0.423547826
52	41	0.4059	0.5616	0.480365217
52	46	0.4554	0.5616	0.506191304
52	58	0.5742	0.5616	0.568173913
52	74	0.7326	0.5616	0.650817391

Table 15: Warp, filling and construction factor of twill weave fabrics made out of 303D filling

Warp Density (t_1), Ends/inch	Pick Density (t_2), Picks/inch	Filling Construction Factor (C_{Weft})	Warp Construction Factor (C_{Warp})	Fabric Construction Factor (C_{Fabric})
52	18	0.2214	0.624	0.425185185
52	28	0.3444	0.624	0.485925926
52	33	0.4059	0.624	0.516296296
52	37	0.4551	0.624	0.540592593
52	58	0.7134	0.624	0.668148148

Table 16: Warp, filling and fabric construction factor of twill weave fabrics made out of 615 D filling

Pick Density (t_2), Picks/inc	Filling Construction Factor	Warp Construction Factor	Fabric Construction factor
14	0.2212	0.715	0.485228426
18	0.2844	0.715	0.51463621
23	0.3634	0.715	0.551395939
37	0.5846	0.715	0.654323181

8.2 Finished fabric tightness calculation

Weft Yarn Diameter calculation

Weave	Count (Denier)	Count (Tex)	Diameter (cm)
Plain	257	29	0.02014699
Twill	275	31	0.020830132
Basket	284	32	0.021163435
Basket (p)	568	63	0.029694871

Warp yarn diameter calculation

Count (Denier)	Count (Tex)	Diameter (cm)
253	28	0.019774862

Thread density calculation of the reference fabric

Weave	Warp Yarn Diameter	Filling yarn Diameter	$T1_{Ref}$	$T2_{Ref}$
Plain	0.019774862	0.02014699	25.04893796	25.04893796
Twill	0.019774862	0.020830132	33.12362969	32.55466589
Basket	0.019774862	0.021163435	32.9417875	32.20522067
Basket (p)	0.019774862	0.029694871	20.21438017	20.21438017

Russell's Fabric Tightness calculation

Weave	Ends/cm	Picks/cm	C_1	C_2	C_f
Plain	34	12	1.357342976	0.479062227	0.918203
Twill*	37	22	1.117027341	0.675786386	0.936466
Basket	40	22	1.214263191	0.683119058	0.951694

C_1= Warp construction factor
C_2= Filling construction factor
C_f=Fabric construction factor

Weave	In-Loom Fabric Tightness	Finished fabric Tightness	Air permeability (Finished fabric)	Fabric thickness (Finished fabric)
Plain	0.566	0.918	101	0.35
Twill*	0.548	0.936	52	0.43
Basket	0.548	0.952	36	0.46

Twill*= Involves Brierley's correction factor (M^0.45/M^0.39)

8.3 Stress strain evaluation results of Type-400 elastomeric yarn (without heat setting)

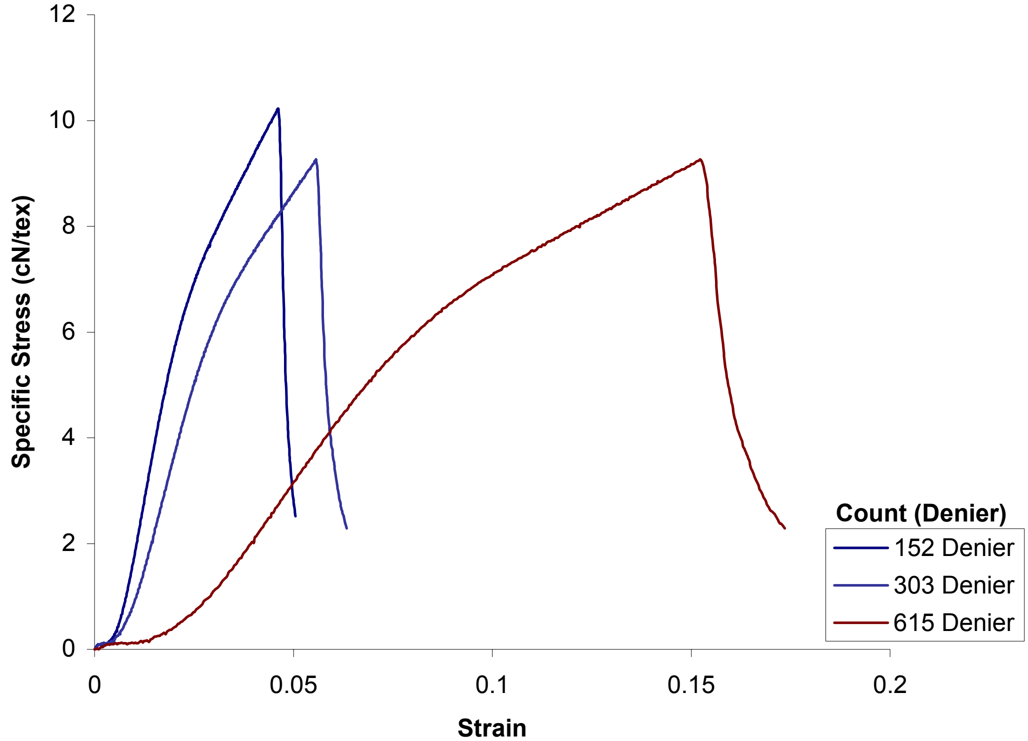

Figure 8. 2: Stress strain evaluation of type 400 elastomeric yarns (without heat setting) of three different yarn counts

8.4 Stress strain Evaluation Results of Type-400 elastomeric yarn (with heat setting)

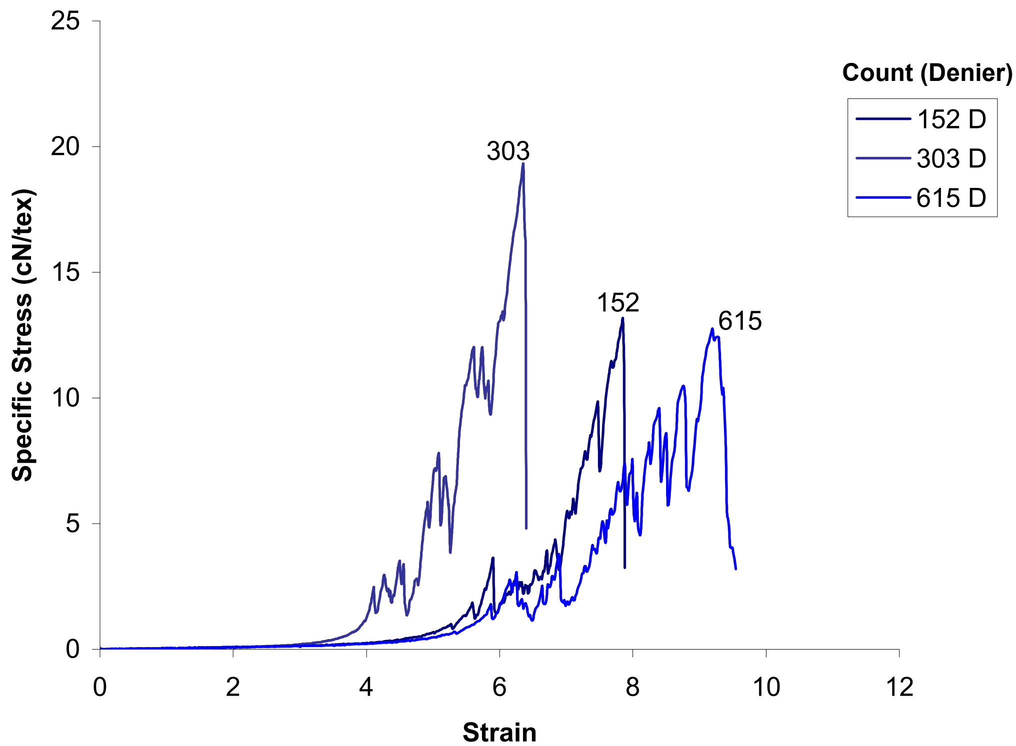

Figure 8. 3: Stress strain evaluation of type 400 elastomeric yarns (After heat setting) of three different yarn counts 152 D (having 68 filaments and 4.45 D per filament), 615 D (having 136 filaments and 4.522 D per filament)

8.5 Stress strain evaluation results of elastomeric fabrics

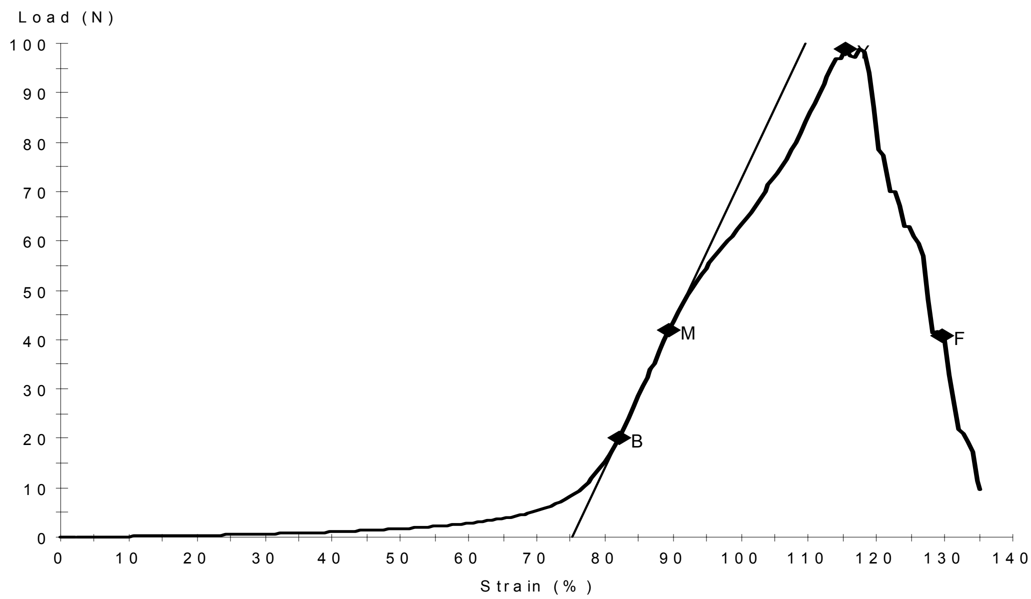

Figure 8. 4: Stress strain evaluation of elastomeric fabric (2x2 basket weave) woven with 152 D filling yarn having a pick density of 60 picks per inch

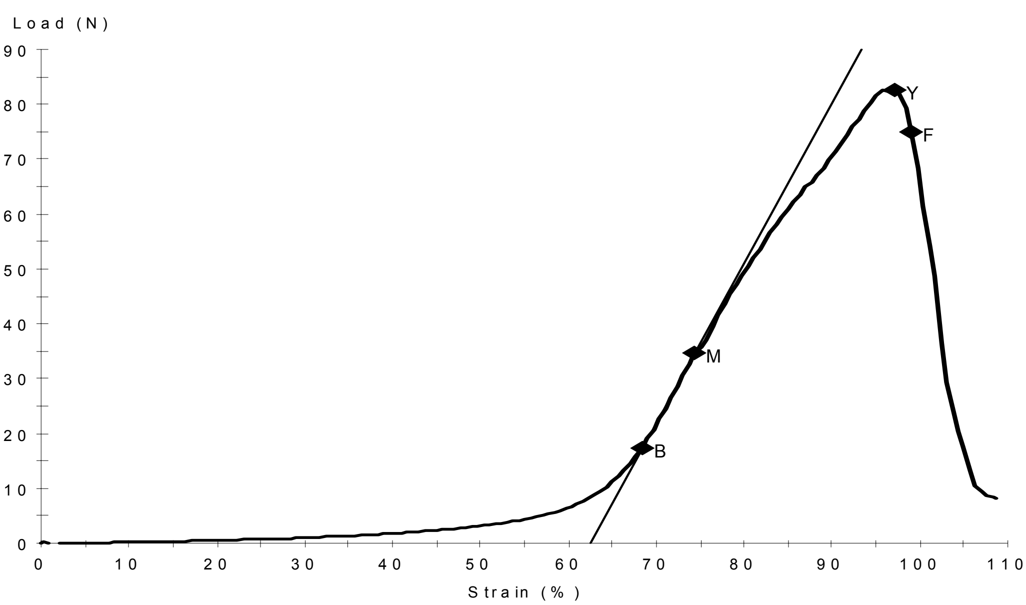

Figure 8. 5: Stress strain evaluation of elastomeric fabric (2x2 Twill weave) woven with 152 D filling yarn and having a pick density of 60 picks per inch

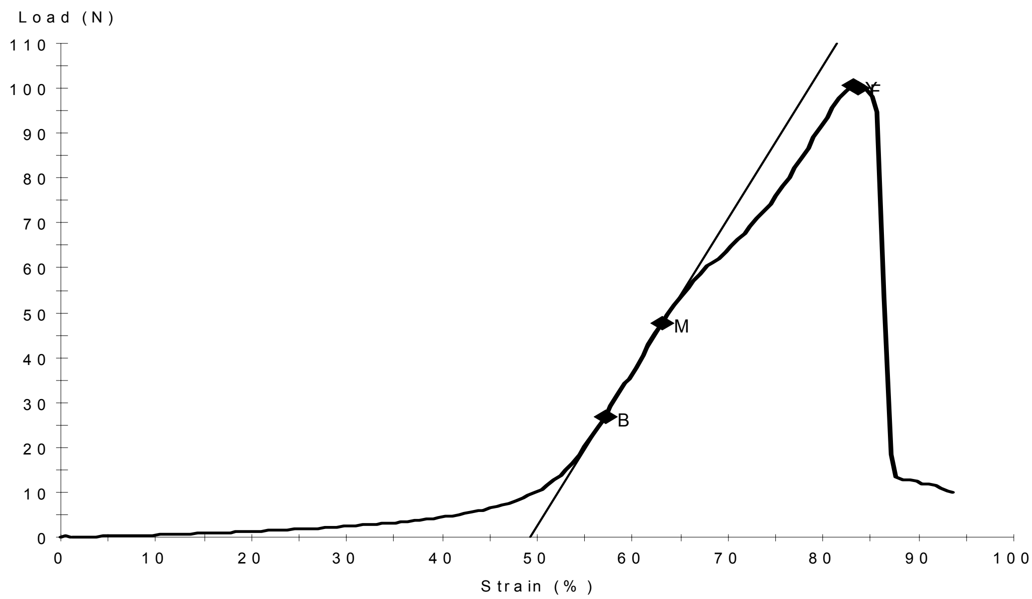

Figure 8. 6: Stress strain evaluation of elastomeric fabric (plain weave) woven with 152 denier filling yarn having a pick density of 60 picks per inch

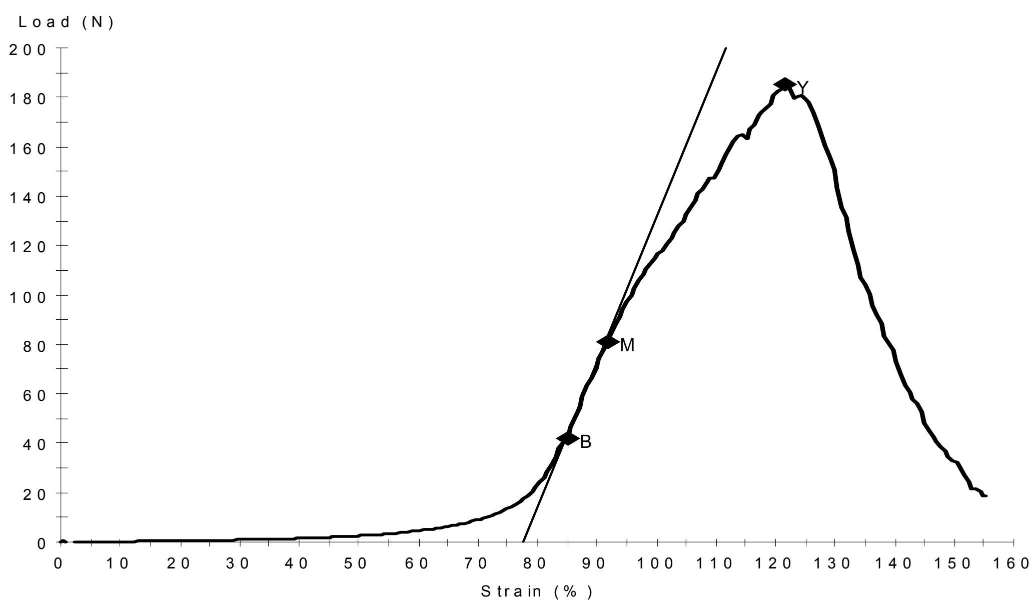

Figure 8. 7: Stress strain evaluation of elastomeric fabric (2x2 Basket weave) woven with 615 D filling yarn having a pick density of 27 picks per inch

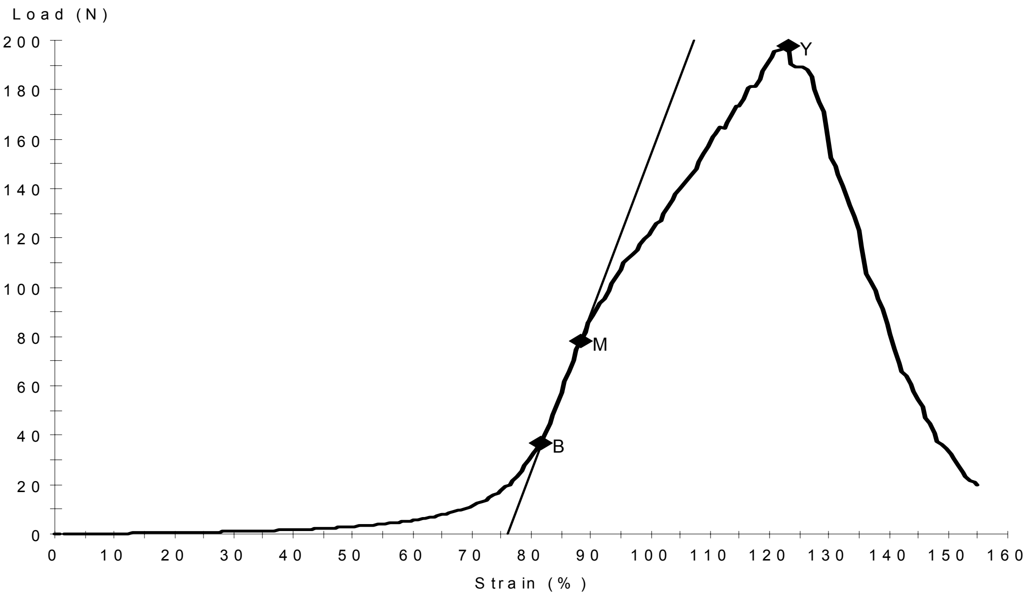

Figure 8. 8: Stress strain evaluation of elastomeric fabric (2x2 Twill weave) woven with 152 Denier filling yarn and having a pick density of 27 picks per inch

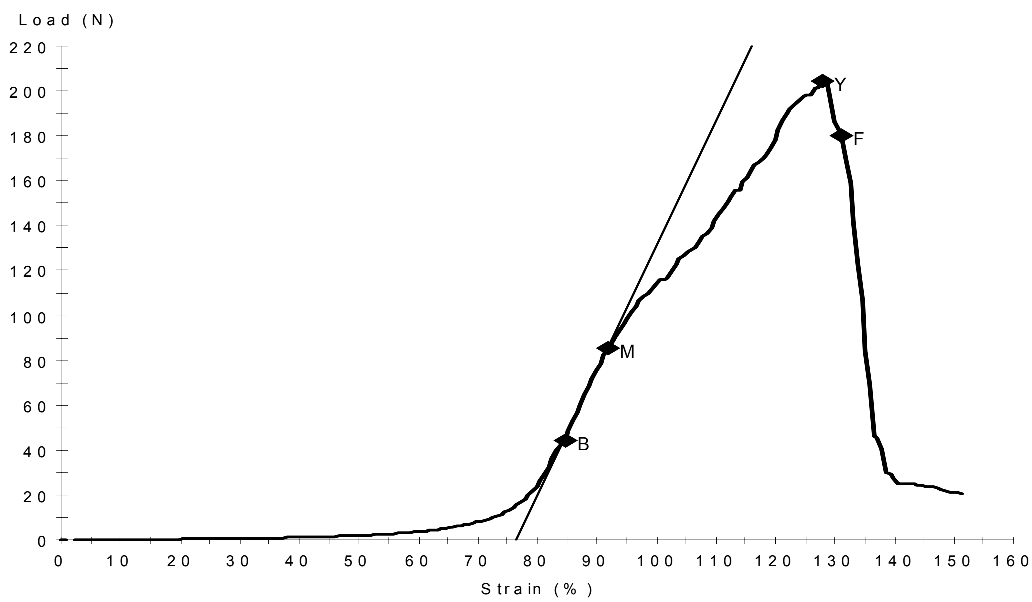

Figure 8. 9: Stress strain evaluation of elastomeric fabric (Plain weave) woven with 615 Denier filling yarn and having a pick density of 27 picks per inch

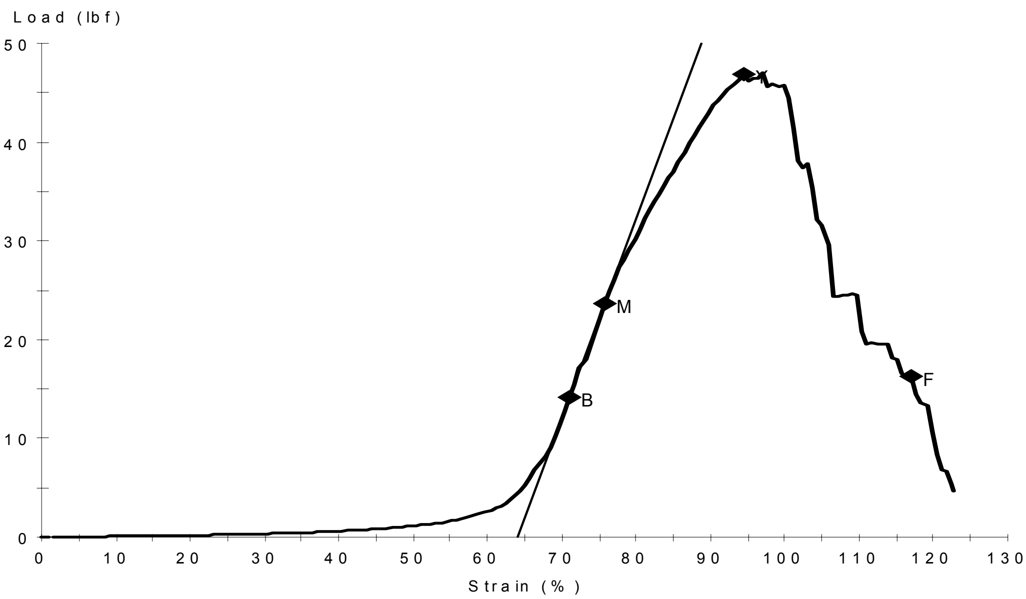

Figure 8. 10: Stress strain evaluation of elastomeric fabric (2x2 basket weave) woven with 303 D filling yarn and having a pick density of 74 picks per inch

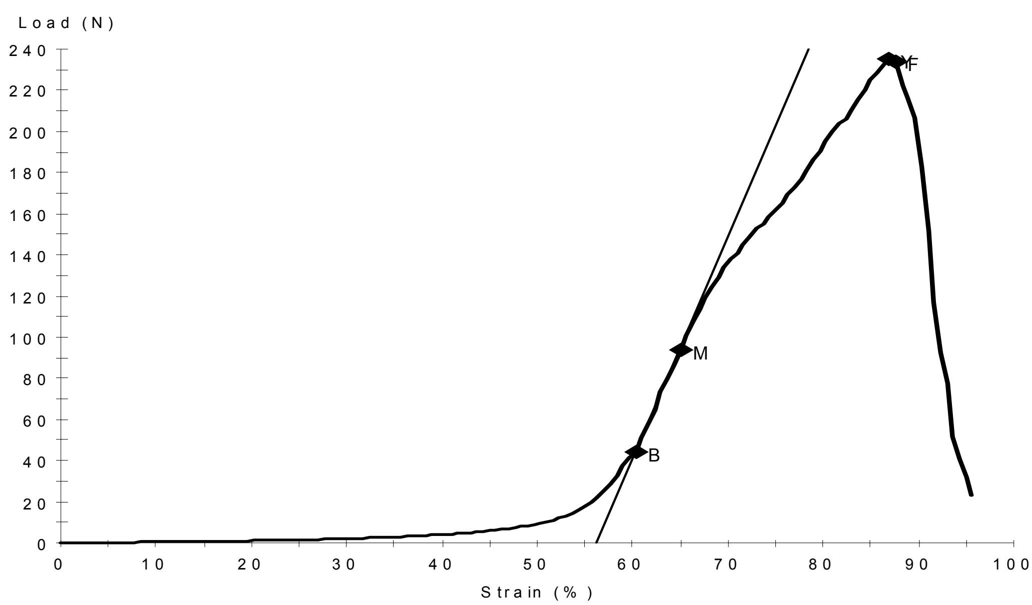

Figure 8. 11: Stress strain evaluation of elastomeric fabric (2x2 Twill weave) woven with 303 Denier filling yarn and having a pick density of 74 picks per inch

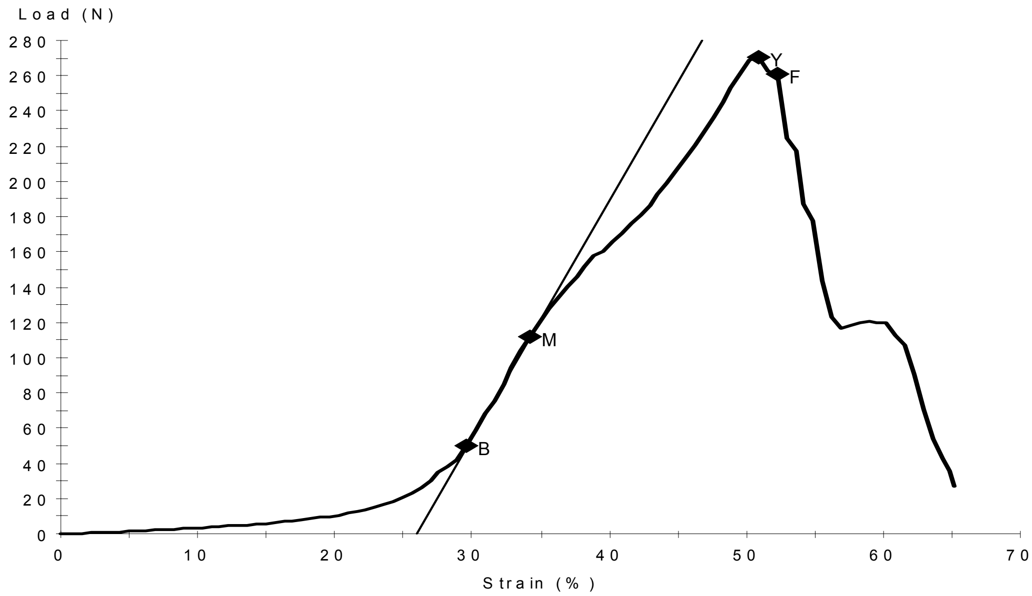

Figure 8. 12: Stress strain evaluation of elastomeric fabric (Plain weave) woven with 303 Denier filling yarn and having a pick density of 74 picks per inch

8.6 Calculating porosity of the fabric:

$$Porosity = \frac{Volume\ of\ \ fabric - Volume\ occupied\ by\ yarns}{Volume\ of\ \ fabric} X100$$

$$Porosity = \frac{100}{t} X \left(t - \left(\left(\frac{epi}{2.54} X \frac{Weight\ of\ \ warp\ Yarn(g/cm)}{Density\ of\ Warp\ Yarn} \right) + \frac{ppi}{2.54} X \frac{Weight\ of\ \ weft\ Yarn(g/cm)}{Density\ of\ Weft\ Yarn} \right) \right)$$

Where

t = Thickness of the fabric in cm

epi = Ends per inch

ppi = Picks per inch

In this experiment warp yarn is made of 100% cotton and weft yarn is Type 400 elastomeric yarn from DuPont. Table (17 – 25) shows the volumetric porosity of fabrics made of three different count (152 D, 303 D, 615 D) of filling yarns and three types of weaves (Plain, twill and basket)

The density of cotton yarn is 1.52

The density of Type-400 elastomeric yarn is 1.4

Table 17: Volumetric porosity of plain weave fabrics woven with 152 Denier filling yarn

Avg PPI	Avg EPI	Avg Fabric Thickness (cm)	Avg weight of warp yarn (g/cm)	Avg weight of weft yarn (g/cm)	Porosity %
30	97	0.043	0.0003	0.0003	75.21
42	99	0.047	0.0003	0.0003	75.12
46	99	0.048	0.0003	0.0003	75.08
54	95	0.050	0.0003	0.0003	74.92
74	94	0.055	0.0003	0.0003	94.31

Table 18: Volumetric porosity of Basket weave fabrics woven with 152 Denier filling yarn

Avg PPI	Avg EPI	Avg Fabric Thickness (cm)	Avg weight of warp yarn (g/cm)	Avg weight of weft yarn (g/cm)	Porosity %
30	102	0.046	0.0003	0.0003	75.45
42	104	0.049	0.0003	0.0003	75.27
54	104	0.054	0.0003	0.0003	75.2
70	98	0.076	0.0003	0.0003	75.09
91	94	0.062	0.0003	0.0003	74.85

Table 19: Volumetric porosity of plain weave fabrics woven with 152 Denier filling yarn

Avg PPI	Avg EPI	Avg Fabric Thickness (cm)	Avg weight of warp yarn (g/cm)	Avg weight of weft yarn (g/cm)	Porosity %
30	88	0.036	0.0003	0.0003	72.99
37	86	0.037	0.0003	0.0003	72.90
42	85	0.037	0.0003	0.0003	72.32
46	86	0.038	0.0003	0.0003	71.97
55	84	0.038	0.0003	0.0003	70.90

Table 20: Volumetric porosity of twill weave fabrics woven with 303 Denier filling yarn (Type 400)

Avg PPI	Avg EPI	Avg Fabric Thickness (cm)	Avg weight of warp yarn (g/cm)	Avg weight of weft yarn (g/cm)	Porosity %
13	94	0.060	0.0003	0.0006	82.24
27	92	0.068	0.0003	0.0006	81.88
33	90	0.068	0.0003	0.0006	80.98
37	89	0.071	0.0003	0.0006	80.68
58	84	0.072	0.0003	0.0006	78.18

Table 21: Volumetric porosity of Basket weave fabrics woven with 303 Denier filling yarn

Avg PPI	Avg EPI	Avg Fabric Thickness (cm)	Avg weight of warp yarn (g/cm)	Avg weight of weft yarn (g/cm)	Porosity %
18	98	0.063	0.0003	0.0006	82.55
28	92	0.070	0.0003	0.0006	82.39
37	92	0.075	0.0003	0.0006	81.23
51	90	0.078	0.0003	0.0006	80.10
70	86	0.080	0.0003	0.0006	77.29

Table 22: Volumetric porosity of Plain weave fabrics woven with 303 Denier filling yarn

Avg PPI	Avg EPI	Avg Fabric Thickness (cm)	Avg weight of warp yarn (g/cm)	Avg weight of weft yarn (g/cm)	Porosity %
19	98	0.088	0.0003	0.0006	87.18
23	79	0.099	0.0003	0.0006	88.97
27	82	0.100	0.0003	0.0006	88.53
34	73	0.040	0.0003	0.0006	73.88
38	73	0.040	0.0003	0.0006	71.91

Table 23: Volumetric porosity of twill weave fabrics woven with 615 Denier filling yarn

Avg PPI	Avg EPI	Avg Fabric Thickness (cm)	Avg weight of warp yarn (g/cm)	Avg weight of weft yarn (g/cm)	Porosity %
14	106	0.075	0.0003	0.0013	81.22
18	98	0.075	0.0003	0.0013	80.17
23	96	0.079	0.0003	0.0012	79.87
37	86	0.080	0.0003	0.0011	76.5

Table 24: Volumetric porosity of the basket weave fabrics woven with 615 Denier filling yarn

Avg PPI	Avg EPI	Avg Fabric Thickness (cm)	Avg weight of warp yarn (g/cm)	Avg weight of weft yarn (g/cm)	Porosity %
14	107	0.084	0.0003	0.0013	82.78
23	96	0.081	0.0003	0.0012	79.90
34	92	0.084	0.0003	0.0012	77.08
50	86	0.087	0.0003	0.0011	73.33

Table 25: Volumetric porosity of the plain weave fabrics woven with 615 Denier filling yarn

Avg PPI	Avg EPI	Avg Fabric Thickness (cm)	Avg weight of warp yarn (g/cm)	Avg weight of weft yarn (g/cm)	Porosity %
10	68	0.107	0.0003	0.0014	90.87
14	69	0.101	0.0003	0.0013	89.22
18	66	0.119	0.0003	0.0013	89.59
23	55	0.069	0.0003	0.0013	82.60